AN ABSTRACT OF THE THESIS OF

Lih-Jong Ko for the degree of Master of Science in Atmospheric Sciences
presented on June 26, 1992.

Title: Factors Influencing the Atmospheric Aerosol Composition at Two Sites in Western Oregon.

Redacted for privacy

Abstract Approved: _____.
Richard J. Vong

Fine and coarse particles were collected for eight weeks during the summer of 1991, at a coastal site (Yaquina Head) and a non-industrial site (Corvallis) in Western Oregon to characterize the aerosol composition and evaluate whether the sites are appropriate for sampling "background" marine air. Concentrations of up to 11 species (SO_4^{2-}, NO_3^-, Cl^-, Na, Fe, Ni, Pb, Cr, Co, Sb, and CH_3SO_3H) for 95 samples were determined using four chemical analysis techniques.

The influences of seasalt and soil dust were identified by analyzing concentrations of Na and Fe in the aerosol samples. Relative elemental composition in fine and coarse fractions indicated that the aerosol composition at Yaquina Head was greatly affected by seasalt. "Seasalt" enrichment factors (relative to Na) indicated that seasalt is the only source of Cl^- and SO_4^{2-} in coarse particles at Yaquina Head. In contrast, the seasalt

influence was relatively weak at the Corvallis site. "Crustal" enrichment factors suggested that soil dust was not a major source of Na^+, Cl^-, or SO_4^{2-} at either site.

A simple conceptual model that relies on meteorological conditions was used to identify sampling periods with long range transport from either marine or continental areas as well as local influences. This model suggested that during 61% of the experiment period the aerosols were advected from marine areas. At Yaquina Head, 52% of the sampling periods are associated with the "clean" background air (marine air with no local influences). Thus, Yaquina Head represents a useful location for collecting marine background air from the Pacific Ocean. The chemical composition of the marine background air collected at the Yaquina Head site is similar to that for other remote sites around the world. At Corvallis, "clean" marine background air can occasionally (21%) be collected even though Corvallis is located 64 km from the ocean.

Factors Influencing the Atmospheric Aerosol Composition at Two Sites in Western Oregon

by

Lih-Jong Ko

A THESIS

submitted to

Oregon State University

in partial fulfillment of
the requirements for the
degree of

Master of Science

Completed June 26, 1992

Commencement June 1993

APPROVED :

Redacted for privacy

Professor of Atmospheric Sciences in Charge of Major

Redacted for privacy

Chairman of Department of Atmospheric Sciences

Redacted for privacy

Dean of Graduate School

Date of thesis presentation June, 26, 1992.

Thesis presented and typed by Lih-Jong Ko.

ACKNOWLEDGEMENTS

Special gratitude is due to my major professor Dr. Richard J. Vong for his guidance and great help throughout my master's years. I would also like to thank Dr. Michael W. Schuyler from Department of Chemistry, Dr. Steven K. Esbensen and Dr. Murray Levine for serving on my graduate committee and for reviewing the manuscript.

Further thanks are due to Joan Sandeno, Charlotte Meredith and Michael Conrady for their help in chemical analysis. Further thanks also are due to George Taylor for his help in discussion about general meteorology.

I especially thank Ms. Hsin-Hua Cheng, my loving fiancee, for her constant encouragement and caring. Finally, I want to express my deepest appreciation to my parents Mr. San-Yuen Ko, Mrs. Wei-Lun Hsu and other members of my family for their continuous encouragement and understanding.

TABLE OF CONTENTS

LIST OF FIGURES

LIST OF TABLES

Factors Influencing the Atmospheric Aerosol Composition at Two Sites in Western Oregon

1. INTRODUCTION

1.0 Introduction

Increases in atmospheric particle concentrations over global scales and their corresponding effects upon climate have been recognized for more than 20 years (Peterson and Bryson, 1968; Mitchell, 1971). To accurately estimate the influence of atmospheric particles on human health and terrestrial ecosystems, the composition of aerosols (i.e., a system of small particles or liquid droplets suspended in a gaseous phase) has also been widely studied over the same period of time (Dzubay and Stevens, 1975; Appel *et al.*, 1978; Pacyna *et al.*, 1984; Davidson *et al.*, 1985; Orsini *et al.*, 1986; Maenhaut and Akilmali, 1987; Mahadevan *et al.*, 1989).

Since contaminants from human activities are minimal in remote areas, compared to urban areas, observation sites in remote areas afford several important experimental simplifications (Vong *et al.*, 1988). For example, the well-aged air present in remote areas usually is well mixed with no vertical stratification, and atmospheric-chemical reactions in remote areas are simpler than in urban areas. Thus, in the study of the mechanisms of global aerosol transport and origin and properties of atmospheric aerosols, the background concentrations of airborne particles obtained in remote areas are more easily interpreted than equivalent concentrations in urban areas.

Over the last two decades, airborne particle investigations have been performed at a number of remote locations over the world, including: the

Arctic area (Pacyna *et al.*, 1984; Maenhaut *et al.*, 1989), North America (Davidson *et al.*, 1985; Vong, 1990), Europe (Clarke *et al.*, 1984; Öblad and Selin, 1986; Amundsen *et al.*, 1992), and isolated locations in the Southern Hemisphere (Zoller *et al.*, 1974; Anngarn *et al.*, 1983; Orsini *et al.*, 1986; Lal and Kapoor, 1989). Seasalt, crustal materials and anthropogenic emissions were generally reported as source contributions for atmospheric particles. In particular, seasalt has been identified as the major source of Na^+ and Cl^- particles (Davidson *et al.*, 1985; Orsini *et al.*, 1986), also contributing a significant amount of K^+, Br^- and SO_4^{2-} (i.e., in particle fractions of a diameter larger than 2.5 μm) (Anngarn *et al.*, 1983). Crustal materials are recognized as the major source of Al, Fe, Ca, Ti and Si in aerosol samples (Anngarn *et al.*, 1983; Pacyna *et al.*, 1984; Braaten and Cahill, 1986; Orsini *et al.*, 1986). Elements which are highly enriched relative to seasalt and crustal materials, such as trace metals (Pb, V, Ni, Cr, Zn and Cd) and SO_4^{2-} (in particle fractions of a diameter smaller than 2.5 μm), are usually transported from populated or industrial areas to remote locations (Pacyna *et al.*, 1984; Öblad and Selin, 1986; Maenhaut *et al.*, 1989; Amundsen *et al.*, 1992).

In addition to anthropogenic emissions and seasalt, biological decay is also an important source of atmospheric sulfur. The major biogenic sulfur species include carbonyl sulfide (COS), carbon disulfide (CS_2), dimethyl sulfide (DMS) and hydrogen sulfide (H_2S), of which COS is the most abundant gaseous sulfur species in the troposphere. However, since the atmospheric residence time of COS is long, the total SO_4^{2-} production from COS is relatively minor (Seinfeld, 1986). DMS is the most abundant volatile sulfur compound in seawater, produced by both algae and bacteria (Seinfeld, 1986). Methane sulfonic acid (MSA) and sulfur dioxide (SO_2) can be formed from the DMS oxidation (Vong, 1985; Charlson *et al.*, 1987), and particulate sulfate is

one of the byproducts of DMS photooxidation (via SO_2). Aerosol nitrate was reported as the end product of variety of reactions for the oxidation of nitrogen oxide (NOx) (Prospero *et al.*, 1983). The oxidation reactions were discussed by Chameides and Davis (1982) in detail. Among the sources of NOx, anthropogenic emissions from the combustion of fossil fuels and biomass burning were known to contribute over half of the total NOx (Prospero *et al.*, 1983).

In addition to studies whose objective is the identification of the origin of atmospheric particles, long range transport of particles is frequently reported in aerosol composition studies. Soil dust has been transported from China to as far as Hawaii (Braaten and Cahill, 1986). Trace elements and sulfates in the Arctic area are transported from U.S.S.R., Europe and North America (Pacyna *et al.*, 1984; Maenhaut *et al.*, 1989). Other long range transport of airborne particle have been identified in studies conducted at a number of remote locations in Europe and North American (Öblad and Selin, 1986; Vong *et al.*, 1988; Amundsen *et al.*, 1992).

For the current study, air particles in two size fractions (i.e., particle diameters both larger than and smaller than 2.5 μm) were collected in Corvallis and Yaquina Head, Oregon, for a eight-week (55 days) period. Chemical analyses were performed to determine aerosol chemical composition. The measured species include sulfate (SO_4^{2-}), nitrate (NO_3^-), sodium (Na), chloride (Cl^-), iron (Fe), nickel (Ni), lead (Pb), chromium (Cr), cobalt (Co), antimony (Sb) and methane sulfonic acid (MSA).

Since NO_3^-, Ni and Pb in the fine fraction (i.e., particle diameters smaller than 2.5 μm) can be formed from combustion processes, including those based on fossil fuels, the concentrations of these species in aerosols provide an indication of combustion source contributions. Fe is a typical marker element

for soil dust. Concentrations of Na^+ and Cl^- in coarse aerosol (i.e., particle diameters both larger than and smaller than 2.5 μm) usually represent seasalt (i.e., when a bubble bursts at the sea surface it produces a mist of droplets, which upon evaporation leave NaCl particles) (Orsini et *al.*, 1986; Vong *et al.*, 1988; Andreas, 1990). Therefore, general source characteristics can be estimated from chemical analysis of the particulate samples. Meteorological data also were collected to investigate the relationship between aerosol chemical composition and meteorological conditions.

1.1 Classification of the Size of Airborne Particles

Airborne particles can be classified into two fractions according to size. Particles less than 2.5 μm diameter are generally referred to as "fine" aerosol and those greater than 2.5 μm diameter are referred to as "coarse" aerosol (Clarke *et al.*, 1984; Seinfeld, 1986; Orsini *et al.*, 1986). In general, the fine and coarse aerosol modes are generated by different processes, removed by different processes, transformed by different processes, and have a different chemical composition and optical properties. Therefore, it is necessary to distinguish between fine and coarse particles to engage in any useful discussion of the physics and chemistry of aerosols.

Fig. 1.1 summarizes the sources of particles as well as particle formation and removal mechanisms for each fraction. Fig. 1.2 shows some of the major species which are found in each fraction.

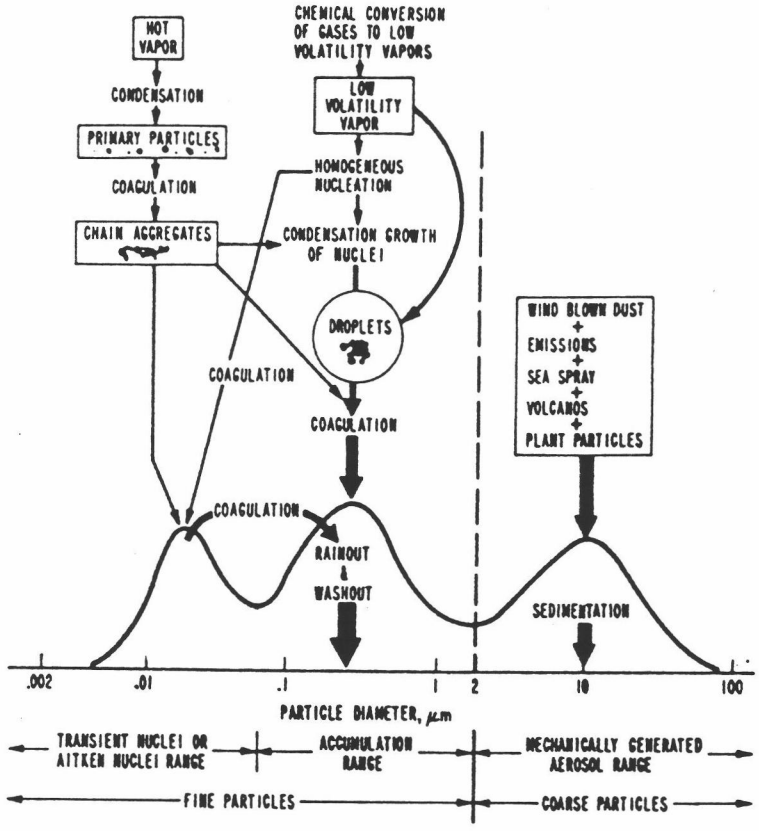

FIG. 1.1. Idealized schematic for aerosol size distribution. Particle sources, formation and removal mechanisms are also indicated. The Y axis represents the total volume of particles (Seinfeld, 1986).

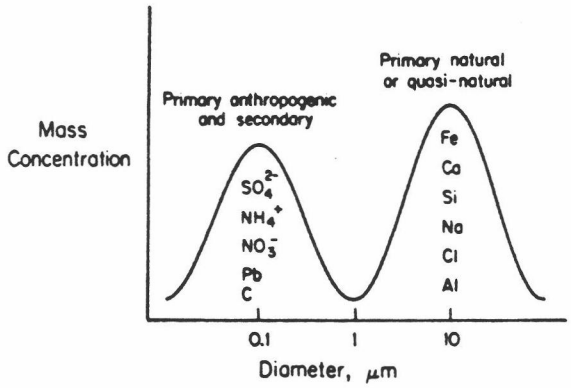

FIG. 1.2. Idealized aerosol mass distribution showing some of the major species usually found within each size fraction (Seinfeld, 1986).

1.2 Characteristics of Fine Particles

Fine particles can be divided into two modes, the nuclei mode and the accumulation mode. Nuclei mode particles, from 0.005 to 0.1 μm diameter, are generated from the condensation of vapors generated during combustion (or other processes). Accumulation mode particles, from 0.1 to 2.5 μm diameter, are generated from the coagulation of particles in the nuclei mode and from the condensation of vapors onto existing particles (Seinfeld, 1986). The nuclei mode contains only a small fraction of the total aerosol mass and may be absent in aerosol collected at some distance (e. g., 100 km or greater) from combustion sources.

Fine particles usually contain considerable quantities of SO_4^{2-}, NH_4^+, NO_3^-, elemental carbon and condensed organic compounds (Mahadevan *et al.*, 1989). Carcinogenic organics such as polycyclic aromatic hydrocarbons (PAH) and some heavy metals, including As, Pb, Ni, Cd and Zn are concentrated in fine particles (Davidson *et al.*, 1985; Seinfeld, 1986; Baeyens and Dedeurwaerder, 1991). Particles in the fine fraction are not significantly affected by gravitational settling (i.e., the terminal fall velocity for 1 μm diameter particles is 0.7 cm/min) and are often transported over long distances (Pacyna et *al.*, 1984). Brownian diffusion followed by coagulation is the key sink for particles in the nuclei mode. The dominant removal mechanism for fine particles in the atmosphere is wet scavenging by precipitating cloud, rain or fog (Seinfeld, 1986). The typical lifetime of fine particle is several days under boundary-layer conditions (Wolff, 1980).

1.3 Characteristics of Coarse Particles

Coarse particles, sized from 2.5 to 100 μm diameter, are generated by mechanical processes, such as grinding, and can be either natural or anthropogenic in origin. Natural coarse particles consist mainly of crustal material, such as Fe, Ca and Si, and seasalt elements, such as Na^+ and Cl^-. The major sources of course particles are windblown dust, sea spray, and volcanic eruption. The anthropogenic coarse particles are principally derived from manufacturing, tire wear and mining (Seinfeld, 1986). Coarse particles are usually removed from the atmosphere by sedimentation (i.e., the terminal fall velocity for 20 μm diameter particles is 2.8 m/min) (Davidson *et al.*, 1985). Sedimentation limits the lifetimes of coarse particles to a range from minutes to hours (Wolff, 1980).

1.4 Meteorological Parameters Affecting the Transportation and Dispersion of Airborne Particles

In general, the transport and dispersion of airborne particles is controlled by meteorology. Thus, the acquisition of meteorological data at the sampling site is desirable to assist in understanding the origins of pollutants and the mechanisms of particle transportation and dispersion (Pacyna *et al.*, 1984). The meteorological parameters which were utilized in the current study for estimation of the pattern of transportation and dispersion of pollutants were: (1) surface wind speed and direction, (2) back trajectories calculated for appropriate heights (950 mb) above the surface, and (3) thermal stability of the atmosphere.

1.4.1 Wind Speed and Direction

The movement of air, and its constituents including airborne particles, is accomplished by the winds. Observations of surface wind speed and direction provide data descriptions of the horizontal movement of air. The area over which wind observations are representative is varied and dependent upon the height of the observation site, topography, and the nature of the surface in question. For example, the distribution of land-sea, mountain-valley, and urban-rural environments plays a significant role in determining wind movements (Eagleman, 1985). In coastal areas, a diurnal pattern in which sea breeze (i.e., a breeze that flows from the sea toward the land) occurs by day and a land breeze (i.e., a breeze that flows from the land toward the water) by night, results from the differentials in solar absorption and radiative characteristics between water and land. Similarly, in a valley area, differential daytime heating and nighttime cooling of the air adjacent to a slope and of the air at the same height, but situated above the valley, results in density differences which drive upslope winds during the day and downslope winds at night. In an urban area, where there is less vegetation and exposed soil, the majority of the solar energy is absorbed by urban structures and asphalt. Hence, during the warm daylight hours, the reduced degree of evaporative cooling in urban areas allows surface temperatures to rise higher than in nearby rural areas. This "heat island effect" generates surface air flows blowing toward the city from the surrounding country (Eagleman,1985; Ahrens,1988).

Corvallis, located near the geographic center of the Willamette Valley, reflects wind patterns related to area topographical characteristics. The Willamette Valley is bag-shaped with the mouth opening towards the north. During the daytime, sea breezes blow from the north (or northwest) into the

valley (near surface). During nighttime, the winds blow downward from the surrounding mountains and a light southerly wind develops (near surface).

1.4.2 Back Trajectory

Aerosol is transported considerable vertical distances from mixing associated with buoyancy forces. At the same time, surface winds are highly influenced by the nature of surface. Therefore, surface winds are usually not good indicators of the history of air masses which have moved into the sampling area while back trajectories estimated from wind fields of certain aloft levels may be more appropriate. However the accuracy of back trajectories is limited by the frequency and density of observed winds at upper levels of the atmosphere (Kuo *et al.*, 1985).

1.4.3 Thermal Stability

Thermal stability determines the vertical mixing characteristics of the atmosphere. The atmosphere is commonly composed of layers, each with different rates of temperature change with altitude (i.e., lapse rates, the rate at which the air temperature decreases with height). In a stable layers, defined as layers in which the lapse rate is less than the dry adiabatic lapse rate (9.8°K decrease per km), mixing is suppressed. The most stable layers are temperature inversions (characterized by increasing temperature with increased height). An inversion tends to trap air below the layer, where emitted pollutants tend to accumulate. Thus, the information about intensity and the height of temperature inversion layers is important for understanding particle mixing.

Over many land areas, including the Willamette Valley in Oregon, the thermal stability of the layer of air adjacent to the surface undergoes a diurnal

change; often during the night a temperature inversion layer occurs and during the day the surface layer is usually unstable due to radiative heating.

1.5 Research Objectives

The principal objectives of this investigation were to appraise the air quality of the Corvallis and Yaquina Head areas by collecting airborne particles, and to characterize the composition and any interelemental relationships in Oregon coastal aerosol. The possibility of sampling background aerosol at each sampling site was assessed. The relationship between meteorological conditions and aerosol composition was addressed.

1.6 Research Hypotheses

The hypotheses for this experiment were as follows:

a) During certain meteorological conditions (westerly local winds and marine air mass trajectories) clean marine air can be collected at the two sampling sites.

b) Since their chemical composition is known, the influences of certain natural sources on aerosol composition (soil and seasalt) can be identified through chemical analysis of appropriate species (Holland, 1978; Duce *et al.*, 1975; Cunningham, 1981). In addition certain anthropogenic source influences (fuel burning and automobile traffic) may be identified by use of the concentrations of other chemical tracers.

c) For the purpose of identifying and distinguishing between periods of marine background air ("clean"), continental background air ("polluted"), and air which has been influenced by local anthropogenic emission

sources, a simple model that relies on meteorological conditions can be utilized to classify the investigated aerosols.

2. EXPERIMENTAL PROCEDURES

2.1 Sampling Overview

For the present study, aerosol samples were collected at two sampling sites, Corvallis and Yaquina Head in Oregon. The sampling filters were weighed and mounted alternatively in an impactor or on a filter holder before it was fixed in a sampling box. After collecting air for two to three days, the sampling filters were removed and reweighed prior to chemical analysis.

2.1.1 Site Selection

The coast of Oregon state, adjacent to the Pacific Ocean, is a potentially good location for the study of background aerosols. During certain weather conditions, (e.g. the period of westerly transport), the Oregon coast is downwind of the eastern Pacific Ocean and upwind of the North American continent. This condition provides an opportunity to collect samples which represent what may be expected to be fairly "clean" air from the Pacific Ocean.

In general, to meet the goals of the monitoring program, sampling sites should be selected at locations which are representative of some larger region. To obtain representative ambient aerosols, the sampling sites should not be dominated by "local" influences such as automobile traffic, fuel combustion, or soil dust. As a practical consideration, a good sampling site should have available electric power to operate sampling equipment and should also provide convenient access for personnel. As shown in Fig. 2.1, Yaquina Head was selected as the "background" site for the collecting marine air, and Corvallis was chosen as the rural site for both marine and continental influences.

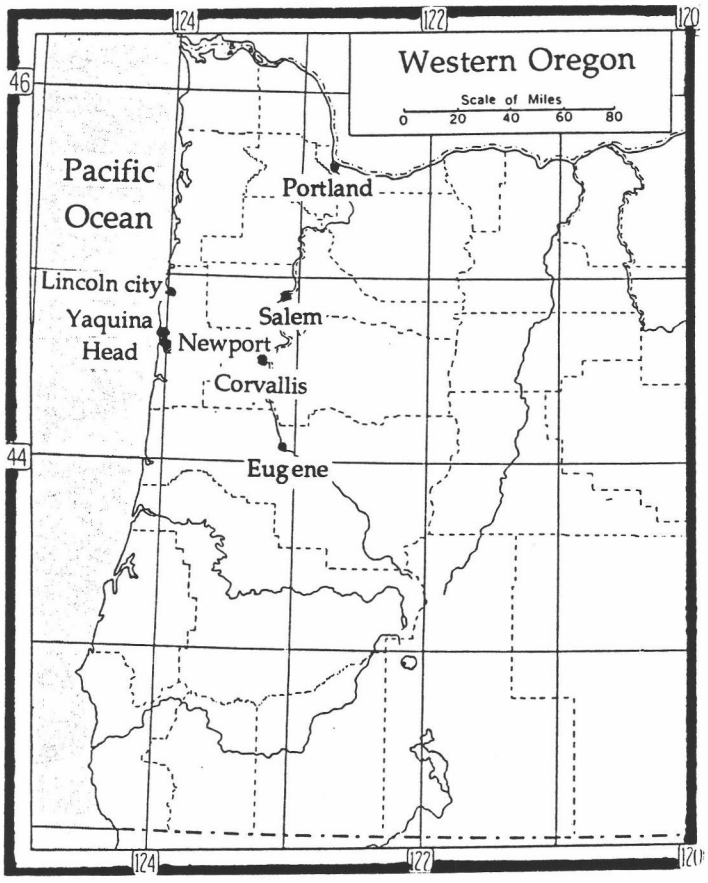

FIG. 2.1. Map of Western Oregon, including urban areas and two sampling sites.

2.1.1.1 Background site. A background site was chosen for the collection of samples with minimal anthropogenic influences. The U. S. Coast Guard rescue communication site near Yaquina Head Lighthouse (about 5 km north of Newport, OR) was chosen as the background site. This site is located at the top of a large hill (height = 120 m) on a small peninsula extending westward into the Pacific Ocean, in an area with no public access. The sampling location was situated immediately adjacent to the ocean, 1000 m east of the Pacific Ocean. The Pacific coast highway (highway 101) is located 600 m to the

east of the sampling site and could have exercised a potential influence upon the site when air was transported from the east.

During westerly winds, the air at the sampling site was transported directly from the Pacific Ocean with no continental influences, other than the road to the lighthouse (located at the extreme westend of the peninsula). Thus, beyond light traffic on the road there were no other potential aerosol sources of influence to the west of the Yaquina Head site. A five-sided box, which served as a rainhood for the aerosol samplers, was attached to an existing tower.

2.1.1.2 Rural site. Corvallis, Oregon, situated in a non-industrial area of the Willamette Valley, was chosen as rural site for the evaluation of the effects of both anthropogenic and marine sources. Located at 64 km east of Newport and 66 km north of Eugene, Corvallis has a population of 43,000 and few industries in its vicinity. Therefore, the aerosol in the Corvallis area was expected to be similar to that of the selected "background site", 69 km away, and was expected to some degree to represent "background" air.

To minimize the influence of human activities, the roof of Strand Agriculture Hall on Oregon State University campus was selected for air sampling. The sampling box that served as a rainhood was installed five meters above the nearest surface (i.e., the roof of a five story building), and 100 meters distant from the principal directions of campus traffic. Human activities were rare in the immediate vicinity of this sampling site since the access door to the roof was maintained in a locked condition and the roof was not used for any purpose except particle sampling during the course of this study. However, emissions from automobiles represent a potential influence at this site.

2.1.2 Sampling Equipment Set-Up

The usual practice was to collect two simultaneous aerosol samples using both an openface filter holder and an aerodynamic impactor; these devices were used to sample particles of different sizes. The filter mounted in an openface filter holder caught all sizes of particles, while the impactor filter caught only those particles which have diameters less than 2.5 μm (details are presented in section 2.1.3). An air pump with an adjusting valve, a dry gas meter, and a mass flow meter (used intermittently) were installed downstream of the impactor or the filter holder, as showed in Fig. 2.2.

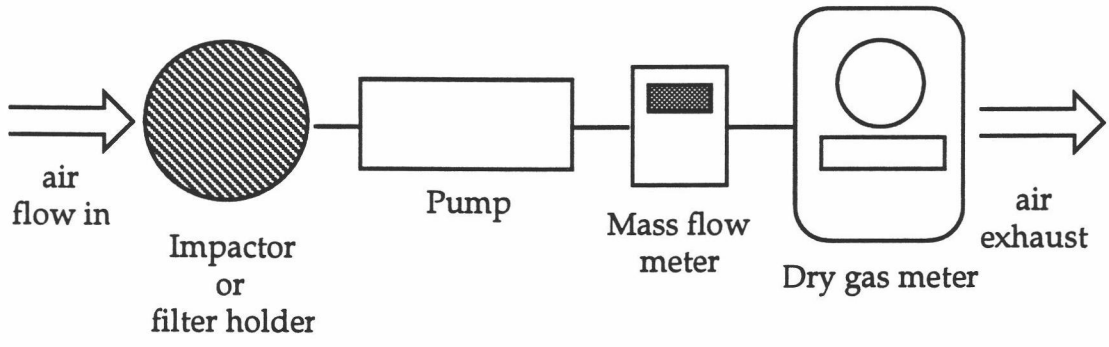

FIG. 2.2. Equipment set-up for airborne particle sampling.

2.1.3 Particle Collection by Openface Filter Holder

When air was drawn through the sampling system, essentially all particles (> 99.9%) in the air were deposited on the openface filter (John and Reischl, 1978). In some sampling periods when collection of nitric acid (HNO_3) vapor was desirable, a nylon back-up filter was used in conjunction with the openface filter holder. After sample collection, all filters were stored in air tight petri dishes at room temperature for further analyses. The total

volume of the air through the system was recorded by a dry gas meter which was compared with the flow rate monitored by a mass flow meter.

2.1.4 Impactor and Size Segregation

An air sampling impactor was used for particle size-segregation. The air flow within the impactor is shown in Fig. 2.3. Impactors are based on the principle that when the flow of the air is a curve, some particles in the air stream will tend to continue to travel in a straight line due to inertia. The larger particles, unable to follow the curved air stream, will then collide onto the impaction plate, where they generally adhere. The smaller particles pass around the plate by following the air streamline and are caught by a filter (Lioy *et al.*, 1988).

Collection efficiency is defined as the fraction of particles of a certain size that are removed from the aerosol stream by the impaction process. The collection efficiency for an impactor collecting airborne particles is a function of the Reynolds number of air stream, the particle Stokes number, and the physical configuration of the impactor (Marple and Willeke, 1979).

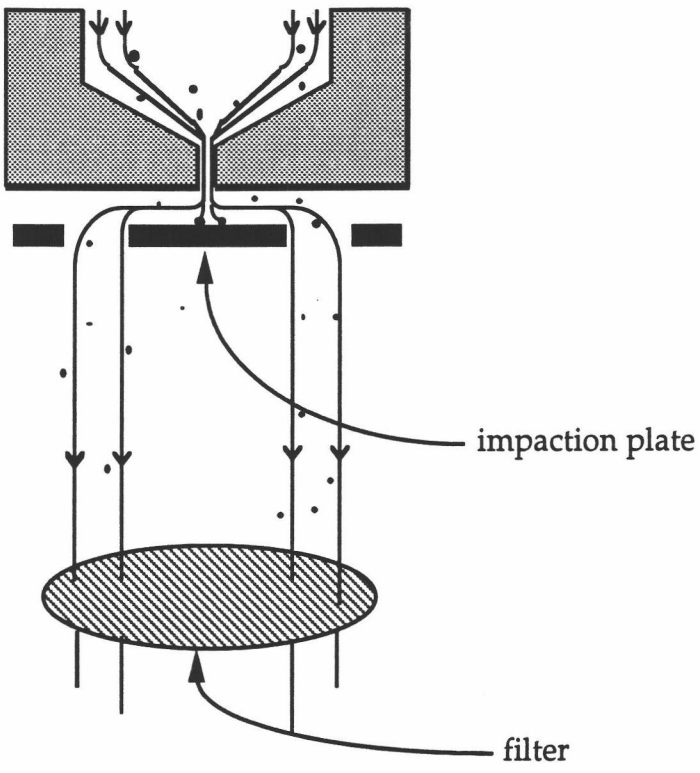

FIG. 2.3. Air flows within an air sampling impactor.

The Reynolds number of air stream for round impactors is defined as (1)

$$Re = \frac{\rho V_o W}{\mu} \qquad (1)$$

where :

ρ = the fluid density,

V_o = the mean velocity at the nozzle throat of impactor,

W = the nozzle diameter, and

μ = the fluid viscosity.

With a Reynolds number for the air stream between 500 and 25,000, collection efficiency will experience a sudden increase (i.e., the accurate cutoff characteristic similar to Fig 2.4) (Marple and Liu, 1974). For a low Reynolds numbers (<500), the poor cutoff characteristics are caused by the thick boundary layer near the impactor nozzle wall. For high Reynolds numbers, the poor cutoff characteristics results from the heterogeneous boundary layer over the impaction plate, resulting in the diffusion of smaller particles to the impaction plate (Marple and Liu, 1974). The Stokes number is defined as the ratio of the aerodynamic particle stopping distance to the nozzle radius of the impactor (Lundgren, 1967; Marple and Willeke, 1979):

$$Stk = \frac{\frac{\rho_p C V_o D_p^2}{18\mu}}{\frac{W}{2}} \qquad (2)$$

where :

ρ_p = the particle density,

C = the Cunnigham Slip correction factor,

D_p = the particle diameter, and

W = the nozzle diameter.

The physical configuration for an impactor can be sufficiently specified by the value of the nozzle diameter of the impactor, W; the nozzle-to-plate distance, S; and the nozzle throat length, T (Marple and Willeke, 1979). Collection efficiency is a function of the square root of the Stokes number (i.e., particle size) for fixed V_o, S, W and T. The impactor used for the current study had a sharp aerodynamic cut size of 2.5 μm diameter for a 10 L/min inlet flow rate, as shown in Fig. 2.4 (Marple *et al.*, 1987).

Bounce-off errors could occur when large particles rebound off the impaction plate. This would result in the collection of too large of a weight on the filter (overestimate of fine particle mass). A silicon oil coating was applied to the impaction plate prior to sampling to decrease bounce-off errors (Marple *et al.*, 1987).

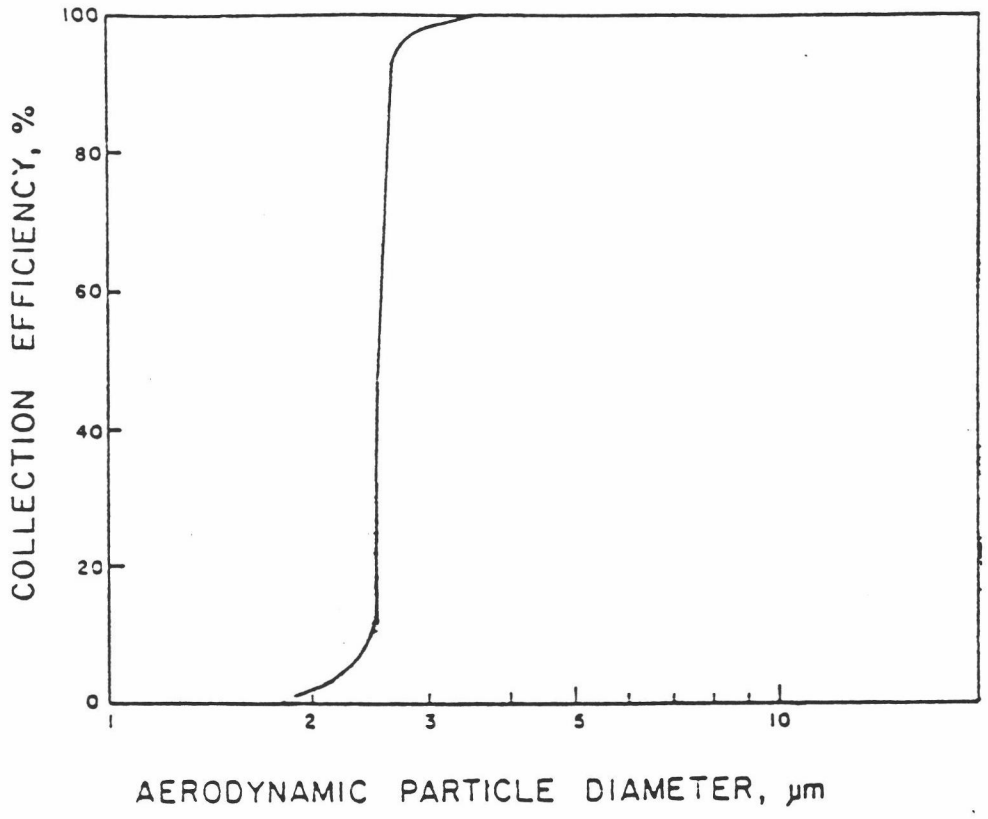

FIG. 2.4. Impactor efficiency curve for 2.5 μm cutoff diameter.

2.1.5 Sample Handling

Usually, background aerosol is very "clean" compared with urban aerosols. In most remote areas, the background concentrations of most elements are as low as one thousandth of those of industrial areas (Davidson *et al.*, 1985). Therefore, the particle concentration of samples collected at a background site will be especially sensitive to any contamination associated

with sample handling; contamination control is emphasized in such a sampling process. Special care was taken in the sample handling process to obtain high quality samples. A glove box with an absolute air filter at the inlet was built to create a particle-free space for sample handling. Sampling procedures are summarized in Fig. 2.5. Prior to collection, all the sample filters were weighed and mounted in an openface filter holder or inserted into a snap ring (which was used to mount the filter in the impactor) within the glove box. The filter holder was wrapped in Saran wrap, while the snap ring was stored in an air-tight petri dish to prevent contamination. Following sample collection, the samples were protected in the same manner and transported to the glove box. After unmounting and re-weighing , the filters were stored in petri dishes.

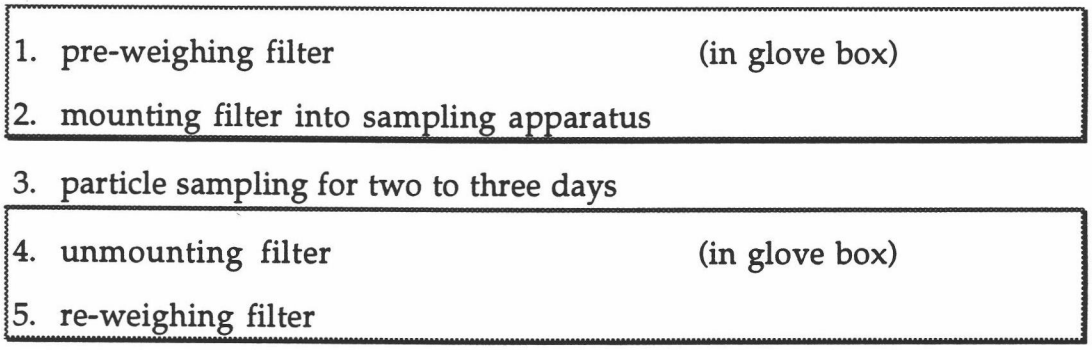

FIG. 2.5. Six steps for collection of atmospheric aerosol.

Two different size of Teflon filters, 37 mm and 47 mm in diameter, with pore size of 2 μm were used for this experiment . The 47 mm diameter filters were fit into openface filter holders for total particle (i.e., all sizes) collection and 37 mm diameter filters were fit in impactors for fine particle (i.e.,

aerodynamic diameter < 2.5 μm) collection. The collection efficiency of the Teflon filters was reported at 99.9% in the range of an inlet flow rate in the range of 3 to 85 L/min (John and Reischl, 1978).

2.1.6 Gravimetric Measurement

For this experiment, each sampling filter was weighed with a Cahn model 1500 electrical balance before and after sample collection. The mass of the collected particles was calculated as the difference between the two measurements. The precision of the balance was ± 20 μg, but the instrument provided to be less reliable because of "drift" within the balance. Standardization of weighing procedures was essential in order to obtain even an "estimate" of accumulated aerosol mass.

2.1.7 Sampling Schedule

Since background aerosol particle concentrations are low, sampling period selection is crucial to the accumulation of sufficient mass for successful chemical analyses. For the present study, the sampling period utilized was from two to three days. Table 2.1 lists the sampling schedule for fine particle collection. The experiment period was subdivided into three phases. In phases I and III, fine particles were collected simultaneously at both the Yaquina Head and Corvallis sites to assess the influence of human activities at both sites and to identify the characteristics of marine aerosols. In phase II, two impactors were placed side-by-side to collect two fine particle samples simultaneously at the Yaquina Head site during each sampling period. One sample was analyzed as a water extract via ion chromatography (IC) and graphite furnace atomic absorption spectroscopy (GFAAS), while the other sample was analyzed without extraction with instrumental neutron

activation analysis (INAA) in order to obtain more detailed information about the aerosol composition.

Table 2.1. Sampling schedule for fine particle collection (particle diameter < 2.5 μm).

		Yaquina Head (background)		Corvallis (rural)	
	Duration	No. of samples	Analyzed compounds	No. of samples	Analyzed compounds
Phase I	7/22 - 8/7	6	SO_4^{2-}, NO_3^-, Cl^-	7	SO_4^{2-}, NO_3^-, Cl^-
		6	Pb, Ni	5	*Pb, Ni
Phase II	8/9 - 9/1	10	SO_4^{2-}, NO_3^-, Cl^-	0	
		10	Pb, Ni		
		10	Na, Cr, Co, Sb		
Phase III	9/11 - 9/27	7	SO_4^{2-}, NO_3^-, Cl^-	7	SO_4^{2-}, NO_3^-, Cl^-
		7	Pb, Ni	7	Ni

* number of Pb samples in phase I at Corvallis is 2

Table 2.2 lists the sampling schedule for total particle collection. The principal objective of total particle collection was to estimate the influence of sea-sprays and soils. This estimation was performed by the measurement of the Na and Fe content in the samples. SO_4^{2-}, NO_3^-, and Cl^- concentrations of total aerosol (i.e., sampling with no size selection) were measured in selected samples for comparison with the concentrations obtained from fine particle samples.

Table 2.2. Sampling schedule for total particle collection (all sizes).

		Yaquina Head (background)		Corvallis (rural)	
	Duration	No. of samples	Analyzed compounds	No. of samples	Analyzed compounds
Phase I	7/22 - 8/7	3	SO_4^{2-}, NO_3^-, Cl^-	3	SO_4^{2-}, NO_3^-, Cl^-
				7	Na^+, Fe^{3+}
Phase II	8/9 - 9/1	8	Na^+, Fe^{3+}	6	SO_4^{2-}, NO_3^-, Cl^-
				6	Na^+, Fe^{3+}
Phase III	9/11 - 9/27	2	SO_4^{2-}, NO_3^-, Cl^-	6	Na^+, Fe^{3+}
		7	Na^+, Fe^{3+}		

2.1.8 Sampling for Experiment Uncertainty

Prior to phase I, a few aerosol samples were collected to estimate experiment uncertainties. A total of nine pairs of total-particle samples were collected at the Corvallis site. Four pairs were analyzed with ion chromatography for sulfate, nitrate and chloride concentrations, and the remaining five pairs were analyzed for sodium concentrations with flame atomic absorption spectroscopy.

To evaluate the extraction efficiency of the ultrasonic bath, four pairs of simultaneous samples were collected side-by-side at the Corvallis site by using openface filter holders. In each pair, one of the filters was extracted (procedure see Section 2.2.1) and analyzed by flame atomic absorption

spectroscopy for Na concentration, another filter was directly analyzed by instrumental neutron activation analysis (INAA) for same element (Na).

2.2 Chemical Analysis

A number of different chemical analysis techniques were employed for the present study. Concentrations of SO_4^{2-}, NO_3^- and Cl^- were determined by ion chromatography analysis (IC) in the Soil Science Department, Oregon State University (OSU). Concentrations of sodium (Na) and iron (Fe) were determined from flame atomic absorption spectroscopy (FAAS) conducted by Lih-Jong Ko at the Department of Chemistry in OSU. Concentrations of nickel (Ni) and lead (Pb) were determined from graphite furnace atomic absorption spectroscopy (GFAAS) at the College of Oceanography, OSU. Concentrations of sodium (Na), chromium (Cr), cobalt (Co) and antimony (Sb) were determined by instrumental neutron activation analysis (INAA) at the OSU Radiation Center. For each procedure, several unused filters were sent laboratory analysis in order to establish "blank" filter concentrations. The blank filter measurements also were necessary to determine the detection limits of the experimental procedure.

2.2.1 Sample Preparation

All of the samples, with the exception of those collected for INAA, were extracted with water prior to chemical analysis. The extraction procedures are summarized in Fig. 2.6. The water used for sample preparation was first distilled and then passed through a Millipore water deionizing system to produce deionized, distilled water with a conductance of less than 0.1 $\mu\Omega^{-1}cm^{-1}$ (Millipore water). The hydrophobic Teflon filters were first

treated with 0.5 ml methanol (99%, analytical reagent grade) to make them wettable, then placed in an acid-washed test tube with 7 to 10 ml of Millipore water. This test tube was then placed in an ultrasonic bath and shaken for 30 min to extract the particles from the filter. Two identical aliquots, approximately 1 ml each, were acidified with 20 µl HNO_3 (16N ULTREX[1]) for GFAAS. The remainder of this sample (5 ml) was transferred to a clean test tube for IC analysis. The extracts from the large filters (47 mm diameter) were transferred to acid washed tubes and acidified with 20 µl HNO_3 (16N ULTREX) for the FAAS. All aqueous sample extracts were stored in a refrigerator until chemical analysis.

The aerosol filters collected for INAA were not extracted, but were placed in polyethylene vials provided by the OSU Radiation Center. The sample vials were stored at room temperature and subsequently delivered to Radiation Center for INAA.

[1] ULTREX is a registered trademark of J. T. Baker Inc.

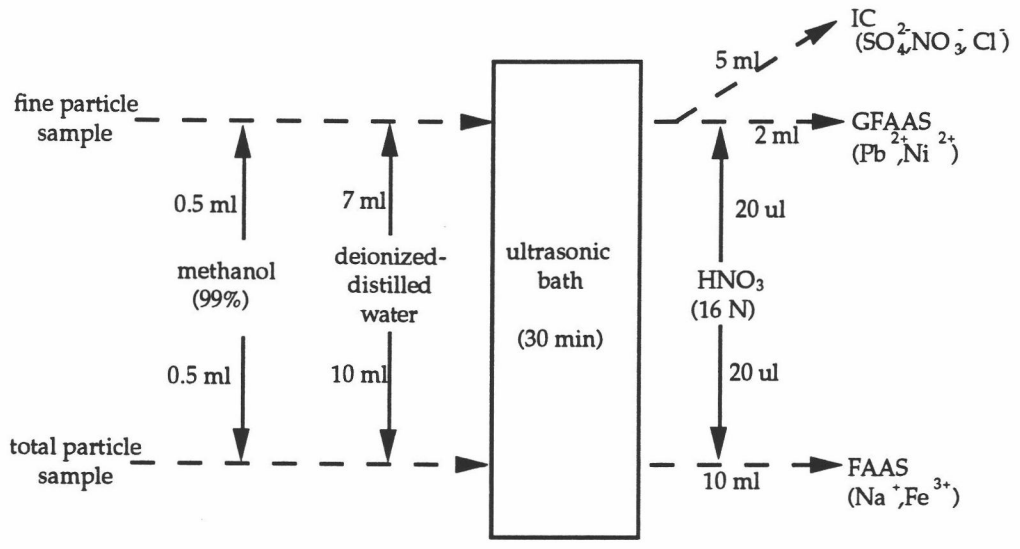

IC: Ion chromatography
FAAS: Flame atomic absorption spectroscopy
GFAAS: Graphite furnace atomic absorption spectroscopy

FIG. 2.6. Flow chart for sample extraction.

2.2.2 Flame Atomic Absorption Spectroscopy

Absorbances for the aerosol filter aqueous extracts were measured with a Buck model 200 atomic absorption spectrophotometer using air/acetylene burner and Varian Techtron Na and Fe hollow cathode lamps as light sources. Stock solution of 1000 μg/ml Na were prepared by dissolving 2.543 g NaCl in water, followed by dilution to 1 liter. A 1000 μg/ml Fe stock solution was obtained from Mr. Dean Johnson, laboratory coordinator at the Chemistry Department, OSU. That solution was prepared by dissolving 1 g of iron wire in aqueous HCl (6N), which was then diluted to 1 liter with water. A general agreement was obtained when the Na and Fe stock solutions were compared with an independent set of calibration standards provided by

college of Oceanography, OSU. Calibration standards were freshly prepared by dilution of the stock solutions. Instrumental operation conditions and the concentration calibration standards for each element are given in Table 2.3.

Table 2.3. Instrumental operation conditions and standard concentrations for flame atomic absorption spectroscopy.

Metal ion	Flame	Lamp current (mA)	Wavelength (nm)	concentration of standards (μg/ml)
Na	Air-C_2H_2	3.0	589.6	0.05, 0.5, 1.0, 1.5, 2.0
Fe	Air-C_2H_2	5.0	248.3	0.05, 0.2, 0.5, 0.7, 1.0

2.2.3 Graphite Furnace Atomic Absorption Spectroscopy

Lead and nickel absorbances were obtained by graphite furnace atomic absorption spectroscopy (GFAAS), performed by a trained technician at the College of Oceanography at OSU . A Perkin-Elmer Zeeman 5000 atomic absorption spectrometer, equipped with a HGA-500 graphite furnace, and an AS-40 autosampler were used for the analysis. Instrumental settings, control programs, and concentration calibration standards for the GFAAS are listed in Tables 2.4 and 2.5.

Table 2.4. Instrumental settings, control program sequence, and concentration of calibration standards* for nickel determination

Purge gas: Argon	Wave length: 232.0 nm
Furnace: graphite tube with L'vov platform	Slit: 0.2 nm
	Lamp: Hollow cathode lamp
Sample volume: 30 µl	Lamp current: 25 mA

*Concentration of calibration standards (ng/ml): 0, 10, 20, 30

Control Program

step	1	2	3	4	5	6
temperature (°C)	130	150	1000	2300	2700	20
ramp (sec)	10	10	10	0	1	1
hold (sec)	0	15	15	4	4	10
recorder				X*	X	
read				X		
int flow (ml/min)				30		

* X means turned on the recorder or the printer

Table 2.5. Instrumental setting, control program sequence, and concentration calibration standards* for lead determination.

Purge gas: Argon	Wave length: 283.3 nm
Furnace: graphite tube with L'vov platform	Slit: 0.7 nm
	Lamp: Electrodeless discharge lamp
Sample volume: 10 µl	Lamp power: 10W

*Concentration of calibration standards (ng/ml): 0, 8, 16, 24

Control Program

step	1	2	3	4	5	6
temperature (°C)	120	140	500	1600	2500	20
ramp (sec)	1	15	15	0	1	1
hold (sec)	0	10	10	4	4	5
recorder				X	X	
read				X		
int flow (ml/min)				30		

2.2.4 Ion Chromatography

Sulfate, nitrate, and chloride concentrations were determined by ion chromatography in the Department of Soil Sciences, OSU. All chromatograms were completed by a trained technician using a Dionex model 2000i with a NGI guard column, an AG4A precolumn, an AS4A separator column, and an anion micromembrane suppressor. The system was controlled by an IBM computer with AI-400 software. A Na_2CO_3(1.8mM)/ $NaHCO_3$(1.7mM) eluant was pumped through columns at a flow rate of 2 ml/min. A 25 mN H_2SO_4 regenerant was used to suppress the background signals. A few methane sulfonic acid (MSA) concentrations were determined via ion chromatography by a second trained technician employed by NOAA-Sand Point, Washington. The MSA analyses were performed using a similar system but with an AS-4 separator column and a weaker eluant.

2.2.5 Instrumental Neutron Activation Analysis

The ten fine particle samples which were collected at the background site were delivered to the OSU Radiation Center for instrumental neutron activation analysis (INAA). The sample vials were heat-sealed, then irradiated in the OSU TRIGA reactor for six hours at 1MW. The irradiation time was limited since the samples became increasingly fragile as irradiation time increased. Following the irradiation process, the filters were transferred to non-radiation-contaminated polyethylene vials and counted three times, using an intrinsic high purity Ge γ-ray detector coupled to a 80K-Adcam multi-channel analyzer. The final count was at least 30,000 seconds for each sample.

3. METHODOLOGY OF DATA ANALYSIS

3.1 Analysis of Variance

An analysis of variance (ANOVA) procedure was used to separate variations in observed atmospheric aerosol composition into two basic components: variation due to assignable causes and the uncontrolled or random variation. Assignable causes include known or suspected sources of variation from variates that were either controlled or measured during the conduct of the experiment. Random variations include the effects of all other sources, which were neither controlled nor measured during the experiments.

In this study, an ANOVA procedure was used to separate variation from time-dependent factors (e.g., weather conditions or emission sources) from measurement errors (e.g., random instrumental response errors in chemical analysis and the variation associated with the sampling apparatus), thus providing an estimate of the experimental uncertainties. If the time-dependant variations were substantially greater than measurement errors, then the experiment is capable of recognizing the data variation from the alteration of controlled variable; if not, the experiment has failed to recognize the variation of interest because the measurement error has a significant effect upon the results.

3.2 Treatment of Sulfate Concentration

As considered in Chapter one, since the major contributors to particulate sulfate concentrations in a coastal region could be seasalt, DMS oxidation, or

anthropogenic emissions, procedural steps were taken to distinguish sulfate contributions from different source types.

Based on a SO_4^{2-}/Cl^- mass ratio of 0.14 in seasalt (Holland, 1978), excess sulfate (SO_4^{2-}ex) concentrations were calculated as

$$[SO_4^{2-}ex] = [SO_4^{2-}] - 0.14\,[Cl^-]\,, \qquad (3)$$

where [ ]: concentration ($\mu g/m^3$). If all Cl^- is seasalt derived then the excess sulfate calculation describes sulfate that is related to sources other than seasalt (Vong, 1990).

To estimate the contribution from DMS oxidation, methane sulfonic acid (MSA) concentrations of 13 fine particle sample extracts were analyzed in this study (see Section 1.0).

3.3 Separation of Fine and Coarse Fractions

Since the behavior of fine and coarse particles is different (see Section 1.2 and 1.3), it was necessary to separate the total particles into two different fractions. For the present study, a number of species were analyzed from both fine and total particle filter samples collected at each sampling site. The concentrations of chemical species in the coarse particle samples were calculated as the difference between total and fine particle concentrations. Given differences in the generation processes for both types of particles (see Sections 1.2 and 1.3), the relative percentages of fine and coarse fraction aerosols were calculated to assess relative contribution from different processes.

3.4 Temporal Variation Among Species

Analysis of the temporal changes in mass concentrations for each species is a useful tool for understanding particle behavior. Species which have similar time variation at a site may have been derived from the same or similar sources or, alternatively, may have been generated by sources at the same location. Similarities in temporal behavior also are the likely result when particle chemical concentrations are controlled by similar processes of transport and dispersion, or similar reactions (i.e, sharing a common participant reactant) for chemical transformation.

3.5 Enrichment Factor Analysis

Enrichment factors (EF) were calculated as

$$EF = (X/R)_{aerosol}/(X/R)_{crust\ or\ seasalt} \qquad (4)$$

where X and R represent, respectively, concentrations of elements X and R. If the reference element (R) is considered to be unique to a source (e.g., the ocean or crustal material), then the ratio of element X to reference element R in ambient aerosol relative to the same ratio in pure crustal or seasalt material is a measure of the source contribution to element X that is not related to the source of element R. From equation (4), if the EF is close to the value of one, then it is implied that element X is also from the specified source (e.g., oceanic or crustal material); if the EF is large, then the element X is from an alternative source to the specified source; and if the EF is less than

one, then either the source of the reference element is not unique or a part of element X has been transformed (e.g., volatilization of aerosol Cl^-) and is not detectable.

Among the elements measured for the present investigation, Fe is generally considered to be unique to crustal material, whereas Na^+ and Cl^- are considered as seasalt tracers. The average compositions of crustal material and sea water were obtained, respectively, from Taylor (1964) and from Holland (1978) The EF relative to seasalt can be calculated from the use of sodium or chloride as the reference element, whereas the EF relative to crustal materials can be calculated from the use of Fe or Al (not measured in this study) as the reference element. For EF calculation with approach the value of one, additional species from either seasalt or crustal material can be identified.

3.6 Principal Component Analysis

Principal component analysis (PCA) is a multivariate method of analysis appropriate for the characterization of complex data sets. PCA has frequently been applied to aerosol data (Adams *et al.*, 1983; Vong, 1985; Cohen *et al.*, 1991). PCA provides a method of writing a matrix (X) of rank r as a sum of r matrices of rank one (M), thus:

$$X = M_1 + M_2 + ... + M_r, \quad (5)$$

These rank one matrices can then be written as products of a column matrix (t_h) and a row matrix (p_h'[1]) or the equivalent of X = TP' as

$$X = t_1p_1' + t_1p_1' + ... + t_rp_r' = T\,P' , \qquad (6)$$

where t is referred to as the score vector and p' is the loading vector.

For atmospheric chemistry applications, the PCA input data are derived from a matrix in which each column represents the measured species (i.e., the variable) and each row represents a sample (in this study, this represents temporal variation). In theory, a few orthogonal components (i.e., less than number of variables), which are the linear combinations of the original variables, can be sorted to provide (hopefully) an explanation of the variance in the original data. The extracted components can be alternatively interpreted as emission source categories from within the study area, particle transport mechanisms, or reactions which generate certain particle species. The data matrix is decomposed as

$$X = TP' + E = \sum_{h=1}^{a} t_h p_h' + E , \qquad (7)$$

where X: data matrix,

T: score matrix,

P': loading matrix,

E: residual variance matrix,

t: score vector,

p': loading vector, and

a: number of components.

---

[1] p' is the transpose of vector p

The sample scores for each component (t_h) represent temporal variation in source categories and/or changes of meteorological conditions which control the transport or transformation of particles. The variable loadings for each component (p_h') represent the correlation coefficients between the original variables and the components. Thus, the closer the loading is to one or negative one, the stronger is the relationship between the variable and the component.

In the NIPALS PCA algorithm used here, the principle components are not all calculated at once. The algorithm calculates t_1 and p_1' from X matrix, then the product of t_1p_1' is subtracted from X and the residual E_1 is calculated. The vectors t_2 and p_2' are calculated from E_1 :

$$E_1 = X - t_1p_1', \quad E_2 = E_1 - t_2p_2', \ldots\ldots \tag{8}$$

Prior to calculation of the principal components, the frequency distributions for each variable should be nearly normal; this allows each sample to participate within the model. If the variables were not normally distributed, appropriate transformations should be performed to assure a normal data distribution. The methodology of data transformation is discussed by Box *et al.* (1978).

In the application of PCA to atmospheric chemistry data, it has been observed that meteorological conditions may strongly influence the data, thus resulting in a PCA model which cannot be used to describe factors other than covariance due to meteorology (Hansson *et al.*, 1984). To reduce this problem, a normalization procedure that involves the division of individual variables by the total particle mass in the same size fraction has been suggested

(Hansson *et al.*, 1984); if the particle mass is dependent upon meteorological conditions, then its use as a normalizing factor should reduce meteorological covariance, thus allowing the PCA model has the opportunity to resolve emission source influences.

Since particle mass determination does not constitute a method as reliable as measured chemical concentrations (Section 2.1.6) in this study, another normalization developed by Hansson *et al.* (1984) was also applied to the data set for the present investigation for comparison. In this alternative normalization method, each individual sample value was divided by the average of the same variable over all sampling periods, then divided by a scaling value (see Step 2, below) for each sample. These two steps are illustrated in Figures 3.1 and 3.2 for, respectively, equations (9) and (10):

Step 1: Divide by the average for the same variable over all sampling periods

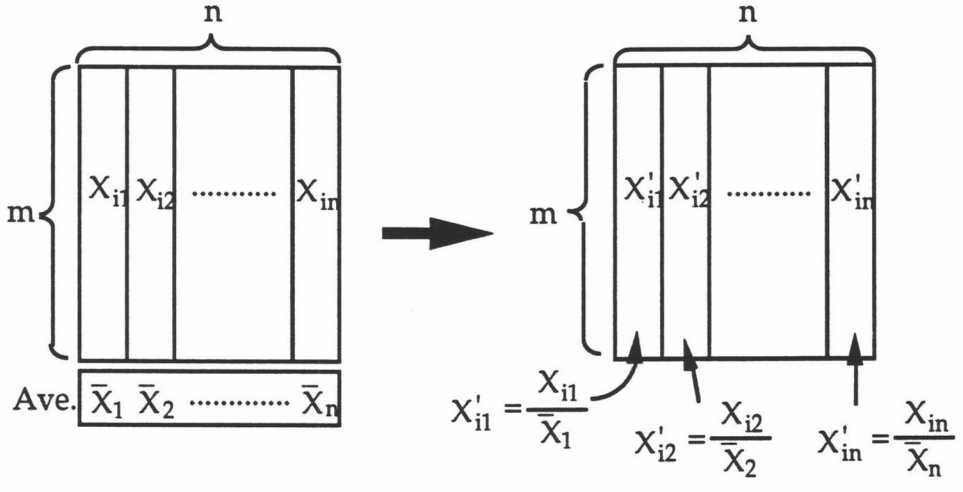

FIG. 3.1 Simple scheme of the procedures used to normalize data for principal component analysis (Step one).

for $$X'_{ij} = \frac{X_{ij}}{\frac{1}{m}\sum_{i=1}^{m} X_{ij}} \quad (9)$$

where X_{ij}=the value for j variable in i sample,

X'_{ij}= data value relative to its mean over all samples,

m=total number of samples, and

n= total number of variables.

Step 2: Divide by a scaling value (sample strength)

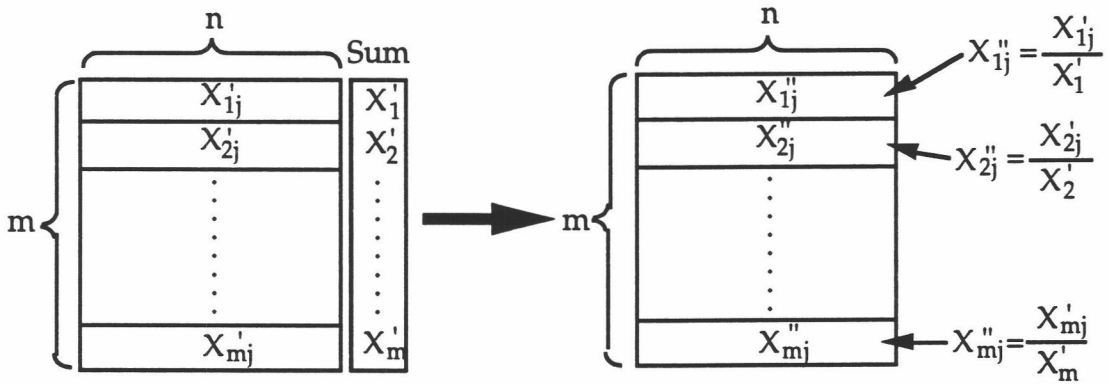

FIG. 3.2 Simple scheme of the procedures used to normalize data for principal component analysis (Step two).

for $$X''_{ij} = \frac{X'_{ij}}{\sum_{j=1}^{n} X'_{ij}} \quad (10)$$

where X''_{ij} is the input value for the PCA model.

The summation of X'_{ij} is the sample strength, representing the overall relative concentration level for each sample. As an alternative to the normalization procedure just described, sample strength can be requested by the measured aerosol gravimetric mass concentration.

3.7 Partial-Least-Square Regression Model

The partial-least-square (PLS) multivariate regression model uses orthogonal components extracted from one data matrix to predict components extracted from a second matrix. To calculate the regression equation, the PLS model calculates components for each of the two matrices, a predictor block (X), and a response block (Y) for extracting variances common to both. The relations of the X block (terminology is analogous to that used for PCA, above) are:

$$X = TP' + E = \sum_{h=1}^{a} t_h p_h' + E \tag{11}$$

and those for the Y block are:

$$Y = UQ' + F = \sum_{h=1}^{a} u_h q_h' + F \tag{12}$$

where X, Y= data matrices,

T, U= score matrices,

t, u= score vectors (column vectors),

P', Q'= loading matrices,

p', q'= loading vectors (row vectors),

E, F= residual matrices, and

a= number of components.

The relations between the X- and Y-block are:

$$u_h = b_h t_h \tag{13}$$

where b is the regression coefficient for each component. To describe Y as completely as possible, $\| F \|$ should be minimized.

The relationships between the components for the X- and Y-matrices can be weak if the components for each matrix are calculated separately (Geladi and Kowalski, 1986) as is done in particle component regression. In the PLS model, the components are calculated by exchanging scores (send information) between X and Y. The scores exchange method is described by Geladi and Kowalski (1986) in detail. With this algorithm, the components in effect are rotated slightly to improve regression model fit to both matrices (i.e., X and Y); PLS provides results which are to be preferred to the separate calculation of the components (Geladi and Kowalski, 1986).

Similar to the PCA, the loading of each variable in the two blocks of the PLS model represents the correlation between variable and the extracted components. Variables with high loadings (i.e., approaching one or negative one) for the same component are said to be correlated. Thus, the relationships among variables within two blocks can be identified.

After component calculation, the prediction model can be developed as

$$Y = BTQ' + F \tag{14}$$

where B= column matrix of regression coefficients (b in equation 13).

3.8 Meteorological Data Processing

Since the aerosol samples are time-integrated data (that is, taken over a period of from two to three days) and the meteorological observations are continuous, the meteorological data have to be processed over appropriate time intervals before data analysis.

3.8.1 Surface Wind Speed and Direction

Local wind speed and wind direction are available for both sampling locations. For Corvallis, continuous data are available 24 hours per day at the Corvallis Airport. For Yaquina Head, continuous data is available 12 hours per day (daytime hours) at Newport.

During the experimental period, the surface winds at both sampling sites display nearly the same pattern. In the Newport area, the wind direction was usually between 360° and 240° (northwesterly). In the Corvallis area, a diurnal pattern with wind direction between 270° and 40° (northerly) during the day and calm winds (0 - 1.8 m/sec) usually existed during the night. In the data processing procedure, the wind direction for each sample period was recognized as either prevailing , in accordance with the general conditions described above, or non-prevailing (that is, any other condition). Wind speed was stratified as high, (greater than 5.3 m/s), medium (between 5.3 m/s and 3.5 m/s), or low (less than 3.5 m/s).

3.8.2 Sounding Data

Vertical temperature "sounding" data were collected at Salem, Oregon for 5:00 a.m. and 5:00 p.m. (local time) daily by the National Weather Service. These data include vertical profile of temperature, pressure, humidity, wind

speed, and wind direction. Atmospheric static stability can be determined by reference to the vertical profile of temperature. A temperature increase with height (or pressure decrease) is called temperature inversion. The existence of atmospheric inversions below 1200 m are recognized as conditions which suppress vertical mixing ("stable"), and any other condition is regarded more favorable for mixing (generally "unstable"). During the aerosol experiments, the sounding data usually followed a diurnal pattern with unstable conditions in the afternoon and stable conditions in the early morning.

The sounding data were transformed to a code representing static stability for each sampling period. In this procedure, the expected diurnal pattern of stability (i.e., unstable in the afternoon and stable in the early morning) was coded as zero. Alternatively, the daytime (afternoon) stable conditions were coded as one and nighttime (early morning) unstable conditions were coded as negative one. The stability code for each two-to three-day sampling period was the sum of the defined numbers of the sounding data within that sampling period. The range for this "stability code" in one sampling period was thus between six and negative six, where the larger stability codes represented a stable atmosphere within the sampling period.

3.8.3 Back Trajectories

To help characterize likely sources of the collected aerosol, back trajectories were calculated to identify the general location of the origin of the collected air (Öblad and Selin, 1986; Daum *et al.*, 1989). In this study, back trajectories were used to recognize the difference between marine and continental air masses.

For the aerosol sampling periods, 48-hour back-trajectories were calculated at 6-hour intervals from a computer code developed at the Department of Atmospheric Sciences, University of Washington, Seattle. These trajectories are based on a 6-hour interval, nested grid model (NGM) from wind velocity fields from the National Meteorological Center (NMC) in Washington, DC. The fields for 00Z and 12Z (i.e., Greenwich time= Z) were based on data, while the 06Z and 18Z fields were 6-hour forecasts. The NGM grided data was for the area 1.25 degree latitude by 2.5 degree longitude. The trajectories were calculated by numerical integration of the velocity backward at 30 min time steps intervals while the velocities for each 30-min period that was between 6-hour NGM velocity fields were determined by interpolating both temporally and spatially to desired space or time point with NGM data. The procedures for calculation of back trajectories with interpolated velocities are summarized in the following two steps:

Step 1: $$x1_{t+dt} = x_t + u(X_t, Y_t)\,dt \qquad (15)$$

$$y1_{t+dt} = y_t + v(X_t, Y_t)\,dt$$

$$p1_{t+dt} = p_t + \dot{p}\,(X_t, Y_t)\,dt$$

Step 2: $$x_{t+dt} = x_t + \frac{(u(x_t, y_t) + u(x1_{t+dt}, y1_{t+dt}))}{2}\,dt \qquad (16)$$

$$x_{t+dt} = y_t + \frac{(v(x_t, y_t) + v(x1_{t+dt}, y1_{t+dt}))}{2}\,dt$$

$$p_{t+dt} = p_t + \frac{(\dot{p}\,(x_t, y_t) + \dot{p}\,(x1_{t+dt}, y1_{t+dt}))}{2}\,dt$$

where: x, y,p = trajectory location,

x1, y1,p1 = the first estimation of trajectory location,

u, v = velocity in X and Y directions,

$\dot{p}$ = dp/dt,

t = time, and

dt = time step (= -30 min).

Back trajectories for two locations in Oregon State, Bay City (45.5N, 124W) and Cape Blanco (42.8N, 124.5W), were available every 12 hours during most of the period of this experiment. Back trajectories for Yaquina Head (44.7N, 124.1W) and (more crudely) Corvallis (44.6N, 123.3W) were estimated, based on the available data for the former two locations.

To simplify the trajectory data, the geographic areas that the trajectories passed through were divided into three regions, as shown in Fig. 3.3, where Region one was open ocean, Region two was continental area, and Region three was the coastal area, the contiguous zone of the continent and the ocean. Note that it is somewhat ambiguous to attempt to identify the

potential sources of collected aerosols when the air is travelling along this coastal area.

Within each two- to three-day sampling period, the back trajectories were further grouped into three classes as either marine, continental, or coastal (i.e., those with a potential for mixed marine and continental sources). Fig. 3.4-3.6 illustrate typical back trajectories for the three different classes. If a sample was classified as having "marine" trajectory, all trajectories within that period were observed to have originated from the ocean area prior to arrival at the observing station (Fig. 3.4); if a sample was classified as "continental", all trajectories within that period were assumed to have originated from continental areas prior to arrival at the observing station (Fig. 3.5); and if a sample was classified as "coastal", the air was observed to have traveled along the coast, as shown in Fig. 3.6, or both "marine" and "continental" trajectories were observed within that aerosol collection period.

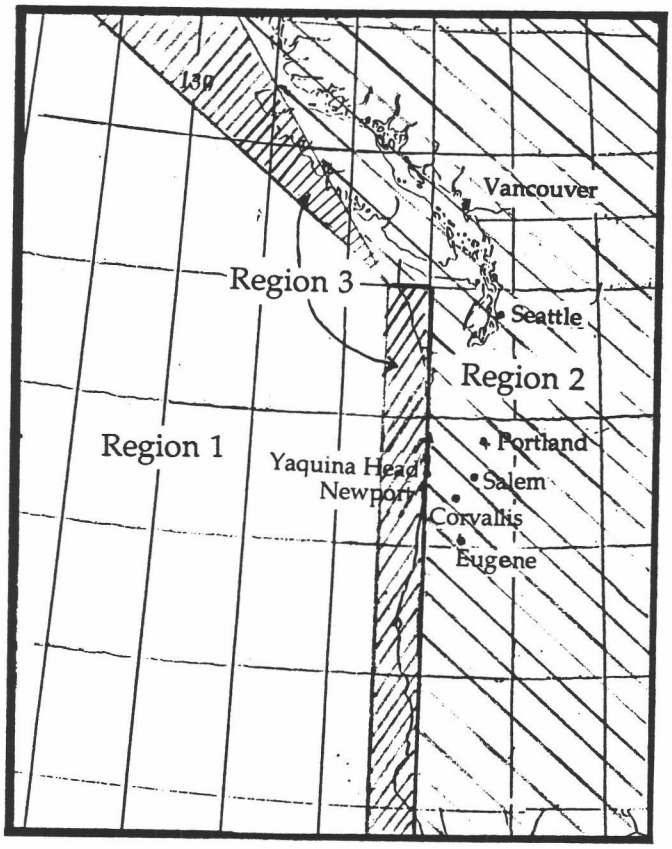

FIG. 3.3. Map of three regions for dividing the back trajectory data.

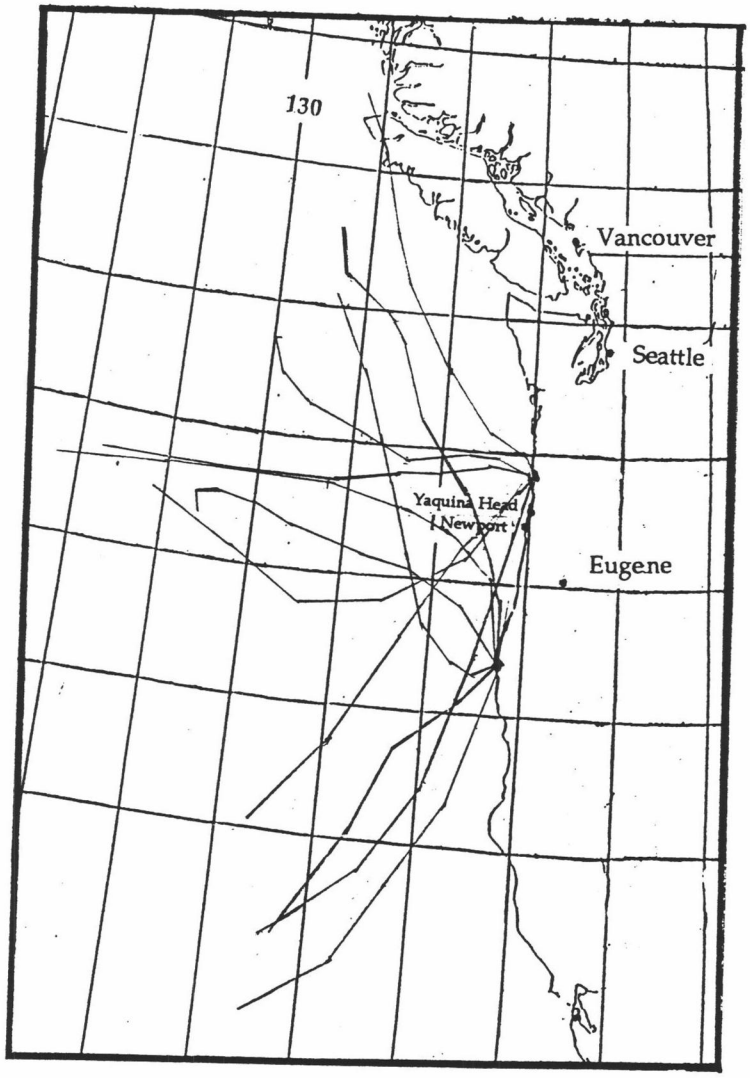

FIG. 3.4. Representative trajectories which were identified as marine trajectory (class "marine").

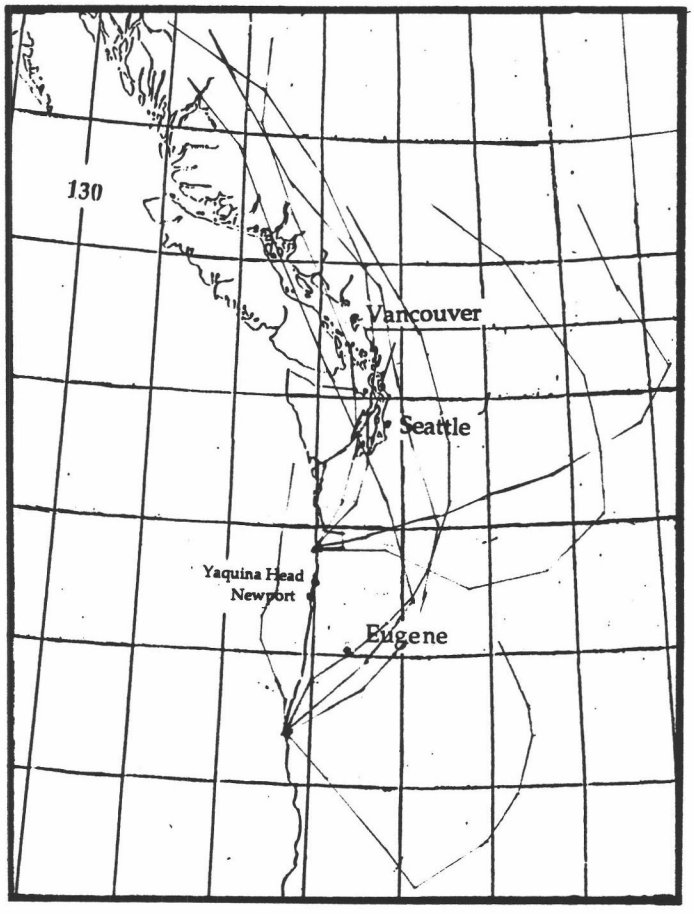

FIG. 3.5. Representative trajectories which were identified as continental trajectory (class "continental").

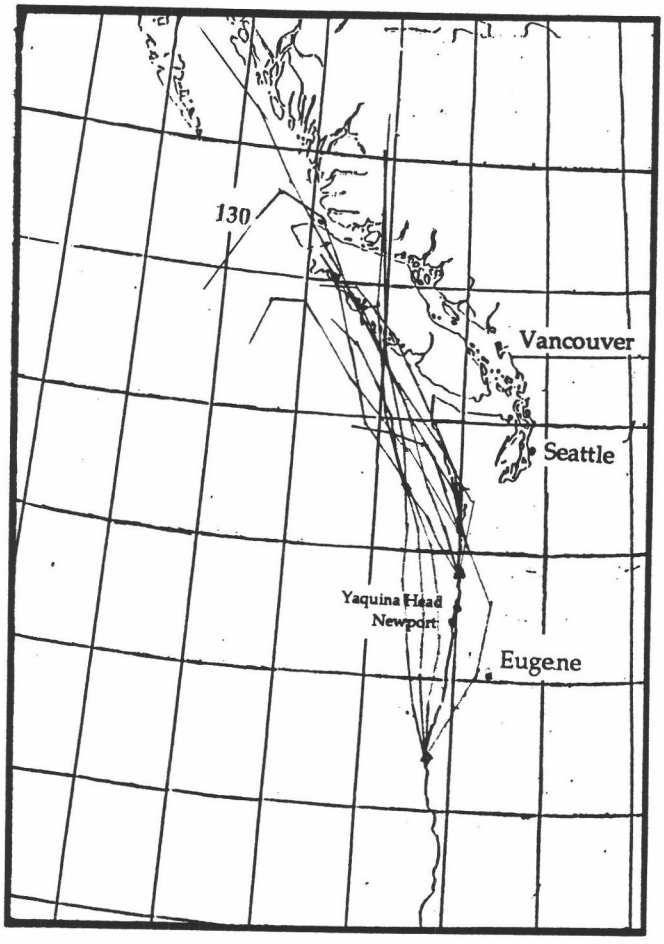

FIG. 3.6. Representative trajectories which cannot be identified as strictly marine or continental (class "coastal").

4. RESULTS

4.1 Experimental Uncertainty

Prior to phase one, nine pairs of total-particle samples were collected for the assessment of experimental uncertainties (see Section 2.1.8). For each paired particle sample, the difference in concentration levels should reflect the sum of the errors from instrument response for chemical analysis and any imprecision caused by the sampling apparatus (e.g. air volume measurements).

Analysis-of-variance (ANOVA) procedures were applied to the results of the nine pairs of samples to separate the concentration variations into two components: controlled and random variations. For this data set, controlled variation was caused by time-dependent factors and the random variations include measurement errors from application of the chemical analysis technique and the differences between the sampling apparatus. The ratio of controlled variations to random variations was calculated (F-value). The results of the ANOVA for SO_4^{2-}, Cl^-, NO_3^- and Na measurements are presented in Table 4.1. The "within pairs" mean square term represents the variance for that analyte due to all experimental procedures.

For these analyses, given that the P-values in the ANOVA tables represented the possibility of accepting, the null hypothesis (H_o) that, compared to random variations, the concentrations for each measured species would not be significantly different among sampling events. The results indicated that the possibility of accepting H_o were less than 1% for the Cl^-, NO_3^- and Na measurements, and less than 2% for the SO_4^{2-} measurement. Thus, the concentrations were significantly different ($P<0.02$) among

sampling events. This implied that the variations related to time-dependent factors (e.g., weather conditions) are significantly greater than the variance from other factors, such as chemical analysis, differences between sampling apparatus, or other sources of random error.

Table 4.1. ANOVA tables for Cl^-, NO_3^-, Na and SO_4^{2-} measurements, experimental uncertainty examination.

Analyte: Cl^-

Source of variances	Degrees of freedom	Sum of squares	Mean square	F-value	P-value
Between pairs	3	1.42	0.474	145	0.0002
Within pairs	4	0.013	0.003		
Total	7	1.43			

Analyte: NO_3^-

Source of variances	Degrees of freedom	Sum of squares	Mean square	F-value	P-value
Between pairs	3	4.56	1.52	1620	0.0001
Within pairs	4	0.004	0.001		
Total	7	4.56			

Analyte: Na

Source of variances	Degrees of freedom	Sum of squares	Mean square	F-value	P-value
Between pairs	4	0.202	0.051	361	0.0001
Within pairs	5	0.001	0.00014		
Total	9				

(continue Table 4.1)

Analyte: SO_4^{2-}

Source of variances	Degrees of freedom	Sum of squares	Mean square	F-value	P-value
Between pairs	3	0.14	0.047	12	0.0172
Within pairs	4	0.015	0.004		
Total	7	0.155			

For Pb and Ni measurements, six sample extracts each were analyzed twice via graphite furnace atomic absorption spectroscopy (GFAA) to assess the uncertainties related to chemical analysis alone. The results of the ANOVA are shown in Table 4.2. Since each sample extract was from a single filter, the difference between two analyses reflected random errors in the GFAA response. The results indicate that the samples collected for different times were significantly different ($p<0.01$). This indicated that the variations caused by time-dependent factors were the major cause of sample variations (assuming that the sampling errors were negligible).

Table 4.2. ANOVA tables for Pb and Ni measurements, experimental uncertainty examination.

Analyte: Pb

Source of variances	Degrees of freedom	Sum of squares	Mean squares	F-value	P-value
Between pairs	5	24.9	4.98	46.8	0.0001
Within pairs	6	0.639	0.11		
Total	11	25.5			

Analyte: Ni

Source of variances	Degrees of freedom	Sum of squares	Mean squares	F-value	P-value
Between pairs	5	13.03	2.6	54.8	0.0001
Within pairs	6	0.29	0.048		
Total	11	13.3			

To evaluate the reliable range of the concentrations for each species, the 75% confidence interval (C.I.) of any aerosol measurement (X) can be calculated as in equation (17) under the assumption that the measurement is normally distributed.

$$C.I. = X \pm Z_{75\%} * \sqrt{MSE} \qquad (17)$$

where X: the concentration for measured species,

C.I.: 75% confidence interval of concentrations for each species,

$Z_{75\%}$: Z value at 75 % confidence level (two tails, = 1.15), and

MSE: mean square within pairs variation in Table 4.1.

The reliable (taken here as the 75% confidence interval) range for Cl^-, NO_3^-, Na^+ and SO_4^{2-} concentrations are 0.06, 0.04, 0.01, 0.07 $\mu g/m^3$, respectively.

Four additional pairs of samples were collected at the Corvallis sampling site to estimate extraction efficiency of the ultrasonic bath (see Section 2.1.8). Fig. 4.1 shows the comparison of the Na concentrations obtained by INAA (no extraction) and FAA (water extraction). The concentrations measured by FAA were lower than by INAA, but these two techniques are highly correlated with each other ($r^2 = 0.95$).

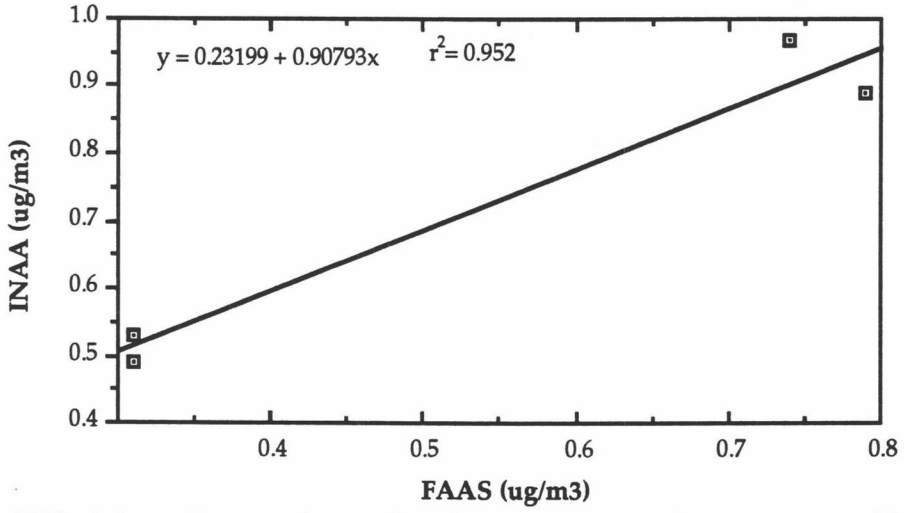

FIG. 4.1. Comparison of sodium concentrations measured by flame atomic absorption spectroscopy (FAAS) and instrumental neutron activation analysis (INAA).

4.2 Aerosol Chemical Composition

The measured chemical composition of individual aerosol samples collected at the Corvallis and Yaquina Head sampling sites is documented in Appendix A; the mean values of aerosol composition over the length of the experiment (i.e., 55 days, ca. eight weeks) are summarized in Table 4.3.

Concentrations listed in Table 4.3 and Appendix A have been corrected to remove the contribution from the blank filter. The composition of blank filters is listed in Appendix B. As described previously, the SO_4^{2-} concentrations were corrected for the contribution from seasalt; this corrected sulfate is referred to as "excess sulfate" (SO_4^{2-}ex) (see Section 3.2).

For the Yaquina Head site, 13 fine particle samples were sent to University of Washington, where the sample concentrations of methane sulfonic acid (MSA) were analyzed for use as a possible tracer of biogenic sulfur (see Section 1.0). In only three out of the 13 samples was MSA detected with measured concentrations of 0.55, 119.7 and 1.8 ng/m^3; MSA concentrations for the remainder of the samples were under detection limits.

Table 4.3. Composition of aerosols collected at Corvallis and Yaquina Head (ng/m^3).

	Yaquina Head		Corvallis	
	fine particles	coarse particles	fine particles	coarse particles
measurement	Mean (S.D.)		Mean (S.D.)	
Mass†	5.78(3.4)	28.5(16.2)	8.6(3.79)	24.4(16.2)
SO_4^{2-}	928(399)	1360(1090)	1150(418)	28(36)
SO_4^{2-}ex	817(382)	-155(422)	1140(418)	15(31)
NO_3^-	200(186)	540(268)	230(129)	336(121)
Cl^-	739(744)	10800(8270)	87(57)	89(102)
Pb	0.492(0.405)	N/A**	0.645(0.15)	N/A
Ni	0.181(0.154)	N/A	0.196(0.145)	N/A
Na	377(295)	3800(3110)	N/A	482(325)††
Fe	N/A	31(33)	N/A	103(36)††
Cr	0.118(0.104)	N/A	N/A	N/A
Co	0.064(0.044)	N/A	N/A	N/A
Sb	0.049(0.069)	N/A	N/A	N/A

† $\mu g/m^3$

†† concentration in total particles (fine particle concentration unavailable for determination of the coarse fraction).

** N/A: not available (no measurement).

4.3 Percentage of Coarse and Fine Particles

Fig. 4.2a-d shows the relative fractions in the fine and coarse size mode for five chemical species and gravimetric mass. From Fig. 4.2a, the percentage of total particle mass in each mode at the Corvallis site was similar to that for the Yaquina Head site. From Fig. 4.2b, the majority of seasalt-derived elements (Na and Cl) were found in the coarse mode at the Yaquina Head site, whereas a larger fine/coarse ratio of Cl existed at the Corvallis site than at the Yaquina Head site. This implied that seasalt particles from the ocean, most of which were coarse particles, represent a weaker influence on total chloride concentration at the site 64 km from the ocean (Corvallis).

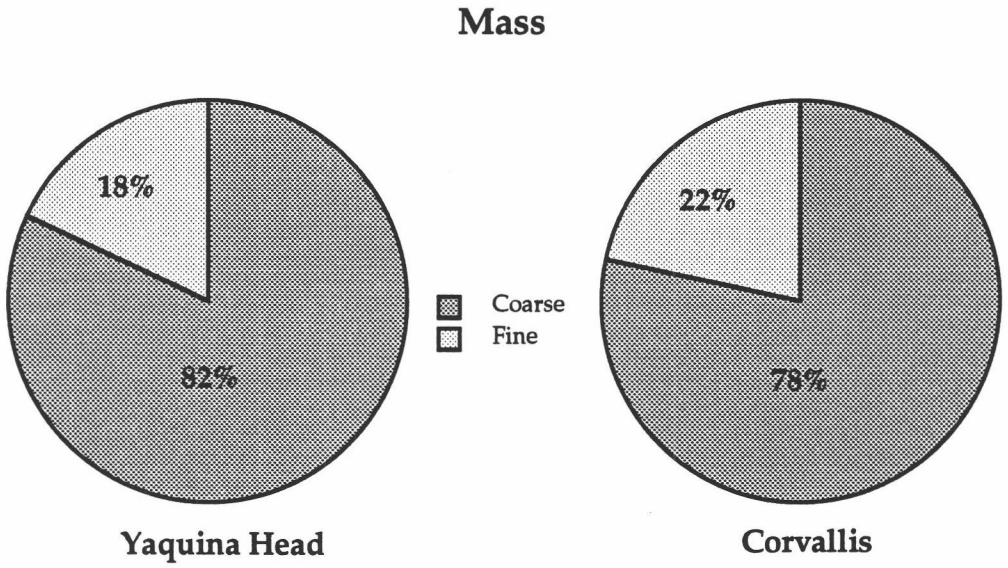

FIG. 4.2a. Relative fractions of particle mass in the fine and coarse modes at two sampling sites.

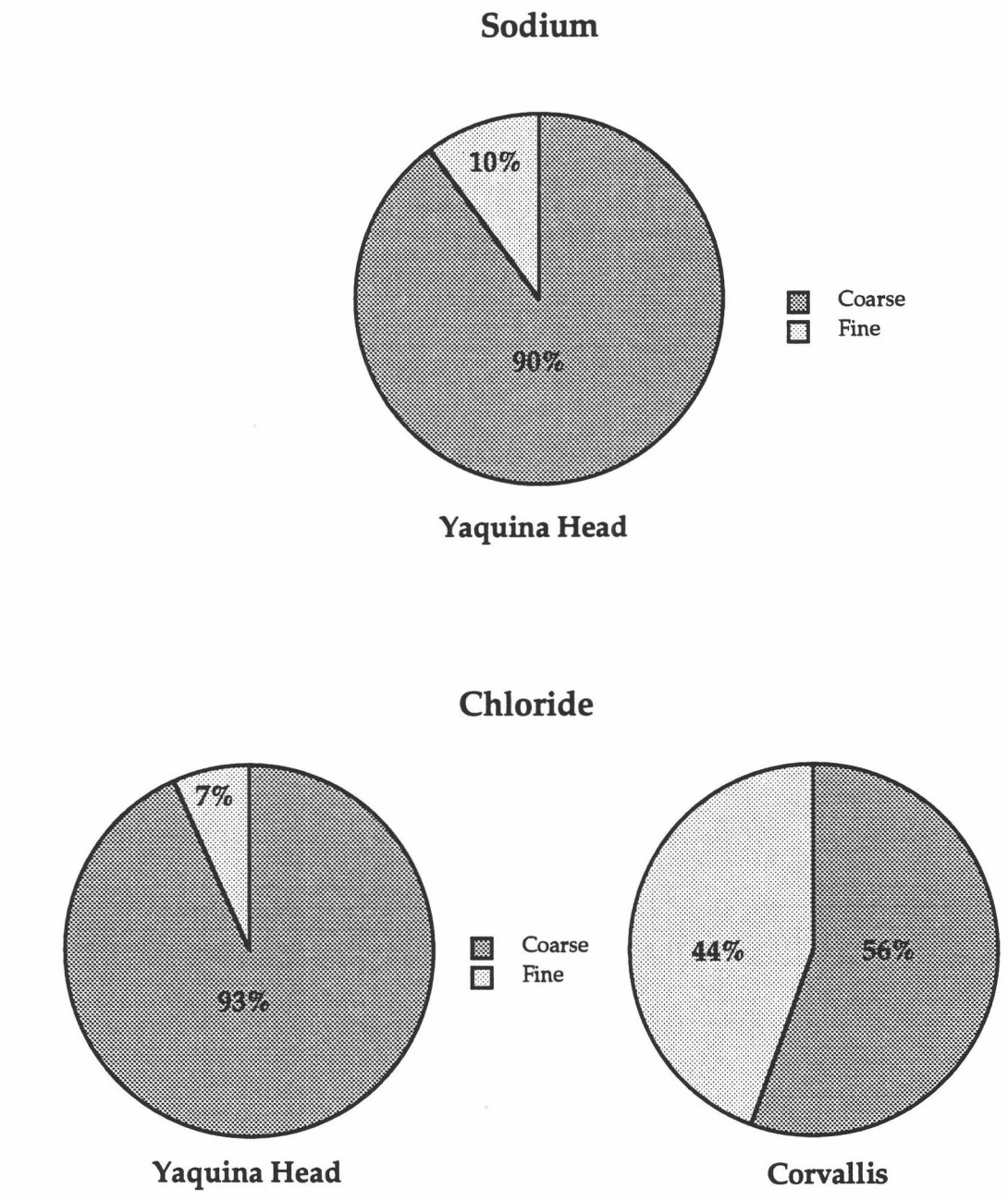

FIG. 4.2b. Relative fractions of sodium and chloride concentrations in the fine and coarse modes at two sampling sites.

The sulfate partitioning between fine and coarse size fractions was quite different for the two sampling sites (Fig. 4.2c). Only 3% of the sulfate at the Corvallis site was found in coarse particles; in contrast, more than half of the measured aerosol sulfate at the Yaquina Head site was found in the coarse mode. The coarse-SO_4^{2-} * at Yaquina Head probably was from seasalt (see Section 1.0). As shown in Fig. 4.2d, the nitrate partitioning was similar at the two sampling sites; the sum of coarse particles and nitric acid vapor held the larger fraction of nitrate at both sites. Since the majority of the atmospheric nitrate is in form of nitric acid vapor (Appel, 1981), the actual coarse particle nitrate was assumed to be less than the quantities shown in Fig. 4.2d.

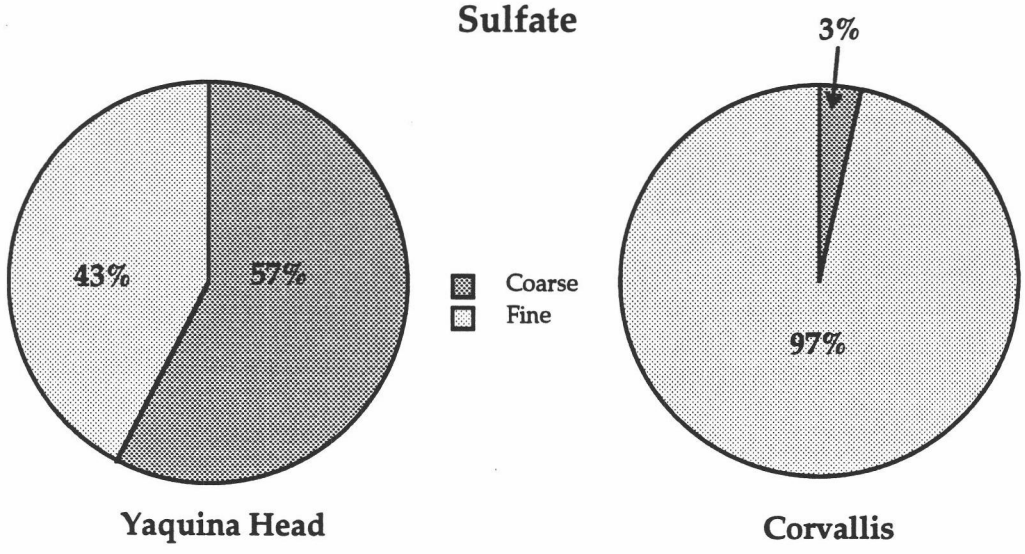

FIG. 4.2c. Relative fractions of sulfate in the fine and coarse modes at two sampling sites.

* coarse-"species name": the "species" in coarse particles.
fine-"species name": the "species" in fine particles.

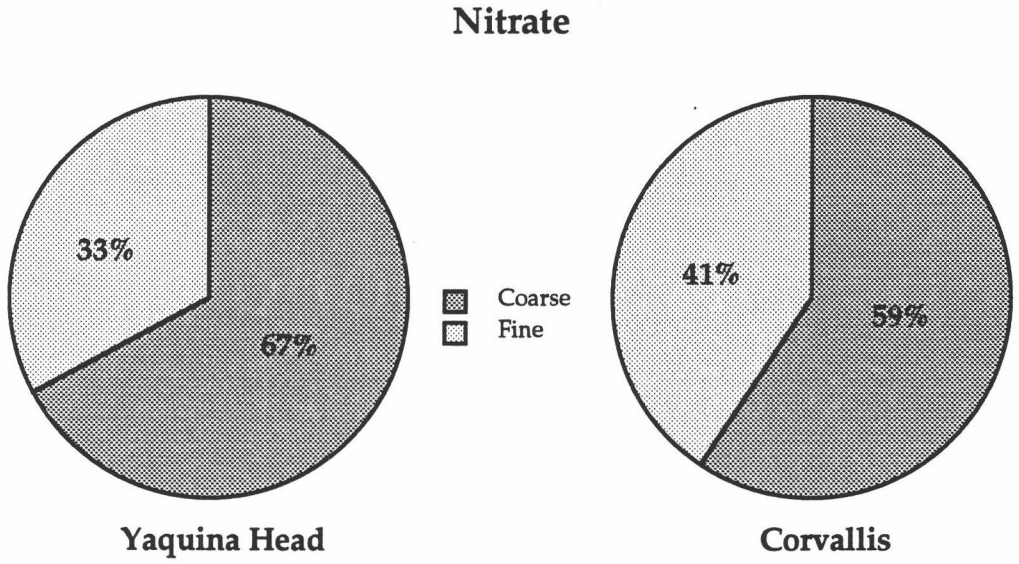

FIG. 4.2d. Relative fractions of nitrate in the fine and coarse (including vapor phase HNO_3) modes at two sampling sites.

4.4 Temporal Variation

The temporal variation in aerosol particle mass, Na concentration, and Cl^- concentrations at the Yaquina Head and Corvallis sites is shown in Figs. 4.3 and 4.4. Because the concentration levels for these measurements were quite different, some of the concentrations were multiplied by scaling factors to facilitate the comparison. From Fig. 4.3, it may be seen that the particle mass for the total and fine fractions was highly correlated (r=0.944) at the Yaquina Head site. Na and Cl for Yaquina Head also were highly correlated (from r=0.92 to r=0.86) and were also correlated with particle mass. These correlations indicate that both the sodium and the chloride at Yaquina Head were derived from a single source (seasalt). For the temporal variation at the Corvallis site (Fig. 4.4), the correlation of particle mass between the total and fine fractions was not nearly as strong as (r=0.18) at the correlations at Yaquina

Head. This indicated that the sources of aerosol particles in the fine and coarse fractions are probably different at the Corvallis site. Total-Cl and total-Na for Corvallis were highly correlated (r=0.96), but neither of these species were correlated with fine-Cl ($|r|<0.1$). This indicated that though the Corvallis site was located 64 Km from the ocean, the coarse-Cl and coarse-Na were still derived from seasalt; however, the fine-Cl probably was derived from sources other than seasalt.

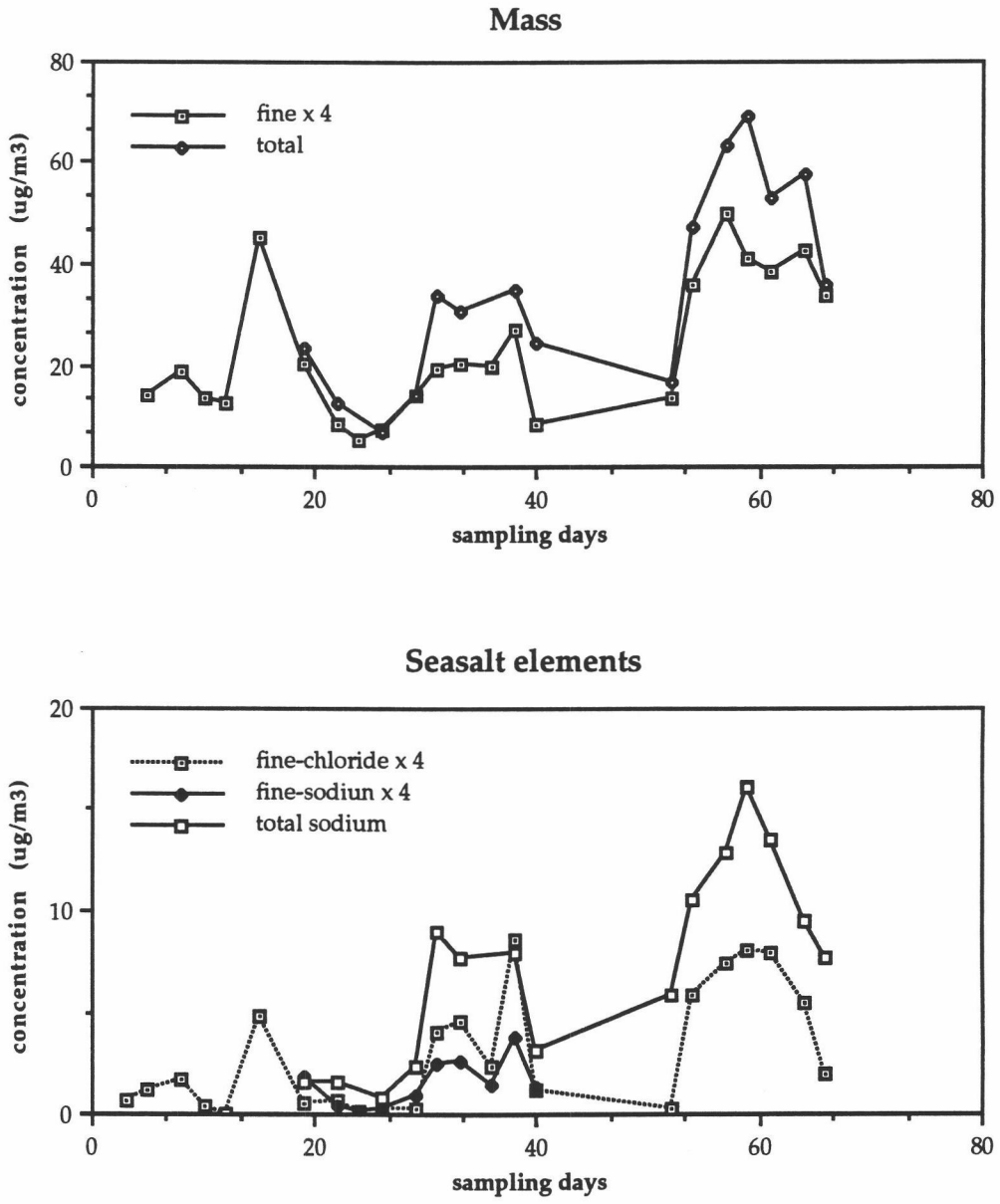

FIG. 4.3. Temporal variation for particle mass and seasalt element concentrations at Yaquina Head.

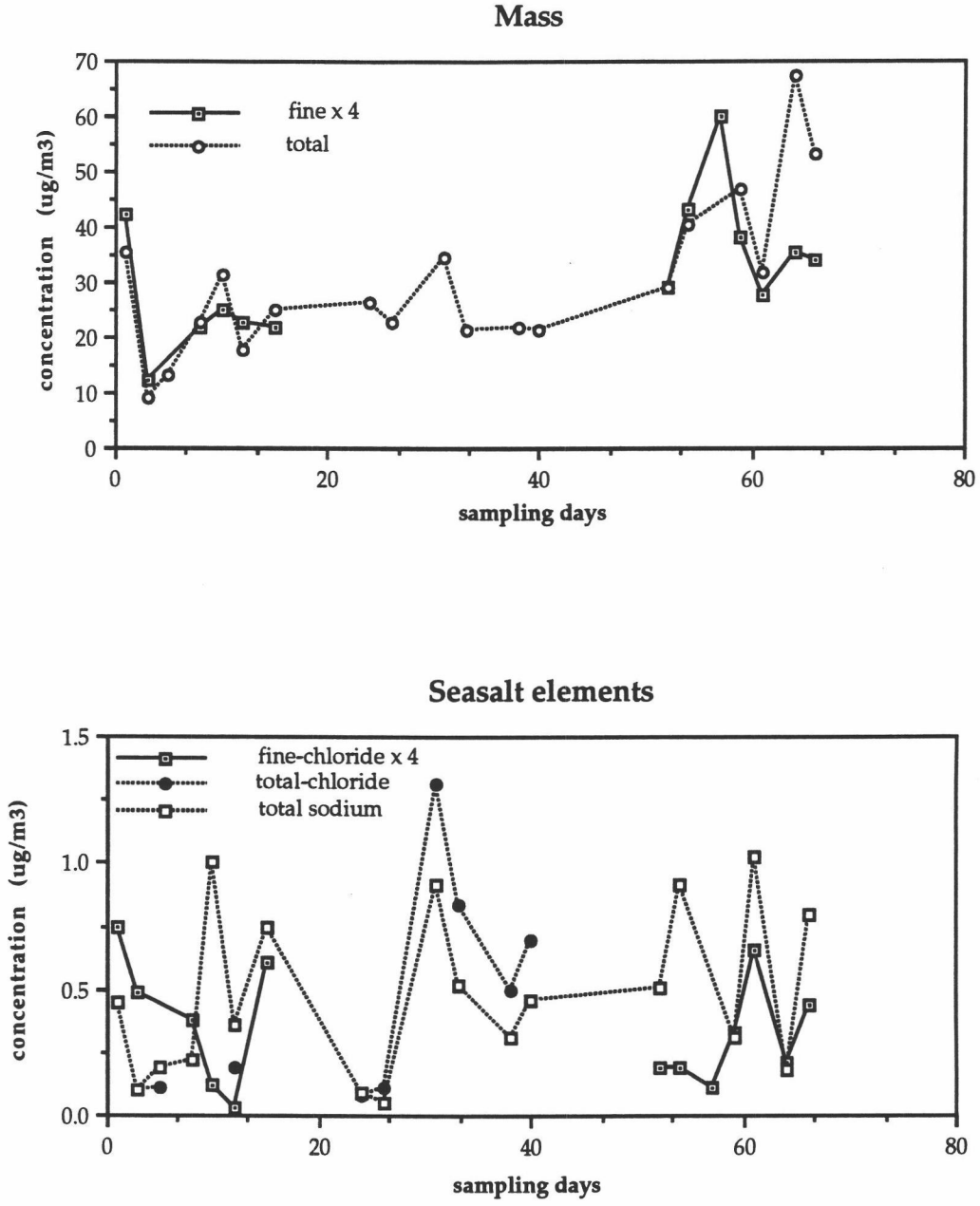

FIG. 4.4. Temporal variation for particle mass and seasalt element concentrations at Corvallis.

Fig. 4.5 indicates the temporal variations of sulfate and excess sulfate in fine particles at both sites. The sulfate concentrations at the two sites are

correlated (r=0.82), suggesting that the processes influencing fine-sulfate concentration were similar for the Corvallis and Yaquina Head areas.

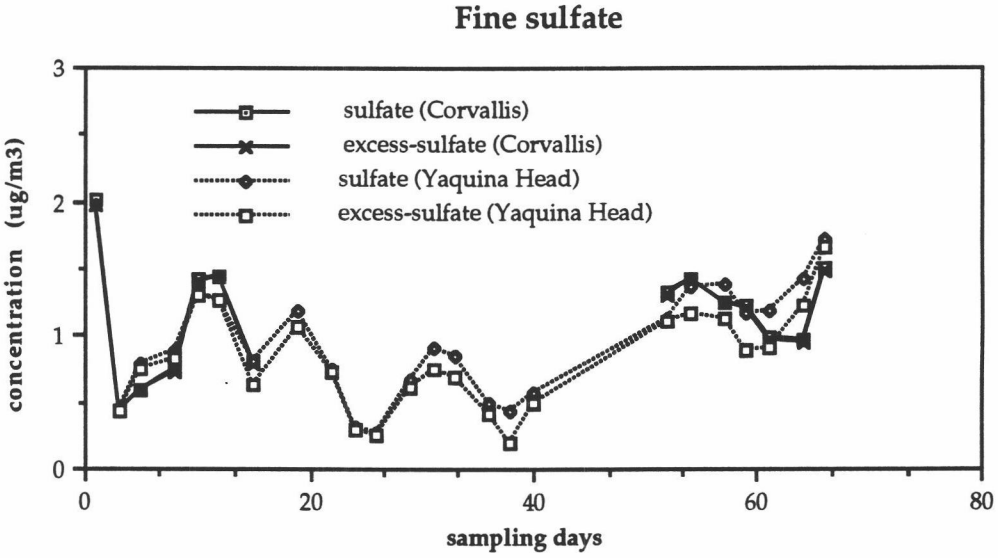

FIG. 4.5. Temporal variation for fine-sulfate and fine-SO_4^{2-}ex concentrations at Corvallis and Yaquina Head.

Fig. 4.6 shows that temporal variations for fine-NO_3^- at both sites and for Sb at the Yaquina Head site. There is no correlation of nitrate ($r<0.1$) between the two sites, and fine-NO_3^- and Sb were correlated with each other (r=0.73) at Yaquina Head.

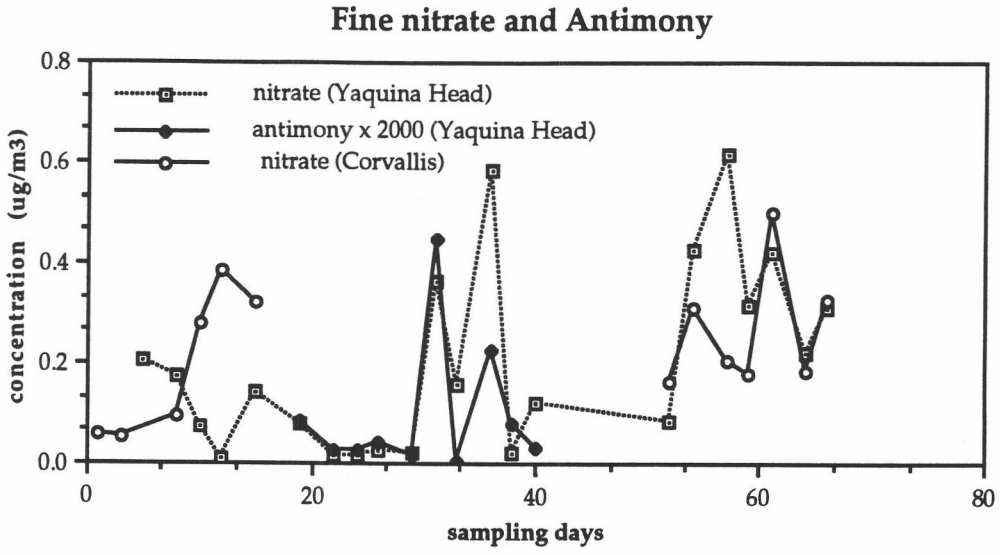

FIG. 4.6. Temporal variation for nitrate and antimony in fine particles at Corvallis and Yaquina Head.

4.5 Enrichment Factors in Relation to Seasalt and Crustal Abundance

Since the number of samples was different for each element, rather than calculating enrichment factors (EF) from mean values, the EF were calculated for every available sample. A large EF can occur when the reference element concentration is small, therefore the geometric means for EF were calculated to avoid bias associate with near detection limit values. The geometric mean values of the EF relative to seasalt composition are listed in Table 4.4.

Table 4.4. Geometric means of enrichment factors (EF) relative to seasalt composition.

	Reference element	Yaquina Head EF	Corvallis EF
$Cr,_f$[1]	Na	27,300,000	
$Co,_f$	Na	62,400,000	
$SO_4^{2-},_f$	Na	9.9	
$SO_4^{2-},_f$	Cl	18.4	122
SO_4^{2-}	Na	0.81[2]	18[3]
Cl	Na	0.94[2]	0.64[3]

1 fine particles
2 coarse particles
3 total particles

The EF for chromium (Cr) and cobalt (Co) were very large, which indicated that the chromium and cobalt were from sources other than seasalt. Sulfate was another enriched species in fine particles at the Yaquina Head site. The large EF for fine-SO_4^{2-} at Yaquina Head (9.9) suggested that there were sources of sulfate other than seasalt at Yaquina Head. In the fine particle fractions, sulfate was more enriched at Corvallis than at Yaquina Head, which confirmed that the influence of seasalt was relatively less important at Corvallis. The EF for coarse-SO_4^{2-} at Yaquina Head was less than one (0.81), indicating that most of the coarse sulfate aerosol collected at Yaquina Head was from seasalt. It should be noted that the EF concept doesn't account for all of the factors which influence aerosol composition. The EF for coarse-Cl at

the Yaquina Head site was close to one (0.94), which is consistent with Cl particles from seasalt. In contrast, in Corvallis (relative to Na) a smaller EF for total-Cl (0.64) indicates that Cl was deficient in the aerosol at Corvallis, a factor which was probably due to the volatilization of HCl following reactions of deposited Cl with the acidic air (Hasson *et al.*, 1984; Daum *et al.*, 1989).

The EF values relative to crustal materials are listed in Table 4.5, indicating that the total-Na and total-Cl were not of crustal origin. The large EF for total-SO_4^{2-} indicates that soil dust was not a major source of particle sulfate at either site.

Table 4.5. Geometric means for enrichment factors (EF) relative to crustal composition.

		Yaquina Head	Corvallis
	Reference element	EF	EF
$Na_{,t}$	Fe	605	9.1
$Cl_{,t}$	Fe	518,000	157
$SO_4^{2-}{}_{,t}$	Fe	1,560	1,000

4.6 Ozone Data

Ozone concentrations were continuously monitored at the Corvallis site during the experimental period. Because of the well-known diurnal variation in ozone concentrations (Karl, 1978; Bruntz *et al.*, 1974), the ozone

data were grouped into four classes according to sampling times: class one, 10 a.m. - 4 p.m.; class two, 4 p.m. - 10 p.m.; class three, 10 p.m. - 5 a.m.; and class four, 5 a.m. - 10 a.m. As shown in Fig. 4.7, a modest positive correlation (r=0.68) was found between nighttime (class three) ozone and the sulfate concentrations.

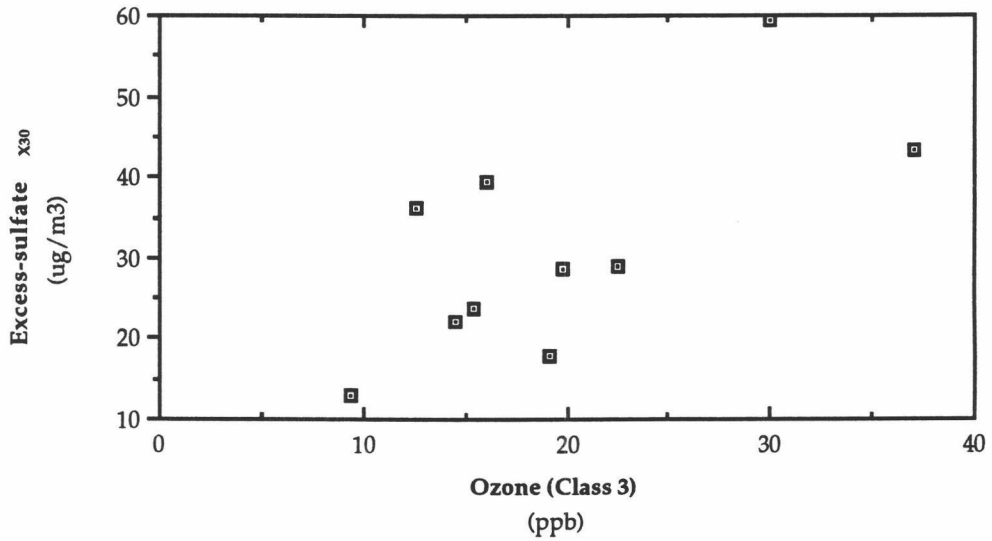

FIG. 4.7. Scatter plot of fine-SO_4^{2-}ex and nighttime ozone (10 p.m. - 5 a.m.) for two or three day sampling periods at Corvallis.

4.7 Principal Component Analysis

Since the number of samples which could be analyzed was limited, only 6 measured variables (mass, SO_4^{2-}, NO_3^-, Cl^-, Ni and Pb) for 22 fine fraction samples at Yaquina Head were chosen for as the subject of principal component analysis (PCA). The PCA results for non-normalized data indicated that the loadings for each variable were at similar levels, thus

demonstrating a correlation between all of the variables. This was caused by the fact that certain external factors control the major variations in sample composition. As noted in section 3.5, the factors which control this variation should be meteorological conditions; for example pollutant concentrations will be high in a stable atmosphere and during low wind speeds. To reduce the effect of meteorological influence in order to perceive other sources of variation (e.g., emission sources), the data were normalized by the two different methods described in section 3.5. Following normalization, since the distributions were skewed, the data were further transformed by square root calculations. The sample strength described in equation (10) was proportional to the particle mass (Fig. 4.8). Thus, the two normalization methods are believed to be equivalent. The PCA results for both methods of normalization were similar.

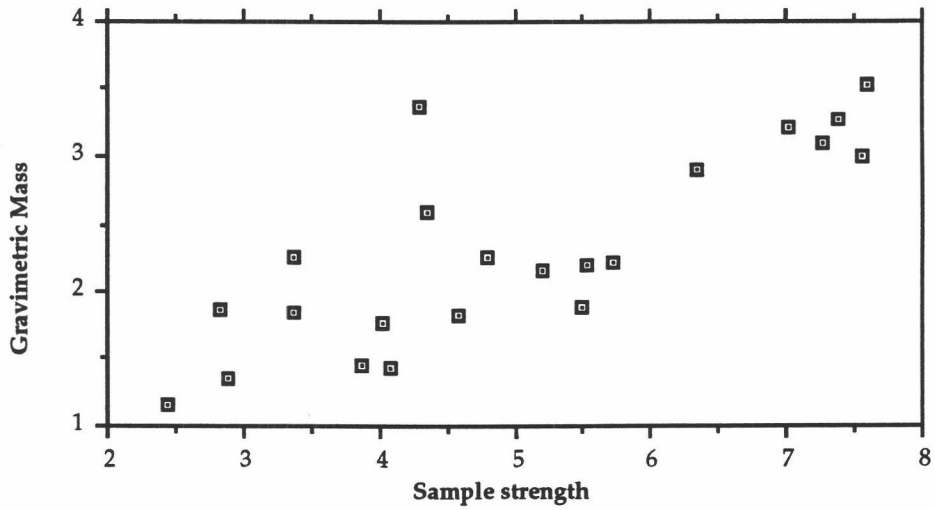

FIG. 4.8. Scatter plot for two normalization factors used to preprocess the data for principal component analysis.

The PCA results for the chemical composition data are summarized in Table 4.6. A total of 57% of the original variance was described by three extracted components. The INAA results (e.g., fine particle Na concentration) are not included in the PCA since the INAA results were not available for every sample period (i.e., data were available for 10 of 23 periods).

Table 4.6. Principal component analysis of the chemical composition normalized by particle gravimetric mass for fine fraction aerosol at Yaquina Head.

	component 1	component 2	component 3
Explained variance	26.3	13.0	17.6
High loading variables	$SO_4^{2-}{}_{ex}$ (0.62)	NO_3^- (0.74)	Pb (0.83)
(loading)	Cl^- (-0.56)	Ni (0.42)	Ni (-0.51)
	Ni (0.41)	Pb (0.44)	

Figs. 4.9 and 4.10 show the relationships among component scores derived from the 22-sample data set and the INAA data for other species (i.e., those measured less frequently). Fig. 4.9 shows that the Na concentrations ($\mu g/m^3$) were anticorrelated with the scores for component one, indicating that the Na concentrations were positively correlated to Cl^- concentrations. Fig. 4.10 shows that the Sb concentrations were positively correlated to the scores for component two; component two depended principally on NO_3^-.

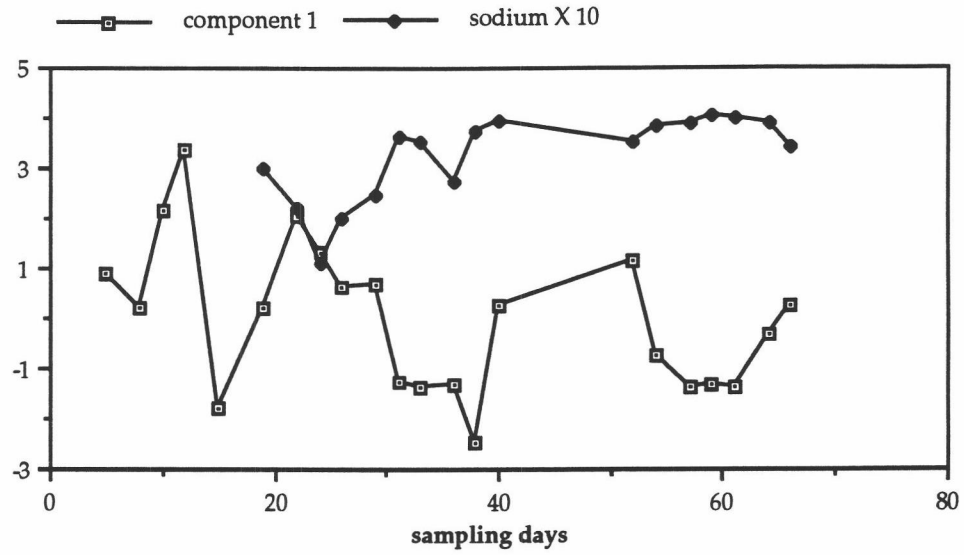

FIG. 4.9. Relationship between sodium concentrations and scores for principal component analysis component one for Yaquina Head.

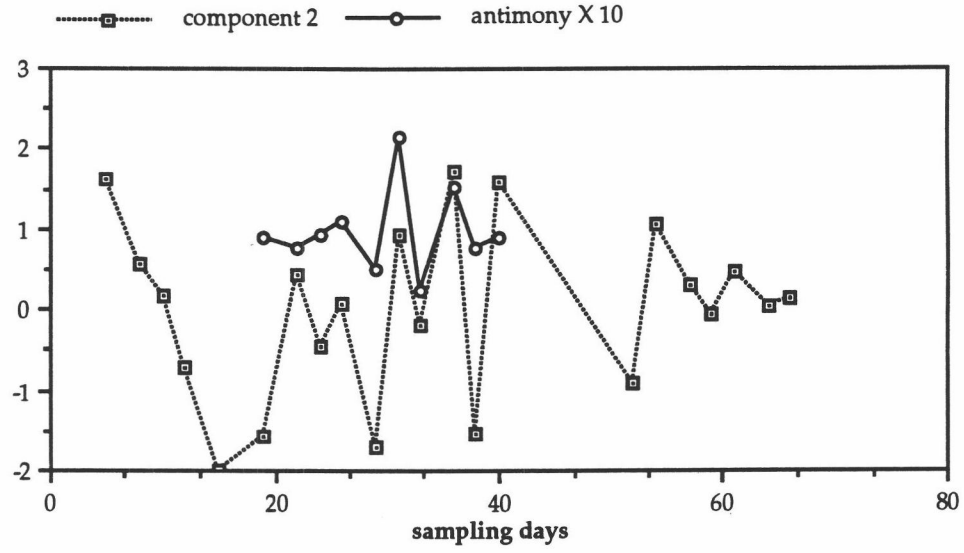

FIG. 4.10. Relationship between the antimony concentrations and scores for principal component analysis component two for Yaquina Head.

4.8 Partial-Least-Square Regression Model

Partial least-square (PLS) multiple linear regression was applied to the collected meteorological and chemical composition data to investigate a model for the prediction of the chemical compositions of airborne particles from meteorological parameters. Only the composition for the fine fraction samples collected at the Yaquina Head site were used in the PLS model.

The meteorological data, including back trajectories, local wind speed and direction, and atmospheric stability were used as the predictor (X) block for the PLS. The chemical compositions were used as the response (Y) block. Prior to the development of the PLS, the chemical composition data were normalized by the two methods discussed in Section 3.6. It is noted that both methods produced similar results.

Table 4.7 shows the results of the PLS model normalized by sample strengths. According to Table 4.7, $SO_4^{2-}{}_{ex}$ concentration tended to be high when the sampling period has a coastal trajectory, and the Cl^- concentration also tended to be high within marine trajectory periods. High Pb concentration was associated with continental trajectory and stable atmosphere. Relationships between the two blocks were fairly weak: the variances explained by the model are 14.3% in the X-block and 14.6% in the Y-block. Component one of the PLS model was similar to component one for the PCA model of chemical composition (see Section 4.7). Thus, the PLS algorithm serves to extract components equivalent to the results produced with the PCA model, but the relationships between components for each block of the PLS demonstrates at least a mild dependence of chemical compositions on meteorology.

Table 4.7. Partial least-square regression model results for meteorological data and the chemical composition of fine fraction aerosol, Yaquina Head site (X-block: meteorological data; Y-block: chemical composition data).

X block	component 1	component 2
Explained variance	1.49	12.8
Key variables (loading)	marine traj.† (-0.63) coastal traj. (0.45) wind speed (-0.45) continental traj. (-0.41)	stability (0.63) continental traj. (0.58)
Y block		
Explained variance	10.2	4.43
Key variables (loading)	$SO_4^{2-}{}_{ex}$ (0.78) Cl^- (-0.47) NO_3^- (-0.40)	Pb (0.87)

†traj.: trajectory

4.9 Characteristics of Marine and Continental Aerosols

To compare the characteristics of marine and continental aerosol, particle mass and chemical composition data were classified according to transport direction (i.e., back trajectory classes). Fig. 4.11 shows classified fine and coarse particle mass for both sampling sites. The number of samples for each trajectory class is indicated below each column; the error bars present the standard deviation for the samples. From Fig. 4.11, it is evident that during the sampling period continental aerosols had a greater particle mass than

marine aerosols, and it is further noted that the difference between the two trajectory types is more obvious for the coarse particles.

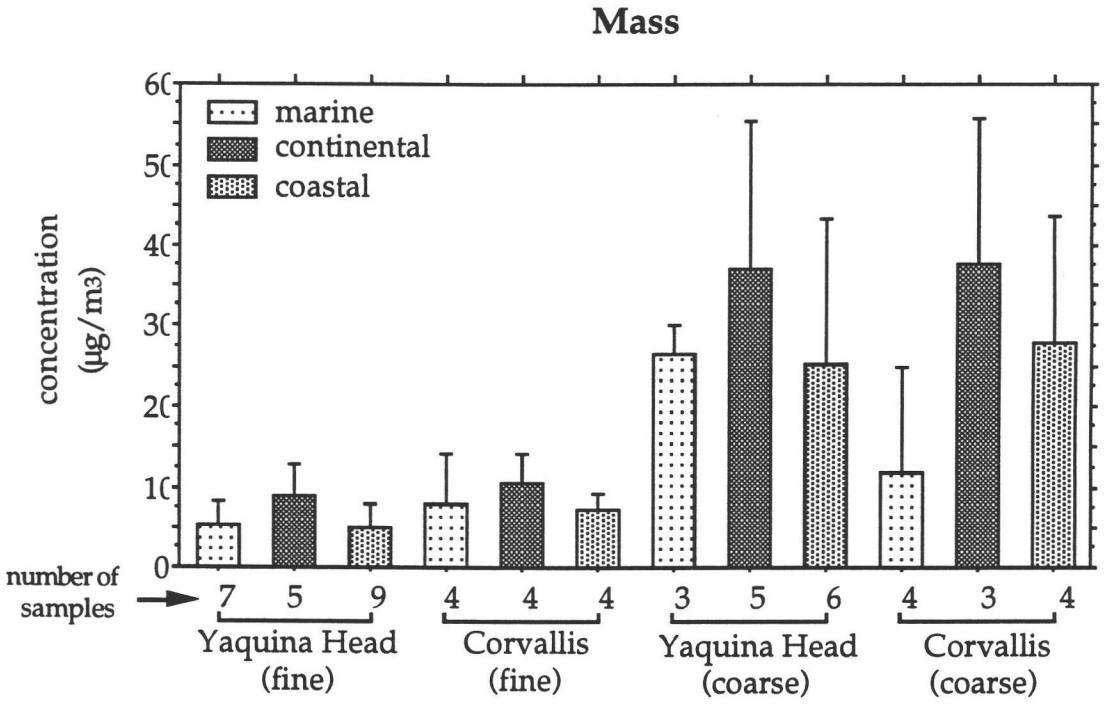

FIG. 4.11. Particle mass classified by back trajectories for Yaquina Head and Corvallis sites (the error bar represent standard deviation).

Fig. 4.12 presents fine and coarse particles SO_4^{2-} for both sites stratified by air trajectories; Fig. 4.13 shows the excess-SO_4^{2-} in both fractions for both sites. The continental aerosols had higher concentrations of both SO_4^{2-} and excess-SO_4^{2-} than the marine aerosols. At the Corvallis site, the coarse-sulfate was very low when compared to the coarse-SO_4^{2-} sample quantities at Yaquina Head. For the greater part, zero excess sulfate was measured for coarse aerosol fractions at both sites.

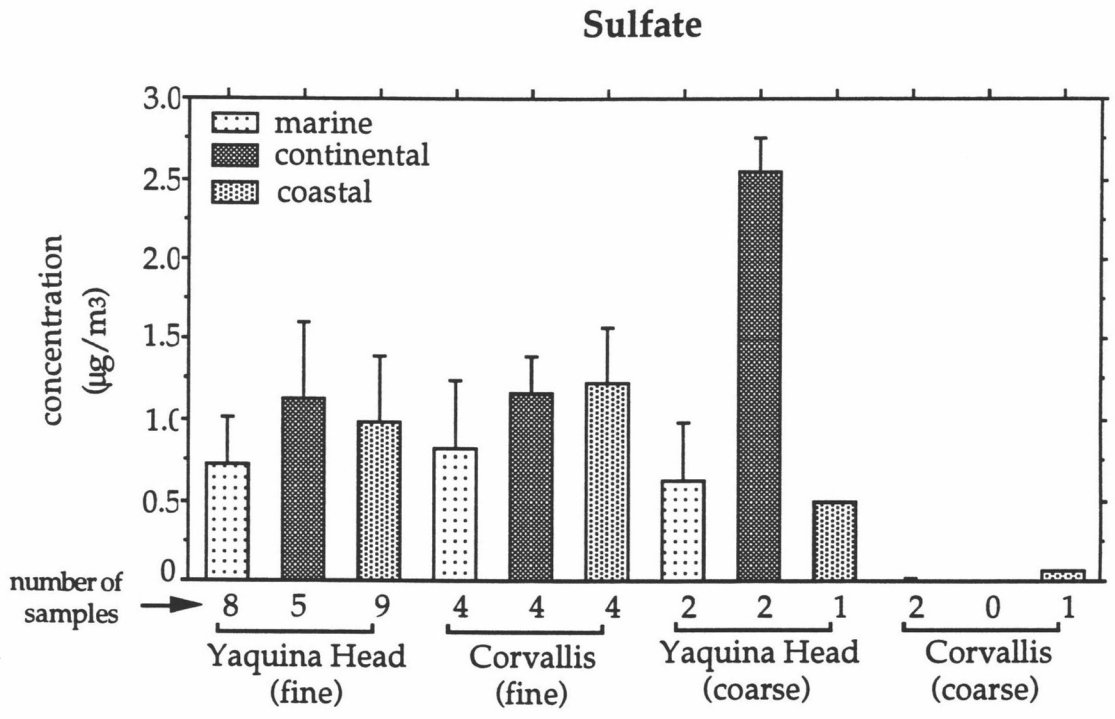

FIG. 4.12. Sulfate classified by back trajectories for Yaquina Head and Corvallis sites (the error bar represent standard deviation).

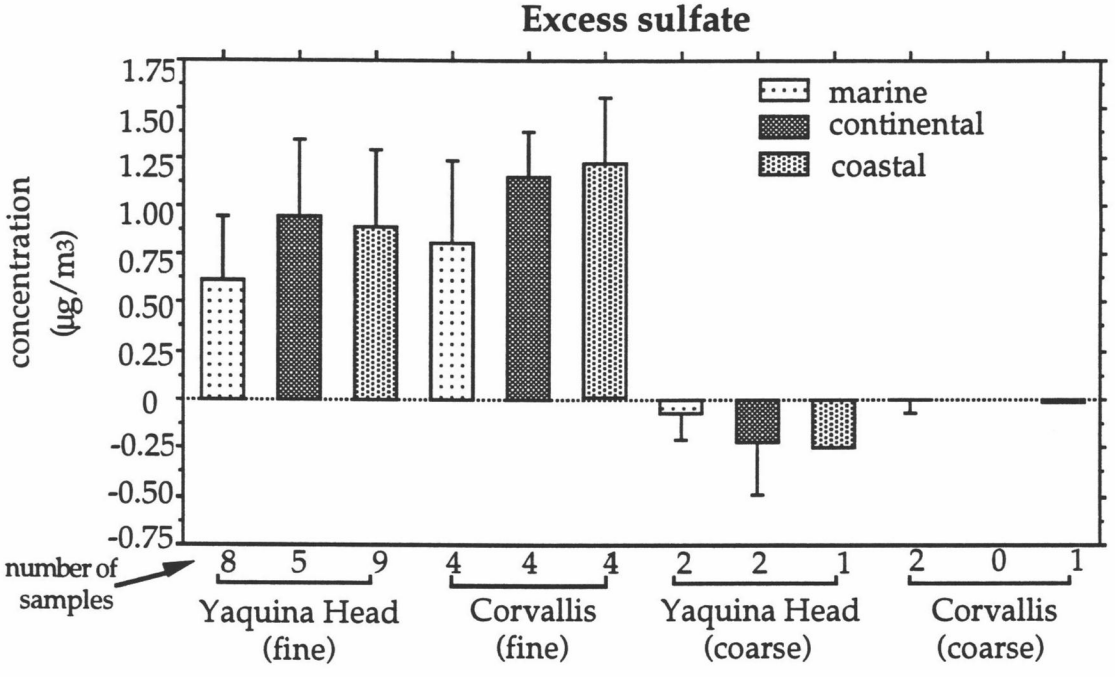

FIG. 4.13. Excess sulfate classified by back trajectories for Yaquina Head and Corvallis sites (the error bar represent standard deviation).

Fig. 4.14 shows NO_3^- for both fine and "coarse + gas" (includes gas phase HNO_3) modes at the two sampling sites classified by back trajectories. Continental aerosols contain more NO_3^- than the marine aerosols. The sum of the coarse-NO_3^- and nitric acid vapor ("coarse+gas") exceeded the amount of fine nitrates but the number of samples was limited. Results for fine-NO_3^- at the two sampling sites were similar. The number of samples was too small for "coarse+gas"-NO_3^-, thus real differences in "coarse+gas"-NO_3^- between the two sampling sites was difficult to perceive.

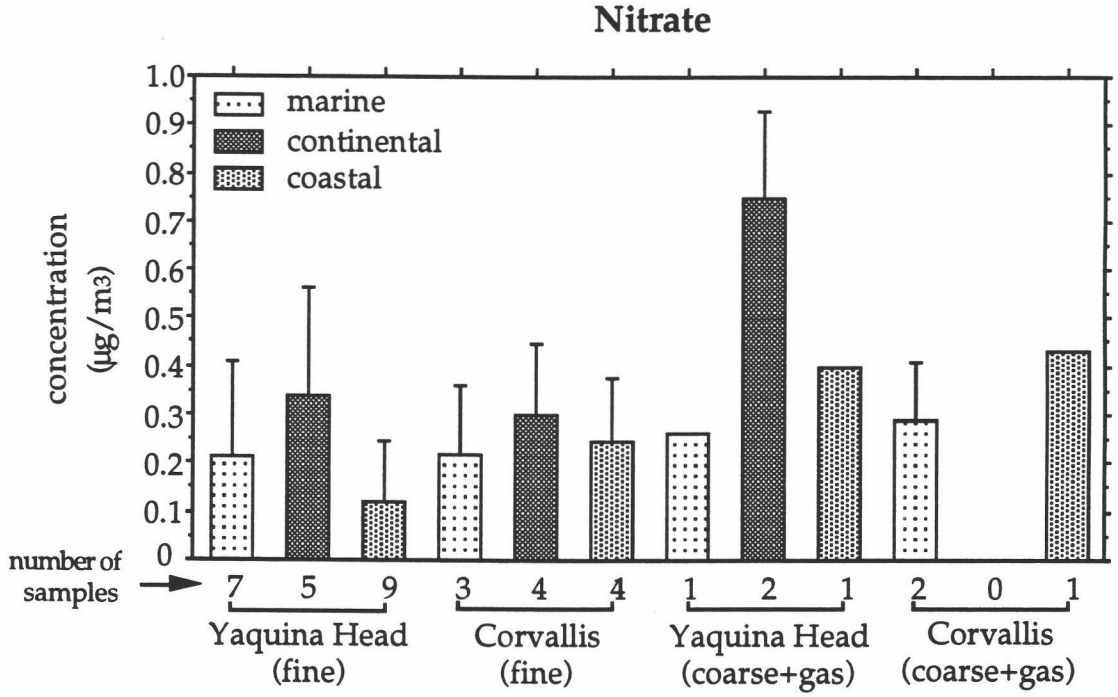

FIG. 4.14. Nitrate classified by back trajectories for Yaquina Head and Corvallis sites (the error bar represent standard deviation).

Fig. 4.15 presents Na concentrations for coarse and fine particles at the Yaquina Head site classified by back trajectories. The coarse particles contained greater quantities of Na than the fine particles, and aerosols with marine trajectories included more Na than the continental aerosols.

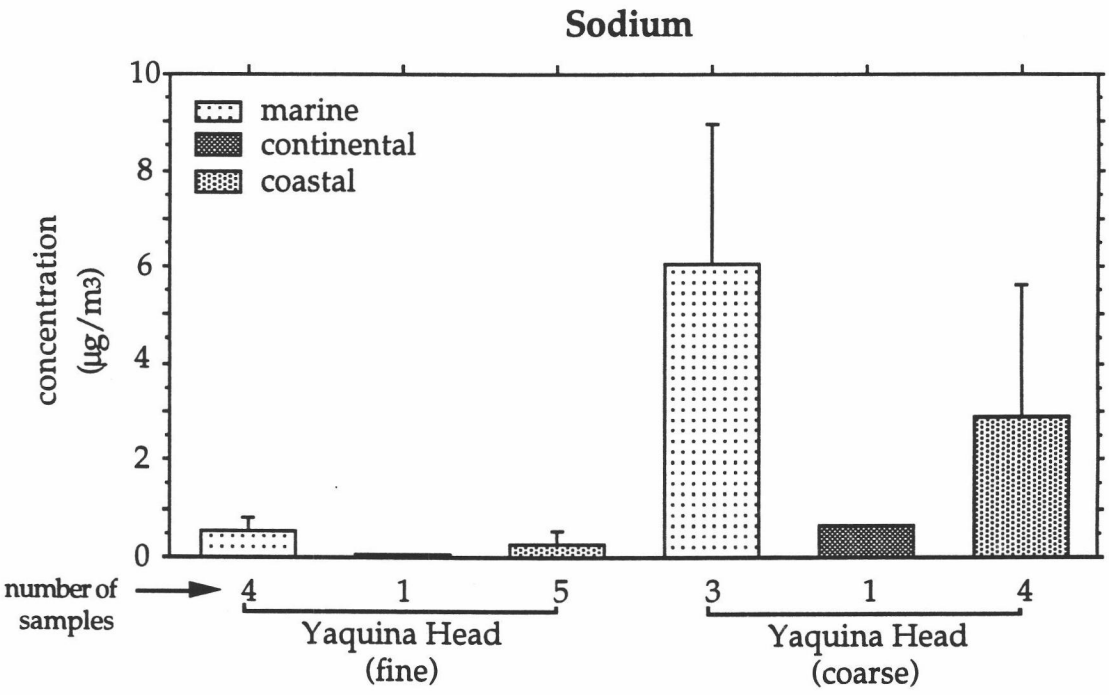

FIG. 4.15. Sodium classified by back trajectories for the Yaquina Head site (the error bar represent standard deviation).

Fig. 4.16 presents a comparison of total Na for the two sampling sites. Yaquina Head received more Na than the Corvallis site, and the continental trajectories had more total-Na than the marine trajectories. This result may have been influenced by the limited number of total particle samples available.

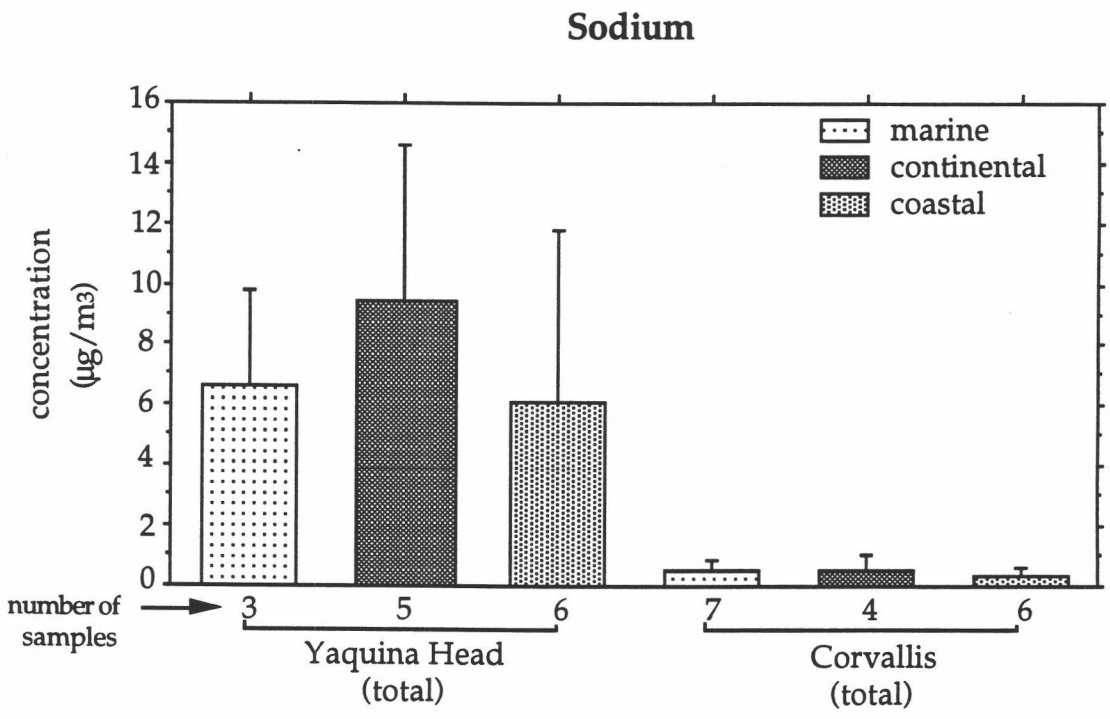

FIG. 4.16. Total-sodium classified by back trajectories for Yaquina Head and Corvallis sites (the error bar represent standard deviation).

Fig. 4.17 shows Cl for the fine and coarse particles at both sites classified by back trajectories. At Yaquina Head, the fine-Cl associated with marine and continental trajectories were similar and at very low concentrations, whereas the continental trajectories contained higher Cl concentrations among the coarse particles than did the marine aerosols. These last results were influenced by the limited number of total particle samples. Compared with the Cl at the Yaquina Head sampling site, Cl at Corvallis site was minimal in both coarse and fine particles.

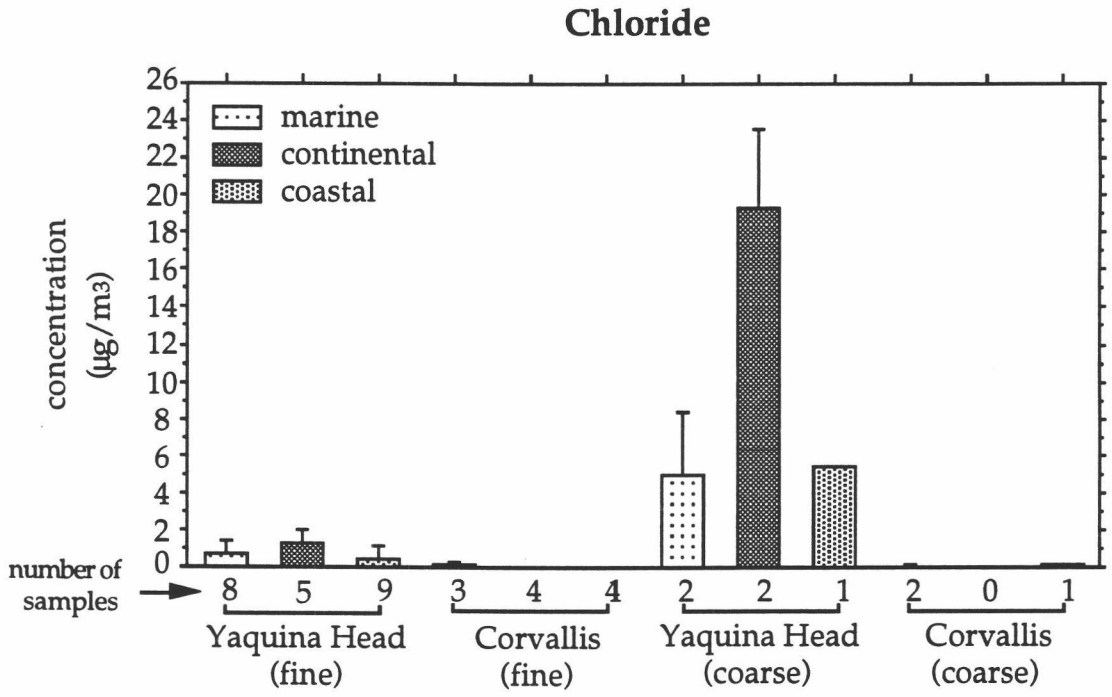

FIG. 4.17. Chloride classified by back trajectories for Yaquina Head and Corvallis sites (the error bar represent standard deviation).

Fig. 4.18 presents Fe concentration in "total" aerosol samples classified by back trajectories for both sampling sites. At both sites, the aerosols collected during periods of continental trajectory contained more Fe than the aerosols collected with marine trajectory, but the differences among trajectory classes was generally small. The Fe concentrations at the Corvallis site were higher than those at Yaquina Head.

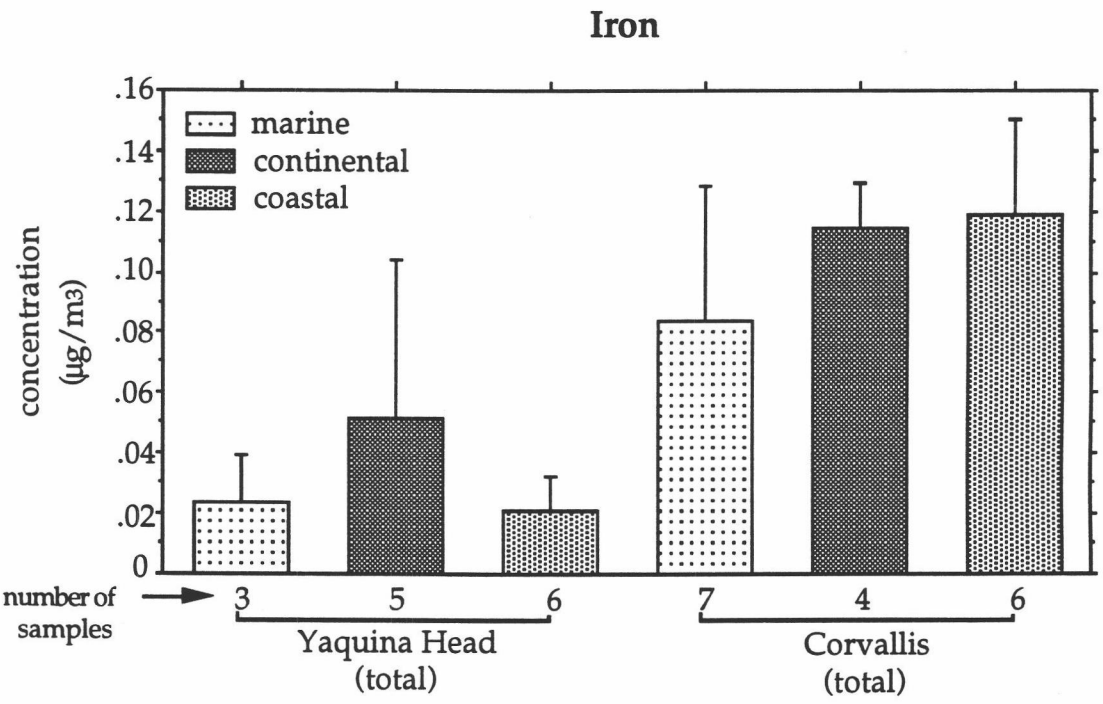

FIG. 4.18. Iron classified by back trajectories for Yaquina Head and Corvallis sites (the error bar represent standard deviation).

Figs. 4.19 and 4.20 show the comparisons, respectively, of Pb and Ni for fine particles at both sites. At Yaquina Head, Pb was trajectory-dependent; in contrast, the Ni concentrations were similar for the different trajectory classes. Both Pb and Ni data display the highest concentrations in the aerosols collected during periods of air flow from the continent but the differences were smaller for Ni.

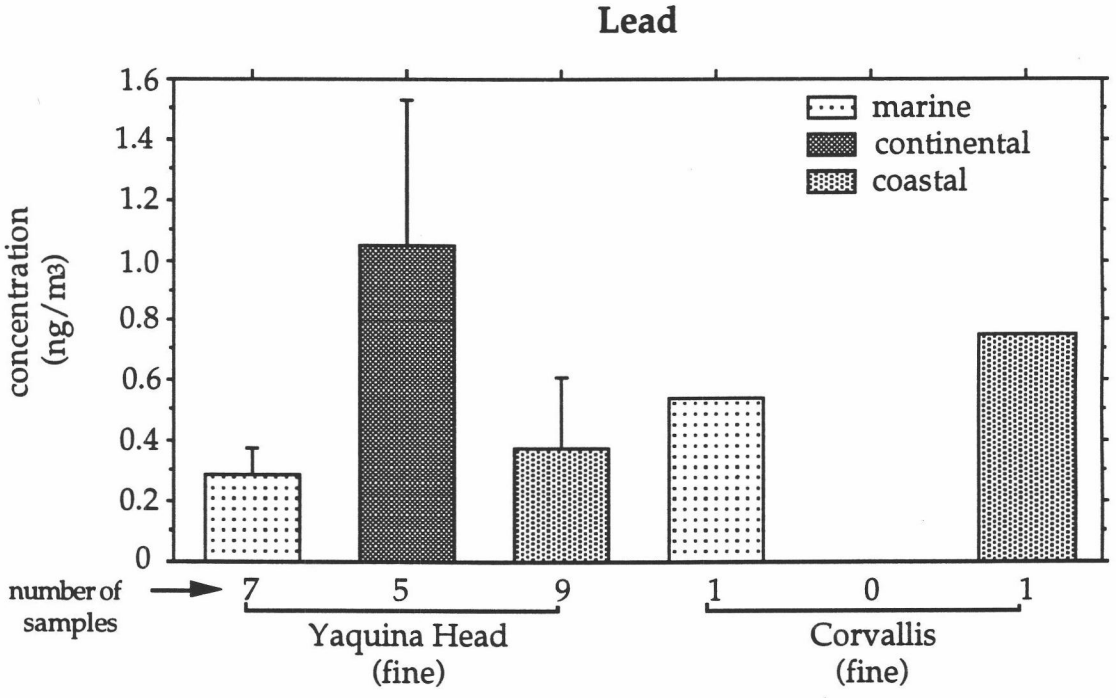

FIG. 4.19. Lead in fine particles classified by back trajectories for Yaquina Head and Corvallis sites (the error bar represent standard deviation).

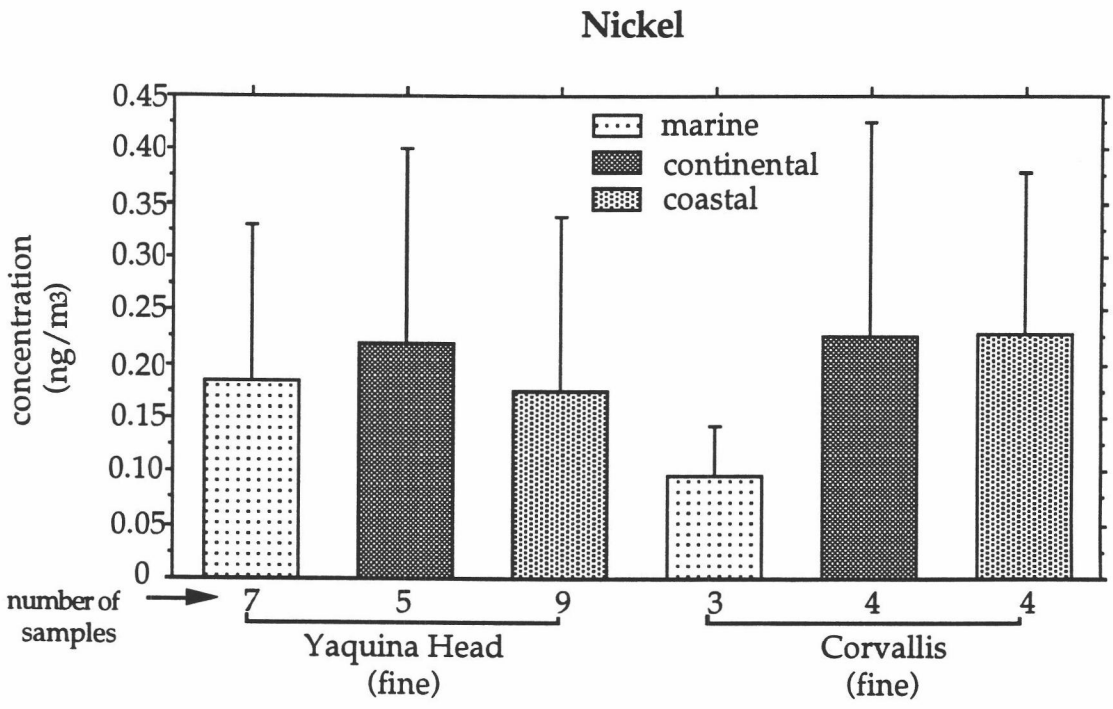

FIG. 4.20. Nickel in fine particles classified by back trajectories for Yaquina Head and Corvallis sites (the error bar represent standard deviation).

4.10 A Conceptual Model for Distinguishing The Air Mass Types and Associated Local Influences

To the extent that SO_4^{2-} is homogeneously distributed between two sampling sites in this experiment, long range transport should be the major influence on the excess sulfate (SO_4^{2-}ex) concentrations of the samples collected at both sites. It also noted that the correlation of SO_4^{2-}ex in fine particles between two sampling sites (r=0.87) suggested that the fine-SO_4^{2-}ex at Yaquina Head was generated in the same way as the fine-SO_4^{2-}ex at Corvallis. However, some difference of SO_4^{2-}ex levels between two sites would result from any local influences. Local influences on SO_4^{2-}ex concentration, adopting a single box model of atmospheric mixing (Butcher and Charlson,

1972) are a function of emission rate, mixing depth and wind speed. The relative position of the two sampling sites is shown in Fig. 4.21.

The long range transport of SO_4^{2-}ex could be either from the North American continent (along a continental trajectory) or from the Pacific Ocean (along a marine trajectory), as shown in Fig. 4.21. If the atmospheric boundary layer is well mixed, the influences of the two types of long range transport on aerosol SO_4^{2-}ex concentration should be the same for two sampling sites separated by 64 km. Local sources, such as areas A and B in Fig. 4.21, can cause different degrees of influence at the two sites with either Yaquina Head or Corvallis having a higher concentration. Therefore, the general location of important local sources of SO_4^{2-}ex can be estimated in each sampling period using chemical and meteorological data (i.e., trajectory and local wind data).

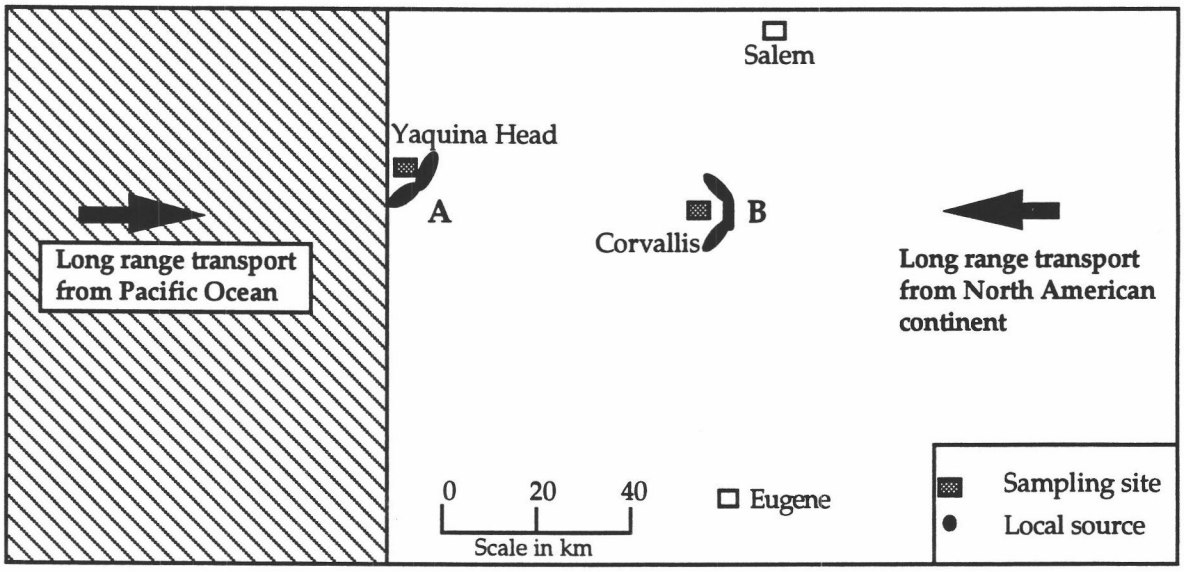

FIG. 4.21. Simple scheme of local (A or B) and regional influences on two sampling sites

Before comparing the sulfate levels at two sampling sites to determine whether any real difference exists, the experimental uncertainty of sulfate measurements was examined. Four pairs of sulfate concentration data (see Section 4.1) were used to calculate the confidence interval associated with the measurement of aerosol sulfate concentration. For each sulfate measurement X, the true concentration can be estimated within the interval of "X ± 0.07" ($\mu g/m^3$) at 75% confidence level (see Section 4.1). A difference smaller than 0.14 is defined as "no difference". Alternatively, since SO_4^{2-}ex concentrations were mainly influenced by long range transport, it seems reasonable to assume the SO_4^{2-}ex differences between two sites is normally distributed with a mean value of zero. The 75% significant level of SO_4^{2-}ex differences can be calculated as 0.2 ($\mu g/m^3$) based on the above assumption. This means the difference larger than 0.2 can be referred to as "significantly different" than the expected value of zero at the 75% confidence level. Thus we consider SO_4^{2-}ex differences above approximately 0.14 to 0.20 to represent "real" differences between the two measurement sites.

In this study, thirteen pairs of simultaneous fine particle samples for the two sampling sites are available for the primary application of a simple conceptual model (i.e., experimental phase I and III). Subsequentially, ten addition sampling periods (i.e., phase II) that lack one or more measured variables will also be investigated with this conceptual model (supplemental model application). The SO_4^{2-}ex concentrations and meteorological data for these sampling periods are listed in Table 4.8. The meteorological data were collected in Newport and Corvallis as described in Section 3.7.

Table 4.8. Excess sulfate concentration and meteorological data for simultaneous sampling periods at the Corvallis and Yaquina Head sites.

	Yaquina Head			Corvallis			
Date	$[SO4^{2-}ex]$ ($\mu g/m^3$)	Wind† Speed	Wind Direction	$[SO4^{2-}ex]$ ($\mu g/m^3$)	Wind Speed	Wind Direction	Trajectory*
7/24	0.43	N/A††	N/A	0.43	M	330	Marine
7/26	0.74	N/A	N/A	0.60	M	360	Marine
7/29	0.84	M	360	0.74	M	340	Coastal
7/31	1.31	M	340	1.41	M	320	Marine
8/2	1.27	N/A	N/A	1.45	N/A	N/A	Coastal
8/5	0.63	M	270	0.79	M	310	Marine
9/11	1.11	M	340	1.31	M	310	N/A
9/13	1.17	M	330	1.42	M	310	Continental
9/16	1.13	M	350	1.25	L	330	Continental
9/18	0.88	M	350	1.21	M	320	Coastal
9/20	0.91	M	340	0.96	M	340	Continental
9/23	1.22	H	180	0.95	M	40	Continental
9/25	1.66	L	220	1.48	M	300	Coastal

† the level of wind speed is classified as high (H), > 5.3 m/s; medium (M), 3.5-5.3 m/s; and low (L), 1.8-3.5 m/s.
†† data is not available.
* trajectories end on the Oregon coast as described in Section 3.8.3

A simple conceptual model was built to examine the relationships between back trajectory, local wind, and SO_4^{2-}ex concentrations. In general, the aerosol traveling along a continental trajectory is assumed to contain more SO_4^{2-}ex (e.g. partly from combustion sources) than the aerosol that has a marine trajectory (e.g., from biogenic sulfur sources). In addition, this conceptual model uses local winds to help identify local emission sources. Some suggestion as to the type of any local SO_4^{2-}ex source can be determined by referring to the concentration level of trace species (NO_3^-, Fe, Pb, Ni, and methane sulfonic acid (MSA)) during the sampling period. For example, the

concentration of Fe reflects the strength of local soil influences since the Fe particles collected in this study, in general, are within coarse fraction (diameter > 2.5 μm) and have a short life time in the air (minutes to hours) for particle transport (see Section 1.1.3). The Ni, Pb and NO_3^- concentration levels in the atmosphere are indices of emissions from human activities (see Section 1.0). MSA concentration is an index of biogenic sulfur (see Section 1.0). Sodium can be a tracer of marine influence, however, sodium was not used in this conceptual model because: a.) the lifetime of Na particle is too short to be transported between sites. b.) six out of 13 sampling periods have no Na data, and c.) earlier analyses of these same data suggest that Na did not work well as a marine tracer (see Section 4.9).

Some ideal cases that characterize this conceptual model are listed in Table 4.9. In case one, the continental background air advects to both sampling sites causing average (or high) SO_4^{2-}ex. Note that one tracer, MSA concentration, should display a totally reverse behavior from other trace species since the major MSA sources are located in marine areas. In case one, the SO_4^{2-}ex difference between the two sampling sites is minimal since no local influence existed. In case two, the "clean" marine background air advects to both sites, which results in relatively low and similar SO_4^{2-}ex and trace species concentrations (but potentially elevated MSA concentration) at the two sampling sites. In case three, the continental background air influences both site equally but local influences near Corvallis leads to a higher SO_4^{2-}ex at Corvallis than at Yaquina Head. In case three, one or more trace species should be elevated at Corvallis. In case four, the continental background air influences both sites equally but local influences near Yaquina Head result in a higher SO_4^{2-}ex at Yaquina Head than at Corvallis; high concentrations of one or more trace species are expected for the Yaquina Head

site. In case five, the marine background air influences both sites while local influences near Yaquina Head results in higher SO_4^{2-}ex concentration at Yaquina Head than in Corvallis. Trace species concentrations, in general, are low for marine air, but the concentrations of any trace element associated with local sources would be elevated at Yaquina Head in case five. In case six, the marine background air influences both sites with local influences near Corvallis leading to higher SO_4^{2-}ex concentration at Corvallis than at Yaquina Head. Concentrations of any trace elements associated with local sources could be elevated at the Corvallis site for case six. In case seven, the marine background air influences both sites with local influences at both Corvallis and Yaquina. Excess sulfate differences in case seven depend on the strength of sources near the two sampling sites and could be any value. Concentrations of any trace elements associated with local sources could be elevated at either or both sites. In case eight, the continental background air influences both sites equally but local influences at each sampling site result in the difference of SO_4^{2-}ex levels between two sampling sites. High concentrations of one or more trace species are expected for both sampling sites.

Table 4.9. Ideal cases for the simple conceptual model

Case No.	Air mass type (local influence)††	Excess sulfate difference†	Excess sulfate concentration (at Yaquina)	Air mass trajectory	Trace species concentrations*
1	continental background (no local influence)	≈0	moderate	continental	average
2	marine background (no local influence)	≈0	low	marine	below average
3	continental background with (Corvallis source)	<0	moderate	continental	potentially high at Corvallis
4	continental background with (Yaquina source)	>0	high	continental	potentially high at Yaquina
5	marine background with (Yaquina source)	>0	moderate to high	marine	potentially high at Yaquina
6	marine background with (Corvallis source)	<0	low	marine	potentially high at Corvallis
7	marine background with (Yaquina, Corvallis)	any value	moderate to high	marine	potentially high at Yaquina and Corvallis
8	continental background with (Yaquina, Corvallis)	any value	high	continental	potentially high at Yaquina and Corvallis

† $[SO_4^{2-}{}_{ex}]_{Yaquina\ Head} - [SO_4^{2-}{}_{ex}]_{Corvallis}$
†† location of local influence
* Except MSA; MSA concentration behaves in reverse.

Results of the comparison for 13 samples in the primary application are summarized in Table 4.10. In Table 4.10, relative sulfate level (RSL) was calculated to show relatively clean (background air) and relatively dirty (long range transport or local sources) sampling periods. As shown in equation (18), RSL is defined as the ratio of sulfate concentration in each sampling period to the average sulfate concentration at the sampling site for the 13 samples collected in experimental phase I and III.

Table 4.10. Summary of case studies (experimental phase I and III) used in the primary application of the conceptual model.

Date	$[SO_4^{2-}{}_{ex}]_Y$ - $[SO_4^{2-}{}_{ex}]_C$†	RSL (Y)††	Meteorology**	Trace species concentration	model evaluation	Air mass type. case* (local influence)
7/24	no difference¶	0.41	marine traj.	low [Fe], $[NO_3^-]$ at Corvallis	fit	marine. case 2
7/26	0.14	0.73	marine traj.	low [Fe], [Ni] at Corvallis high [Ni] at Yaquina	fit	marine.case 5 (Yaquina)
7/29	no difference	0.82	coastal traj.	near average	fit	marine.case 2
7/31	no difference	1.29	marine traj.	low [Pb], $[NO_3^-]$ at Yaquina	no fit	unknown
8/2	-0.18	1.25	coastal traj.	low [Pb], $[NO_3^-]$, high [Ni] at Yaquina	fit	continental.case 8 (Corvallis,Yaquina)
8/5	-0.16	0.61	marine traj.	low [Pb], [Ni] at Yaquina low [Ni] at Corvallis	fit	marine.case 6 (Corvallis)
9/11	• -0.2	1.09	no trajectory data	low [Pb], $[NO_3^-]$, and [Ni] at Yaquina	insufficient	unknown
9/13	• -0.26	1.40	continental traj.	high [Pb] and $[NO_3^-]$ at Yaquina	fit	continental.case 8 (Corvallis,Yaquina)
9/16	no difference	1.11	continental traj.	high [Pb], $[NO_3^-]$ at Yaquina high [Ni] at Corvallis	fit	continental.case 8 (Corvallis,Yaquina)
9/18	• -0.32	0.86	coastal traj.	high [Ni] at Yaquina and Corvallis	fit	marine.case 7 (Corvallis,Yaquina)
9/20	no difference	0.59	continental traj.	high $[NO_3^-]$ at Corvallis	no fit	unknown
9/23	• 0.27	1.21	continental traj. southernly wind at Yaquina	high [Fe], [Ni] at Yaquina	fit	continental.case 4 (Yaquina)
9/25	0.18	1.63	coastal traj. southernly wind at Yaquina	near average	fit	continental.case 4 (Yaquina)

† excess sulfate concentration at Yaquina Head subtracted by at Corvallis

†† RSL(Y): the relative sulfate level for Yaquina Head sample; 1.0 = mean value

** traj: trajectory

*case: case number in Table 2.

¶ sulfate difference smaller than 0.14 µg/m3

• significantly different (> 0.2 µg/m3)

$$RSL = \frac{[SO_4^{2-}ex]_{sample}}{Ave([SO_4^{2-}ex]_Y)} \quad (18)$$

where $Ave([SO_4^{2-}ex]_Y)$: the average of SO_4^{2-}ex concentration for 13 samples at Yaquina Head.

In the four out of 13 sampling periods (July 24, July 26, July 31 and August 5), the collected aerosols were identified as moving along a marine trajectory (see Table 4.10). The samples collected on July 24 revealed low SO_4^{2-}ex concentrations (smaller than the average of SO_4^{2-}ex concentration) and no difference in SO_4^{2-}ex concentrations between two sampling sites. The SO_4^{2-}ex in this period is presumed to be mainly derived from the long range transport of marine background air (model case #2, see Table 4.9). For samples collected on July 26, the SO_4^{2-}ex at Yaquina Head was higher than at Corvallis; this difference taken with the high nickel concentration at Yaquina Head implied the existence of local influence at Yaquina Head (model case #5). The samples collected on August 5 showed a higher SO_4^{2-}ex concentration at Corvallis than at Yaquina Head but the analysis of trace species did not identify a local influence. The SO_4^{2-}ex difference suggests that a local influence may exist at Corvallis area but that our tracers were not markers for this source type (model case #6). The samples collected on July 31 indicated no significant difference in SO_4^{2-}ex between two sampling sites and no local influences at Yaquina Head in terms of trace species levels. However, the fact that the concentration of SO_4^{2-}ex was higher than the average during marine trajectories can not be explained by our simple model. This suggests that either the trajectory classification is inappropriate or that

biogenic sources may at times elevate the SO_4^{2-}ex concentration in background air to higher levels than are assumed in the model.

Among the 13 sampling period listed in Table 3, four sampling periods (September 13, 16, 20 and 23) were identified as associated with continental trajectories. The samples collected on September 13 showed high SO_4^{2-}ex concentrations at both sites and high Pb and NO_3^- concentrations at Yaquina Head. The elevated Pb and NO_3^- concentrations are consistent with anthropogenic influence either as polluted background air from continental areas or some local sources. The higher SO_4^{2-}ex at Corvallis than at Yaquina Head suggests that local influences existed at Corvallis, but the available trace species data did not reveal the influences. Therefore, the local influences seem existed at both site based on the information of SO_4^{2-}ex difference and trace species analysis (model case #8). For the samples collected on September 16, the high Ni concentration at Corvallis and the high Pb and NO_3^- concentrations at Yaquina Head indicated the existence of a local influences at both Corvallis and Yaquina Head (model case #8). The samples collected on September 23 suggest that local sources influenced Yaquina Head in that measured SO_4^{2-}ex at Yaquina Head was higher than in Corvallis (model case #4). The southerly wind direction at Yaquina Head (only present in two sampling periods: September 23 and 25) are consistent with the location of a local SO_2 source (a pulp mill located in Toledo, Oregon). The samples collected on September 20 show relatively low SO_4^{2-}ex at both sites, however, which can not be explained by our simple model for a continental trajectory. This result might represent either a "cleaner" than expected continental air mass or an incorrect trajectory from the NGM model (see Section 3.8.3). The high NO_3^- at Corvallis indicated potential local influences at that site, but the influence on SO_4^{2-}ex concentration is not obvious, since the SO_4^{2-}ex levels at

the two sampling sites are quite low and similar to each other. For the September 20 samples, one would have expected a marine trajectory according to our simple model (probably model case #2).

Of the 13 sampling periods listed in Table 4.10, four sampling periods (July 29, August 2, September 18 and 25) were identified as associated with coastal trajectories. For coastal trajectories it is somewhat more difficult to identify air mass type than for clearcut marine or continental cases. The samples collected on August 2 had higher than average SO_4^{2-}ex at Yaquina Head and higher SO_4^{2-}ex concentration at Corvallis than at Yaquina Head. Available trace species data did not reveal any local influence at Corvallis but high Ni concentration was measured at Yaquina Head. According to the SO_4^{2-}ex difference, local influences were expected to be existed at Corvallis. The high SO_4^{2-}ex concentration suggests that this sample fits the model if the air was more like continental than marine air (model case #8). The samples collected on September 18 showed that SO_4^{2-}ex at Corvallis was higher than at Yaquina Head. High Ni concentrations were measured at both sites suggesting local influences at both. The relatively low SO_4^{2-}ex concentration suggests the advection of marine background air during this period (model case #7). The samples collected on September 25 showed that SO_4^{2-}ex at Yaquina Head was higher than at Corvallis but concentrations of trace species do not reveal any local influence at Yaquina head. However, the special case of southerly wind associated with the highest SO_4^{2-}ex concentration at Yaquina Head implies that potential sulfur sources located south of Yaquina Head (possibly the Toledo, OR, pulp mill) may have influenced that site. The high SO_4^{2-}ex for both sites indicates that continental background air probably advected into sampling area during this period (model case #4).

As shown in Table 4.10, the different types of sulfate sources usually can be distinguished by applying a simple model where high SO_4^{2-}ex levels, in general, are associated with long range transport from continental areas or with local influences. The sampling periods with low SO_4^{2-}ex at both sites are interpreted as the long range transport from marine areas. The difference of SO_4^{2-}ex levels between the two sampling sites, taken in conjunction with any elevated trace species concentrations, reflects the presence of local influences.

In addition to the data evaluated in table 4.10, from August 9 to September 1, ten sulfate samples were collected at Yaquina Head. In six out of the ten sampling periods, total-SO_4^{2-}ex concentrations were available at the Corvallis site. To evaluate the possibility of using the Corvallis total-SO_4^{2-}ex concentration as a surrogate for Corvallis fine-SO_4^{2-}ex concentration, three pairs of simultaneous total- and fine-SO_4^{2-}ex concentrations from Corvallis samples (experimental phase I) were compared. In addition, five pairs of total- and fine-SO_4^{2-}ex concentrations for Yaquina Head samples were compared for the same purpose. For Corvallis samples, the difference between fine and total SO_4^{2-}ex was about 5% of the mean values. For Yaquina Head samples, the difference is comparatively large and the total-SO_4^{2-}ex was inexplicably smaller than fine-SO_4^{2-}ex. Thus, the the total-SO_4^{2-}ex is considered to be equivalent (based on the Corvallis comparison) or smaller than the fine-SO_4^{2-}ex concentrations. The conceptual model was applied to these ten samples to distinguish air mass types during these periods (supplemental model application).

Table 4.11 summarizes the result of the application of the model to these ten samples. In these ten sampling periods, concentrations of SO_4^{2-}ex and trace species at Yaquina Head were quite low, indicating that "clean" background air advected to thesampling sites and that no local influence

existed at Yaquina Head. From the available SO_4^{2-}ex difference for six sampling periods, the SO_4^{2-}ex concentrations at Corvallis were significantly higher than at Yaquina Head in five of the six periods; this suggested that local influences existed at Corvallis (model case #6) in these five sampling periods. The use of total SO_4^{2-}ex comparison for fine-SO_4^{2-}ex (see above) could affect this comparison only in the sense that one might underestimate local Corvallis sources. For the samples collected on August 30, the SO_4^{2-}ex concentrations at two sites were consistent with the absence of local influences (model case #2). The only sample from the August 9 - 30 period that does not fit the simple conceptual model is the sample collected on August 16. In this case, continental trajectory was associated with low SO_4^{2-}ex concentration, this could be caused either by an incorrect classification of trajectory or by "cleaner" then expected continental background air (similar to the September 20 sample, see Table 4.10).

Table 4.11. Summary of case studies (experimental phase II) used in a supplemental application of the conceptual model.

Date	$[SO_4^{2-}{}_{ex}]_Y$-$[SO_4^{2-}{}_{ex}]_C$†	RSL (Y)††	Meteorology*	Trace species concentration** (Yaquina Head)	model evaluation	Air mass type (local influence)	Model Case No.
8/9	not available	1.00	coastal traj.	low [Pb], $[NO_3^-]$ and [Ni]	fit	probably marine	2
8/12	not available	0.71	coastal traj.	low $[NO_3^-]$, MSA detectable	fit	marine	2
8/14	•-1.59	0.30	coastal traj.	low [Pb], $[NO_3^-]$ and [Ni]	fit	marine (Corvallis)	6
8/16	•-1.55	0.26	continental traj.	low $[NO_3^-]$ and [Ni]	no fit	unknown	-
8/19	not available	0.60	coastal traj.	low [Pb], $[NO_3^-]$ and [Ni]	fit	marine	2
8/21	•-1.08	0.75	marine traj.	low [Pb] and [Ni]	fit	marine (Corvallis)	6
8/23	-0.19	0.68	coastal traj.	low [Pb], $[NO_3^-]$ and [Ni], high MSA	fit	marine (Corvallis)	6
8/26	not available	0.41	marine traj.	low [Pb]	fit	marine	2
8/28	•-0.64	0.14	marine traj.	low [Pb] and $[NO_3^-]$, MSA detectable	fit	marine (Corvallis)	6
8/30	no difference	0.53	marine traj.	low [Pb], $[NO_3^-]$ and [Ni]	fit	marine	2

† excess sulfate concentration at Yaquina Head subtracted by at Corvallis
†† RSL(Y): the relative sulfate level for Yaquina Head sample
* traj: trajectory
** trace species concentrations were not available at Corvallis
• significantly different (> 0.2 μg/m3)

From the analysis of air mass type using the simple model, the fraction of the experimental period that the sampling sites were affected by marine background air can be estimated. As listed in Table 5, 14 out of 23 (61%) of the sampling periods were consistent with transport from marine areas. Within these 14 periods, local influences were present at Yaquina Head during two sampling periods. In other words, according to the model, Yaquina Head has a 52% chance (12 out of 23) of receiving "clean" background air advected from marine areas without any local emission source influences. Five out of 23 sampling periods received air transported from continental areas. Three out of these five sampling periods also were associated with local influences at Corvallis; local influences at Yaquina Head also showed up in all these five sampling periods.

Table 4.12. The number of sampling periods associated with each air mass type and with local influence at two sites.

Air Mass type					
	total number	Samples with local source influences			
		none	near Corvallis	near Yaquina	both sites
Marine	14	7	5	1	1
Continental	5	0	0	2	3

5. DISCUSSION

In the current study, fine and coarse particle fractions were collected separately based on knowledge of the aerosol size distribution (see Section 1.1). The relative elemental compositions of fine and coarse particle fractions demonstrate that the inertial impactor used in this study can effectively separate fine and coarse particles. Sodium concentrations that were typically found in the samples collected at two Oregon sampling sites can be accurately determined by FAAS. Contamination associated with sample handling was considered to be low due to the low blank filter concentrations (see Appendix B) and the consistent values for paired samples (see Section 4.1). Apparently the glove box limited potential contamination associated with sample handling. From the analysis of variance for the paired samples (see Section 4.1), the variance associated with aerosol sampling and chemical analysis is relatively small compared with the variance caused by time-dependent variables. This indicated that this experiment could successfully detect the time variation caused by meteorology and emission sources.

Ten of the fine particle samples were analyzed by INAA in the OSU Radiation Center. In the application of INAA to the samples, the irradiation time was comparatively short since the Teflon filters become increasingly fragile as irradiation time increased. The short irradiation time resulted in a high detection limit for each measured element. To improve the detection limit, it is suggested that the sample filter should be pressed into a pellet prior to irradiation for extending the irradiation time.

In contrast to Na concentration, the fine-Cl concentration of Corvallis samples and the Fe concentration of Yaquina Head samples was not well determined due to the relatively high detection limit compared to ambient

aerosol concentration. The extraction efficiency of ultrasonic bath can not be determined with certainty. The small number of samples (four pairs) used for the evaluation of extraction efficiency did not contradict the assumption that Teflon filters can be effectively extracted (Appel, 1981).

5.1 Background Site

In order to test the proposed use of Yaquina Head as a background aerosol ("clean") site, the chemical compositional data for sampling periods which were evaluated as marine background air (see Section 4.10) are summarized in Table 5.1. Concentrations of trace species are similar but slightly higher at Yaquina Head than those at other remote marine sites (Vong, 1985; Orsini *et al.*, 1986; Parungo *et al.*, 1990; Harvey *et al.*, 1991).

Eleven sampling periods were identified to have aerosols from marine areas and no local influence at Yaquina Head. At Yaquina Head, 52% of sampling periods were associated with "clean" background marine air. Thus, Yaquina Head represents a useful location for collecting marine background air from the Pacific Ocean under specified meteorological conditions.

The characteristics of aerosol at Yaquina Head are highly influenced by the ocean. The concentrations of the seasalt elements (Na and Cl) are higher than the concentrations observed at other remote locations around the world (Vong, 1985; Orsini *et al.*, 1986; Parungo *et al.*, 1990; Harvey *et al.*, 1991). The seasalt-derived elements are abundant in the particles of Yaquina Head and seasalt is the major (probably only) source of Na and Cl. This is borne out by a.) the high percentage of Na and Cl mass in the coarse fraction, b.) the consistency in the temporal variation for Na and Cl which was confirmed by

principal component analysis, and c.) the coarse-Cl "seasalt" enrichment factor of about one.

Multiple sources of sulfate particles were demonstrated in this study. The fact that coarse-SO_4^{2-} accounts for a majority (57%) of total sulfate mass and the lack of enrichment in coarse sulfate relative to seasalt (0.81) suggested that coarse-SO_4^{2-} was probably seasalt derived. The higher enrichment factor for fine-SO_4^{2-} relative to seasalt (9.9) is consistent with a fine-sulfate influence at Yaquina Head from sources other than seasalt. According to "crustal" enrichment factors, the influence of soil dust on these samples probably was minor.

Table 5.1. Chemical composition of the particles collected at Yaquina Head within the "marine" background air (defined in Section 4.10 according to the simple conceptual model)

	particle fraction	concentration (ng/m^3)	number of samples
Mass	fine	4031	10
	coarse	20590	7
SO_4^{2-}	fine	684	11
	coarse	no data	-
NO_3^-	fine	155	11
	coarse	no data	-
Cl^-	fine	555	11
Pb	fine	0.3	10
Ni	fine	0.1	10
Na	fine	411	9
	coarse	4250	7
Fe	total	U/D*	8
Cr	fine	U/D	9
Co	fine	0.065	9
Sb	fine	0.052	9

* U/D = under detection limit.

The "coarse+gas"-NO_3^- and fine particle Pb were sensitive to the air mass trajectory (Fig. 4.13 and Fig. 4.18); the concentrations for both were higher with continental trajectory than with marine trajectory. Aerosol NO_3^- has been reported as the end product of variety of reactions for the oxidation of nitrogen oxide (NOx) which are mainly from anthropogenic emissions and biomass burning (see Section 1.0). Lead in the atmosphere is widely thought to derived by human activities such as metal refining and automobile traffic (Davidson *et al.*, 1985; Öblad and Selin, 1986). Thus, the relatively strong trajectory dependence of "coarse+gas"-NO_3^- and Pb concentrations are consistent with larger anthropogenic influences with continental background air than with marine background air.

5.2 Rural Site

The concentrations for the measured species were 8% to 49% higher for the Corvallis site than at the Yaquina Head site except Fe and seasalt-derived species. The higher Fe concentration (Corvallis had 3.3 times the Yaquina Head Fe concentration) and lower seasalt concentrations (Corvallis had 12% of Na and 2% of Cl concentrations observed at Yaquina Head) reflects the geographical difference between two sampling sites (Corvallis is continental influenced- 64 km away from the Pacific Ocean; Yaquina Head is marine influenced- 1 km from the Pacific Ocean). The soil influence at Corvallis was greater than at Yaquina Head but not especially important for the Corvallis site according to the "crustal" enrichment factors. The high percentage of SO_4^{2-} in the fine fraction (97%) and the high "seasalt" enrichment factor for

fine-SO_4^{2-} (122) at Corvallis showed that SO_4^{2-} in the fine aerosol size fraction was mainly from sources other than seasalt.

According to the conceptual model results, ten out of 19 available sampling periods for Corvallis site were identified as having marine background, and four of these ten periods had no local source influences at the Corvallis site. Therefore, the sampling site at Corvallis would occasionally (21%) collect "clean" marine background air even though Corvallis is located 64 km from the ocean.

Ozone concentration during the nighttime was shown to be correlated with average sulfate concentration at Corvallis (two to three full day sampling period). A high correlation between sulfate and ozone has been previously reported in the literature (Wolff *et al*, 1985a; Altshuller, 1985); these authors suggested this result was due to photochemical activity since both sulfate and ozone are typically formed by oxidation reactions involving atmospheric free radicals (Seinfeld, 1986). The correlation decreased when mid-day ozone was compared to sulfate. This suggests that the sulfate and ozone concentrations although both produced by photochemical activity, may be controlled by the reduced degree of mixing in the stable atmosphere during the night time. However, in the daytime under unstable conditions, the correlation decreased due to better mixing in the lower troposphere which resulted in concentrations which are more a function of individual emission sources or specific reaction pathway for each species than the mixing process itself.

5.3 Behavior of Excess Sulfate

Excess-sulfate at Corvallis is correlated with that at Yaquina Head (r=0.87) suggesting a fairly widely distributed sulfur source. This result is consistent Wolff *et al.* (1985b) who concluded that fine fraction sulfate was fairly homogeneously distributed across southeastern Michigan. Sulfate in the fine fraction can be either from biogenic or anthropogenic sources (see Section 1.0). According to the fact that ten out of 13 MSA concentrations collected in this experiment are under detection limit (see Section 4.2), the fine-SO_4^{2-} from DMS oxidation should be fairly small in these ten sampling periods. Thus, the sulfate particles in these ten fine fraction samples might reasonably be assumed to be transformed from anthropogenic SO_2 emissions (burning of coal and oil) located far west of the Oregon coast.

According to the simple conceptual model described in Section 4.10, continental aerosol advected to the sampling sites during about 22% of the experiment period while 61% of the experiment period represented marine aerosol.

5.4 Relationships between Meteorological Condition and Aerosol Composition in Partial-Least-Square Regression Model

Only a small percentage of variance in chemical composition data were explained by meteorological condition in the PLS model described in Section 4.8. The weak relation is believed to be caused by several factors. First, the local meteorological data are not measured in the same location as the chemical data. The day-to-day variation in the chemical composition could easily be affected by other micro-meteorological factors at the sampling site which can not be detected at the weather station (local circulation or thermal stratification). Thus, co-locating meteorological data collection at the aerosol sampling site may be necessary if one is to detect the day-to-day variation of the particle composition that is driven by meteorology. Secondly, the meteorological parameters were not continuously monitored during the experimental period. Trajectory and stability data were generated twice per day while local wind speed and wind direction were available during the daytime (at Yaquina Head). The meteorological data density was less than ideal for this experiment. Thirdly, the observed degree of variation in meteorological condition is probably too limited to show the full extent of potential meteorological influences on airborne particle composition.

To improve the present experiment in terms of ability to recognize the relationships between meteorological condition and aerosol composition in the Corvallis and Yaquina Head areas, a longer experimental period (e.g. for two seasons) is recommended to get different meteorological patterns for comparison to those documented here.

6. SUMMARY AND CONCLUSIONS

In this study, aerosol samples were collected at Corvallis and Yaquina Head to estimate the air quality at the two sampling sites and assess the possibility of sampling marine background air at these locations. Forty seven fine particle (particle diameter < 2.5 μm) samples were collected by using inertial impactors while 48 total particle (all size) samples were collected by using openface filter holders. For 85 of the 95 particle samples, the filters were extracted with deionized-distilled water by using an ultrasonic device. The corresponding extraction efficiency was uncertain in this study since the number of the samples used for estimating extraction efficiency was too small for firm conclusions. However, other studies have suggested nearly complete extraction for SO_4^{2-} particles from similar Teflon filters (Appel, 1981; Clarke *et al.*, 1984). Although the complete extraction for Ni and Pb was expected, any losses would be more important in estimating actual concentrations than in the use of these species as tracers of relative source influences. Further work is required to estimate the extraction efficiency.

The results of chemical analysis indicated that seasalt contributions were important for the coarse particle aerosol at Yaquina Head, but that the seasalt influence was comparatively small in Corvallis. Fine particle excess sulfate (SO_4^{2-}ex) concentrations were quite similar at the two sampling sites. In this study, the SO_4^{2-}ex concentrations were calculated using Cl as the reference element for seasalt. Since aerosol Cl may be lost to the gas phase in acidic samples, the concentration of Na would be useful to accurately estimate the SO_4^{2-}ex concentration. For ten fine particle samples where both fine-Na and fine-Cl were measured, SO_4^{2-}ex calculated from Na typically was 2% (median of ten values) smaller than SO_4^{2-}ex calculated from Cl.

A simple conceptual model was used in conjunction with air trajectory and aerosol chemical composition to distinguish air mass types and help identify any local influences at the two sampling sites. During the experimental period for this study, 61% of the sampling periods described air transported from marine areas. At Yaquina Head, 52% of all sampling periods received "clean" marine background air without any observation of local influences. In contrast, only 21% of sampling periods at Corvallis received "clean" marine background air without local influences.

For the purpose of identifying local influences, NO_3^-, Ni, and Pb were selected. Among the eight sampling periods with SO_4^{2-}ex difference between the two sampling sites, three periods have high NO_3^-, Ni, or Pb concentration at the site with "extra" SO_4^{2-}ex. For the purpose of identifying marine air, the MSA concentrations were analyzed in fine particle samples to assess the potential influence of biogenic sulfate sources. Limited data suggested a small biogenic component to aerosol SO_4^{2-}. The influence of soil dust in this study was minimal according to the Fe measurements. To further check this potential crustal influence, other soil-derived elements, such as Al and Ca, should be analyzed. GFAAS is recommended for Fe measurements because the concentration of Fe was near the detection limit of FAAS.

The experimental procedures were not a significant factor influencing the measured aerosol composition. In general, the key factors which influence the aerosol composition at these two sampling sites are the type of air mass which advects to the sampling area (marine or continental background air) and any local source influences at the sampling sites. The extent to which these two factors affect the aerosol composition depend on the meteorology (i.e., back trajectory and local winds).

REFERENCES

Adams, F., P. Van Espen and W. Maenhaut, 1983: Aerosol composition at Chacaltaya, Bolivia, as determined by size-fractionated sampling. *Atmospheric Environment*, **17**, 1521-1536.

Ahrens, C. D., 1988: Meteorology Today, Western Publishing Company, St. Paul, 596 pp.

Altshuller, A. P., 1985: Relationships involving fine particle mass, fine particle sulfur and ozone during episodic periods at sites in and around St. Louis, MO. *Atmospheric Environment*, **19**, 265-276.

Amundsen, C. E., J. E. Hanssen, A. Semb, and E. Steinnes, 1992: Long-range atmospheric transport of trace elements to southern Norway. *Atmospheric Environment*, **26A**, 1309-1324.

Andreas, E. L., 1990: Time constants for the evolution of sea spray droplet. *Tellus*, **42B**, 481-497.

Anngarn, H. J., R. E. Van Grieken, D. M. Bibby and F. Von Blottnitz, 1983: Background aerosol composition in the Namib desert, south west Africa (Namibia). *Atmospheric Environment*, **17**, 2045-2053.

Appel, B. R., E. L. Kothny, E. M. Hoffer, G. M. Hidy and J. J. Wesolowski, 1978: Sulfate and nitrate data from the California Aerosol Characterization Experiment (ACHEX). *Environ. Sci. Technol.*, **12**, 418-425.

Appel, B. R., 1981: Studies in atmospheric particulate characterization techniques, in *Air/particulate instrumentation and analysis*. P. N. Cheremisinoff, *et al.*, Ann Arbor Science Publishers Inc., Ann Arbor, Michigan, 423 pp.

Baeyens, W. and H. Dedeurwaerder, 1991: Particulate trace metals above the southern bight of The North Sea- I. Analytical procedures and average aerosol concentrations. *Atmospheric Environment*, **25A**, 293-304.

Box, G. E. P., W. G. Hunter and J. S. Hunter, 1978: Statistics for experimenters. John Wiley & Sons, New York, 653 pp.

Braaten, D. A. and T. A. Cahill, 1986: Size and composition of Asian dust transported to Hawaii. *Atmospheric Environment*, **20**, 1105-1109.

Bruntz, S. M., W. S. Cleveland, T. E. Graedel, B. Kleiner and J. L. Warner, 1974: Ozone concentrations in New Jersey and New York: statistical association with related variables. *Science*, **186**, 257-259.

Butcher, S. S. and R. J. Charlson, 1972: An introduction to air chemistry. Academic Press, New York, P. 17-18.

Chameides, W. L. and D. D. Davis, 1982: Chemistry in the troposphere. *Chem. and Eng. News.*, **60 (40)**, 39-52.

Charlson, R. J., J. E. Lovelock, M. O. Andreae and S. G. Warren, 1987: Oceanic phytoplankton, atmospheric sulphur, cloud albedo and climate. *Nature*, **326**, 655-661.

Clarke, A. G., M. J. Willison and E. M. Zeki, 1984: A comparison of urban and rural aerosol composition using dichotomous samplers. *Atmospheric Environment*, **18**, 1767-1775.

Cohen, M. A., P. Barry Ryan, J. D. Spengler, H. Özkaynak and C. Hayes, 1991: Source-receptor study of volatile organic compounds and particulate matter in the Kanawha Valley, WV-II. analysis of factors contributing to VOC and particle exposures. *Atmospheric Environment*, **25B**, 95-107.

Cunningham, W. C. and W. H. Zoller, 1981: The chemical composition of remote area aerosol. *J. Aerosol Sci.*, **12**, 367-384.

Daum, P. H., T. J. Kelly, R. L. Tanner, X. Tang, K. Anlauf, J. Bottenheim, K. A. Brice and H. A. Wiebe, 1989: Winter measurements of trace gas and aerosol composition at a rural site in southern Ontario. *Atmospheric Environmen.*, **23**, 161-173.

Davidson, C. I., G. B. Wiersma, K.W. Brown, W.D. Goold, T.P. Mathison and M.T. Reilly, 1985: Airborne trace elements in Great Smoky Mountains, Olympic, and Glacier National Parks. *Environ. Sci. Technol.*, **19**, 27-35.

Duce, R. A., G. L. Hoffman and W. H. Zoller, 1975: Atmospheric trace metals at remote northern and southern hemisphere sites: pollution or natural. *Science*, **187**, 59-61.

Dzubay, T. G. and R. K. Stevens, 1975: Ambient air analysis with dichotomous samplers and X-ray fluorescence spectrometer. *Environ. Sci. Technol.*, **9**, 663-668.

Eagleman, J. R., 1985: Meteorology, 2nd Edition. Wadsworth Publishing Company, Belmont, CA., p. 323-328.

Geladi, P. and B. R. Kowalski, 1986: Partial least-squares regression: a tutorial. *Analytica Chimica Acta*, **185**, 1-17.

Hansson, H. C., B. G. Martinsson and H. O. Lannefors, 1984: Long range aerosol transport in southern Sweden: an example of multivariate statistical evaluation methodology. *Nucl Instrum. Methods Phys. Res.*, **B3**, 483-488.

Harvey, M. J., G. W. Fisher, I. S. Lechner, 1991: Summertime aerosol measurements in Ross Sea region of Antarctica. *Atmospheric Environment*, **25A**, 569-580.

Holland, H. D., 1978: The chemistry of the atmosphere and oceans. John Wiley & Sons, New York, 351 pp.

John, W. and G. Reischl, 1978: Measurement of the filtration efficiencies of selected filter types. *Atmospheric Environment*, **12**, 2015-2019.

Karl, T. R., 1978: Day of the week variation of photochemical pollutants in the St. Louis area. *Atmospheric Environment.*, **12**, 1657-1667.

Kuo, Y., M. Skumanich, P. L. Haagenson and J. S. Chang, 1985: The accuracy of trajectory models as revealed by the Observing System Simulation Experiments. *Mon. Wea. Rev.*, **113**, 1852-1867.

Lal, M. and R. K. Kapoor, 1989: Certain meteorological features of submicron aerosols at Schirmacher Oasis, east Antarctica. *Atmospheric Environment*, **23**, 803-808.

Lioy, P. J., T. Wainman, W. Turner and V. A. Marple, 1988: An intercomparison of the indoor air sampling impactor and the dichotomous sampler for a 10-μm cut size. *J. Air Pollut. Control Assoc.*, **38**, 668-670.

Lundgren, D. A., 1967: An aerosol sampler of determination of particle concentration of size and time. *J. Air Pollut. Control Assoc.*, **17**, 225

Maenhaut, W. and K. Akilimali, 1987: Study of the atmospheric aerosol composition in equatorial Africa using PIXE as analytical technique. *Nucl. Instrum. Methods Phys. Res.*, **22**, 254-258.

Maenhaut, W., P. Cornille, J. M. Pacyna andV. Vitols, 1989: Trace element composition and origin of the atmospheric aerosol in the Norwegian Arctic, *Atmospheric Environment*, **23**, 2551-2569.

Mahadevan, N. T., B. S. Negi and V. Meenakshy, 1989: Measurements of elemental composition of aerosol matter and precipitation from a remote background site in India. *Atmospheric Environment*, **23**, 869-874.

Marple, V. A. and B. Y. H. Liu, 1974: Characteristics of laminar jet impactors, *Environ. Sci. Technol.*, **8**, 648-654.

Marple, V. A. and K. Willeke, 1979: Inertial Impactors, in *Aerosol Measurement*. D. A. Lundgren, *et al.*, The University Press of Florida, Gainesville, Florida, 716 pp.

Marple, V. A., K. L. Rubow, W. Turner and J. D. Spengler, 1987: Low flow rate sharp cut impactors for indoor air sampling: design and calibration. *J. Air Pollut. Control Assoc.*, **37**, 1303-1307.

Mitchell, J. M., Jr., 1971: A preliminary evaluation of atmospheric pollution as a cause of the global temperature fluctuation of the past century, in *Global effects in environmental pollution*. S. F. Singer, D. Reidel Publishing Company, Dordrecht, Holland, 498 pp.

Öblad, M. and E. Selin, 1986: Measurement of elemental composition in background aerosol on the west coast of Sweden. *Atmospheric Environment*, **20**, 1419-1432.

Orsini, C. Q., M. H. Tabacniks, P. Artaxo, M. F. Andrade and A. S. Kerr, 1986: Characteristics of fine and coarse particles of natural and urban aerosols of Brazil. *Atmospheric Environment*, **20**, 2259-2269.

Pacyna, J. M., V. Vitols and J. E. Hanssen, 1984: Size-differentiated composition of the arctic aerosol at Ny-Ålesund, Spitsbergen. *Atmospheric Environment.*, **18**, 2447-2459.

Parungo, F. P., C. T. Nagamoto and P. J. Sheridan, 1990: Aerosol characteristics of Arctic haze sampled during AGASP-II. *Atmospheric Environment*, **24A**, 937-949.

Peterson, J. T. and R. A. Bryson, 1968: Atmospheric aerosols: increased concentrations during the last decade. *Science*, **162**, 120-121.

Prospero, J. M., R. J. Charlson, V. Mohnen, R. Jaenicke, A. C. Delany, J. Moyers, W. Zoller and K. Rahn, 1983: The atmospheric aerosol system: an overview. *Rev. Geophys. Space Phys.*, **21**, 1607-1629.

Schultz, P. and T. T. Warner, 1982: Characteristics of summertime circulations and pollutant ventilation in the Los Angeles Basin. *J. Appl. Meteorol.*, **21**, 672-681.

Seinfeld, J. H., 1986: Atmospheric chemistry and physics of air pollution. John Wiley & Sons, New York, 738 pp.

Taylor, S. R., 1964: Abundance of chemical elements in the continental crust: a new table. *Geochim. Cosmochim. Acta*, **28**, 1273-1285.

Vong, R. J., 1985: Simultaneous observations of rainwater and aerosol chemistry at a remote mid-latitude site. PhD Dissertation, University of Washington.

Vong, R. J., H, C. Hansson, H. B. Ross, D. S. Covert and R. J. Charlson, 1988: Northeastern Pacific sub-micrometer aerosol and rainwater composition: a multivariate analysis. *J. Geophy. Res.*, **93**, 1625-1637.

Vong, R. J., 1990: Mid-latitude northern hemisphere background sulfate concentration in rainwater. *Atmospheric Environment*, **24**, 1007-1018.

Wolff, G. T., 1980: Mesoscale and synoptic scale transport of aerosol, in *Aerosol: anthropogenic and natural, source and transport.* T. J. Kenip and P. J. Lioy, The New York Academy of Sciences , New York, 618 pp.

Wolff, G. T., P. E. Korsog, N. A. Kelly and M. A. Ferman, 1985a: Relationships between fine particulate species, gaseous pollutants and meteorological parameters in Detroit. *Atmospheric Environment*, **19**, 1341-1349.

Wolff, G. T., P. E. Korsog, D. P. Stroup, M. S. Ruthkosky and M. L. Morrissey, 1985b: The influences of local and regional sources on the concentration of inhalable particulate matter in southeastern Michigan. *Atmospheric Environment*, **19**, 305-313.

Zoller, W. H., E. S. Gladney and R. A. Duce, 1974: Atmospheric concentrations and sources of trace metals at the South Pole. *Science*, **183**, 198-200.

APPENDICES

Appendix A.1. Chemical composition of airborne particles collected at Corvallis

		FINE							TOTAL						
Date begin	Date end	Mass con.[1] ($\mu g/m^3$)	SO_4^{2-} con. ($\mu g/m^3$)	SO_4^{2-} ex. ($\mu g/m^3$)	NO_3^- con. ($\mu g/m^3$)	Cl^- con. ($\mu g/m^3$)	) con. ;/m^3)	Ni con. (ng/m^3)	Mass con. ($\mu g/m^3$)	SO_4^{2-} con. ($\mu g/m^3$)	SO_4^{2-} ex. ($\mu g/m^3$)	NO_3^- con. ($\mu g/m^3$)	Cl^- con. ($\mu g/m^3$)	Na con. ($\mu g/m^3$)	Fe con. ($\mu g/m^3$)
7/22	7/24	10.59	2.006	1.980	0.059	0.187	J/A	N/A	35.38	N/A	N/A	N/A	N/A	0.450	0.124
7/24	7/26	3.11	0.443	0.426	0.052	0.121	J/A	N/A	9.02	0.463	0.449	0.253	0.101	0.101	0.062
7/26	7/29	16.85	0.599	0.598	0.163	U/D[3]	.539	0.090	13.24	0.595	0.579	0.537	0.112	0.196	0.072
7/29	7/31	5.49	0.752	0.739	0.096	U/D	J/A	0.005	22.64	N/A	N/A	N/A	N/A	0.225	0.145
7/31	8/2	6.22	1.413	1.411	0.277	U/D	J/A	0.147	31.21	N/A	N/A	N/A	N/A	1.001	0.127
8/2	8/5	5.73	1.448	1.447	0.382	U/D	.751	0.281	17.52	1.515	1.488	0.815	0.189	0.356	0.116
8/5	8/7	5.48	0.807	0.786	0.320	0.152	J/A	0.053	24.87	N/A	N/A	N/A	N/A	0.745	0.131
8/9	8/12	N/A[2]	N/A	N/A	N/A	N/A	J/A	N/A	N/A	N/A	N/A	N/A	N/A	N/A	N/A
8/12	8/14	N/A	N/A	N/A	N/A	N/A	J/A	N/A	N/A	N/A	N/A	N/A	N/A	N/A	N/A
8/14	8/16	N/A	N/A	N/A	N/A	N/A	J/A	N/A	26.43	1.908	1.896	0.817	0.087	0.093	0.148
8/16	8/19	N/A	N/A	N/A	N/A	N/A	J/A	N/A	22.81	1.827	1.811	1.405	0.114	0.053	0.122
8/19	8/21	N/A	N/A	N/A	N/A	N/A	J/A	N/A	N/A	N/A	N/A	N/A	N/A	N/A	N/A
8/21	8/23	N/A	N/A	N/A	N/A	N/A	J/A	N/A	34.62	2.028	1.844	1.899	1.312	0.912	0.129
8/23	8/26	N/A	N/A	N/A	N/A	N/A	J/A	N/A	21.28	1.002	0.886	0.595	0.829	0.521	0.061
8/26	8/28	N/A	N/A	N/A	N/A	N/A	J/A	N/A	N/A	N/A	N/A	N/A	N/A	N/A	N/A
8/28	8/30	N/A	N/A	N/A	N/A	N/A	J/A	N/A	22.03	0.846	0.777	0.514	0.495	0.314	U/D
8/30	9/1	N/A	N/A	N/A	N/A	N/A	J/A	N/A	21.42	0.680	0.583	0.376	0.695	0.459	U/D
9/11	9/13	7.22	1.323	1.311	0.164	U/D	J/A	0.248	28.96	N/A	N/A	N/A	N/A	0.512	0.078
9/13	9/16	10.85	1.427	1.424	0.312	U/D	J/A	0.144	40.66	N/A	N/A	N/A	N/A	0.917	0.110
9/16	9/18	14.96	1.251	1.249	0.205	U/D	J/A	0.503	N/A	N/A	N/A	N/A	N/A	N/A	N/A
9/18	9/20	9.57	1.216	1.206	0.178	U/D	J/A	0.324	46.94	N/A	N/A	N/A	N/A	0.306	0.113
9/20	9/23	6.88	0.985	0.962	0.501	0.164	J/A	0.218	31.94	N/A	N/A	N/A	N/A	1.021	0.096
9/23	9/25	8.86	0.965	0.956	0.183	U/D	J/A	U/D	67.45	N/A	N/A	N/A	N/A	0.186	0.131
9/25	9/27	8.54	1.498	1.483	0.327	0.109	J/A	0.305	53.15	N/A	N/A	N/A	N/A	0.798	0.131

1 con.: concentration
2 N/A: concentration is not avaliable
3 U/D: under detection limit

Appendix A.2. Chemical composition of airborne particles collected at Yaquir Head

		FINE											TOTAL						
Date begin	Date end	Mass con.[1] ($\mu g/m^3$)	SO_4^{2-} con. ($\mu g/m^3$)	SO_4^{2-} ex. ($\mu g/m^3$)	NO_3^- con. ($\mu g/m^3$)	Cl^- con. ($\mu g/m^3$)	Pb con. (ng/m^3)	Ni co (ng/n	Na con. ($\mu g/m^3$)	Cr con. ($\mu g/m^3$)	Co con. ($\mu g/m^3$)	Sb con. ($\mu g/m^3$)	Mass con. ($\mu g/m^3$)	SO_4^{2-} con. ($\mu g/m^3$)	SO_4^{2-} ex. ($\mu g/m^3$)	NO_3^- con. ($\mu g/m^3$)	Cl^- con. ($\mu g/m^3$)	Na con. ($\mu g/m^3$)	Fe con. ($\mu g/m^3$)
7/22	7/24	N/A[2]	N/A	N/A	N/A	N/A	N/A	N/A	N/A	N/A	N/A	N/A	N/A	N/A	N/A	N/A	N/A	N/A	N/A
7/24	7/26	N/A	0.450	0.425	N/A	0.177	N/A	N/A	N/A	N/A	N/A	N/A	N/A	0.827	0.436	0.142	2.791	N/A	N/A
7/26	7/29	3.57	0.780	0.741	0.203	0.282	0.396	0.42	N/A	N/A	N/A	N/A	N/A	1.661	0.577	0.466	7.744	N/A	N/A
7/29	7/31	4.69	0.896	0.838	0.172	0.413	0.585	0.17	N/A	N/A	N/A	N/A	N/A	N/A	N/A	N/A	N/A	N/A	N/A
7/31	8/2	3.33	1.324	1.310	0.072	0.103	0.212	0.31	N/A	N/A	N/A	N/A	N/A	N/A	N/A	N/A	N/A	N/A	N/A
8/2	8/5	3.11	1.272	1.272	0.012	0.004	0.149	0.47	N/A	N/A	N/A	N/A	N/A	1.759	1.009	0.413	5.360	N/A	N/A
8/5	8/7	11.36	0.801	0.631	0.141	1.211	0.278	U/I	N/A	N/A	N/A	N/A	N/A	N/A	N/A	N/A	N/A	N/A	N/A
8/9	8/12	5.09	1.178	1.021	0.080	0.120	0.240	0.01	0.462	0.232	0.054	0.041	23.45	N/A	N/A	N/A	N/A	1.568	U/D
8/12	8/14	2.10	0.753	^0.728[3]	U/D[4]	U/D	0.485	0.14	0.102	U/D	0.135	0.012	12.37	N/A	N/A	N/A	N/A	1.498	U/D
8/14	8/16	1.36	0.306	^0.302	0.015	U/D	0.183	0.05	0.017	U/D	U/D	0.012	N/A	N/A	N/A	N/A	N/A	N/A	N/A
8/16	8/19	1.84	0.277	0.266	0.025	0.078	0.603	U/I	0.072	0.334	0.061	0.022	6.77	N/A	N/A	N/A	N/A	0.721	U/D
8/19	8/21	3.49	0.662	^0.608	0.023	U/D	0.203	0.05	0.215	U/D	0.033	0.009	14.09	N/A	N/A	N/A	N/A	2.326	U/D
8/21	8/23	4.85	0.904	0.764	0.361	0.997	0.178	0.15	0.633	U/D	0.081	0.223	33.86	N/A	N/A	N/A	N/A	8.960	U/D
8/23	8/26	5.08	0.857	0.698	0.158	1.139	0.274	0.05	0.641	U/D	0.024	0.003	30.55	N/A	N/A	N/A	N/A	7.613	U/D
8/26	8/28	4.89	0.499	0.419	0.583	0.571	0.350	0.19	0.365	0.192	0.120	0.113	N/A	N/A	N/A	N/A	N/A	N/A	N/A
8/28	8/30	6.69	0.436	0.139	0.021	2.143	0.218	0.11	0.939	U/D	U/D	0.040	34.82	N/A	N/A	N/A	N/A	7.970	U/D
8/30	9/1	2.07	0.579	0.538	0.123	0.296	0.367	0.07	0.323	U/D	0.105	0.016	24.35	N/A	N/A	N/A	N/A	3.111	U/D
9/11	9/13	3.40	1.121	1.112	0.082	U/D	0.211	U/I	N/A	N/A	N/A	N/A	16.77	N/A	N/A	N/A	N/A	5.824	U/D
9/13	9/16	8.98	1.369	1.166	0.424	1.449	1.786	0.15	N/A	N/A	N/A	N/A	47.11	3.748	0.408	1.299	23.86	10.518	U/D
9/16	9/18	12.44	1.388	1.130	0.615	1.841	1.171	0.12	N/A	N/A	N/A	N/A	63.30	N/A	N/A	N/A	N/A	12.812	0.081
9/18	9/20	10.32	1.165	0.883	0.317	2.014	0.397	0.40	N/A	N/A	N/A	N/A	69.23	N/A	N/A	N/A	N/A	16.159	U/D
9/20	9/23	9.59	1.187	0.908	0.421	1.994	0.642	0.30	N/A	N/A	N/A	N/A	53.09	3.875	1.309	1.044	18.33	13.502	0.028
9/23	9/25	10.68	1.414	1.223	0.222	1.364	1.033	0.48	N/A	N/A	N/A	N/A	57.69	N/A	N/A	N/A	N/A	9.455	0.129
9/25	9/27	8.39	1.725	1.658	0.313	0.478	0.869	0.18	N/A	N/A	N/A	N/A	35.77	N/A	N/A	N/A	N/A	7.618	0.042

1. con.: concentration
2. N/A: concentration is not avaliable
3. ^: excess-sulfate is calculated with sodium concentration
4. U/D: under detection limit

Appendix B. The chemical composition of blank filters

	analysis technique	unit	mean±S.D.
SO_4^{2-}	IC[1]	ppm	U/D[5]
NO_3^-	IC	ppm	0.256±0.041
Cl^-	IC	ppm	0.216±0.263
Pb	GFAAS[2]	ppb	0.063±0.077
Ni	GFAAS	ppb	0.325±0.216
Na	FAAS[3]	ppm	0.128±0.050
Fe	FAAS	ppm	U/D
Na	INAA[4]	μg	0.23±0.014
Cr	INAA	ng	11.5±2.120
Co	INAA	ng	2.15±0.495
Sb	INAA	ng	1.25±0.410

1 IC: Ion Chromatography
2 GFAAS: Graphite Furnace Atomic Absorption Spectroscopy
3 FAAS: Flame Atomic Absorption Spectroscopy
4 INAA: Instrumental Neutron Activation Analysis
5 U/D: under detection limit